POLITECNICO DI TORINO

Master of Science in Electronic Engineering

Master's thesis

Energy Harvesting and Wireless Power Transfer at Radio-Frequency

Advisor
Prof. Giuseppe Vecchi

Coadvisors:
Dott. Giorgio Giordanengo
Dott. Marco Righero

Candidate
Carlo Curina
Matricola: 231389

Academic year 2017–2018

Abstract

Energy Harvesting is one of the most relevant issues in today green economy; use of the "stray" energy radiated at Radio-Frequency (RF) by countless wireless devices is one of the many aspects of present and future Energy Harvesting. On the other hand, the intentional use of RF sources is also one of the possible approaches to Wireless Power Transfer (WPT). A common energy harvesting device is the *rectenna*, a circuit composed of an antenna, a matching circuit and a rectifier. The main objective of this work is to understand how the antenna impedance affects the charge of the capacitor used as load, to find a trade-off between charge time and maximum achievable voltage.
The antenna choice drops on a patch antenna since it is quite easy to implement in a circuit, modeled as a sinusoidal voltage generator connected in series to an impedance starting from some specifications (shape, dielectric, physical dimensions and so on). The rectifier is a half-wave rectifier, due to a high power conversion efficiency and no matching circuit is used to prevent additional losses to obtain the impedance matching.
The circuit was studied initially assuming the impedance purely resistive, then using its complete model. From the analysis it can be noted that::

- the maximum input voltage achievable from the antenna is related to the radiation resistance;
- fixing the antenna quality factor, the smaller is the radiation resistance the faster is the charge;
- fixing the radiation resistance, the higher is the antenna quality factor the faster is the charge. It is observed that the limit case with the resistance alone has the slowest charge;
- the output voltage in steady state depends mainly on the diode.

These results are coherent with simulations performed by circuit simulators.
From tests done on half-wave rectifier and single stage voltage multiplier in the anechoic chamber to charge a small capacitor, connecting them to a patch antenna and a dipole and used to charge a small capacitor it can be concluded that:

- the half-wave rectifier produces a higher output voltage than the other topology independently on the receiver antenna used;
- the patch allows to get a higher output voltage due to a higher gain with respect the dipole;

- the measured voltages are lower than the theoretical expectations, since the model does not consider any losses.

Contents

Chapter 1

Introduction

Wireless power transfer (WPT) is the transmission of electrical energy without wires. This technology enables to charge electrical devices where the connection with a wire is difficult or not feasible. Wireless power technique can be subdivided in three categories:

- *near-field*, or non-radiative technique in which the power is transferred over short distance exploiting inductive coupling between coils of wires, or by electric field using capacitive coupling between metal electrodes; It is widely commercialized but is suffers from extremely short charging distances:
- *far-field* directive, or radiative technique in which the power is transferred by means of electromegnetic radiation such as laser beams or microwaves;
- *far-field* ambient radio frequency (RF) energy harvesting, in which the power source is the ambient RF energy;

Far field techniques allows to overcome the distance problem. Furthermore, RF energy harvesting becomes more fascinating during the last decades for growing transmission broadcast RF energy. This ambient energy can be seen as "free" powering source. In this case the receiver efficiency is crucial due to the low input power.

1.1 Objective and motivations

An RF power harvester capable to generate enough DC power to supply a wireless system can be used as starting point for future wireless systems, such as portable devices or mobile phones, with a self powered scheme without restoring the batteries [1].
A common energy harvesting device is the rectenna, made up with an antenna ad a rectifier circuit, used to convert the RF incident power to DC power. This

device usually is connected to a storage element in order to collect all the received electromagnetic power. In this thesis it is studied how the antenna parameters (impedance and quality factor) impacts on the charge a capacitor used as load.

1.2 Thesis outline

This thesis is subdivided in many chapters:

- in chapter 2 it is described the rectenna structure, focusing on the antenna and the rectifier:
  - starting from the mathematical description of the antenna an equivalent circuit is obtained;
  - it is discussed about the proper rectifier topology for this application and then the component choice.
- in chapter 3 the complete circuit is analyzed and simulated with many circuit simulators;
- in chapter 4 are reported the experimental results obtained in laboratory, testing the proposed circuit and commercial energy harvesting kit.

1.3 Thesis contribution

In this thesis it is studied the transient of the output voltage of a rectenna, focusing on the charge time an the maximum achievable voltage level which is important in an optic to use this collected energy to supply other circuits. In a low power input scenario the charge time is quite long, so a complete simulation to estimate the transient can take much time using standard circuit simulators, for this reason an algorithm is developed to simulate the circuit in a much faster way. From these results it is possible to choose the antenna and the other components in order to get the best performances.

Chapter 2

Rectenna

A *rectenna* is a circuit used to collect wireless transmitted power and to convert it on DC power. A typical rectenna is composed by an antenna, a matching circuit, a rectifier and a load (figure 2.1).

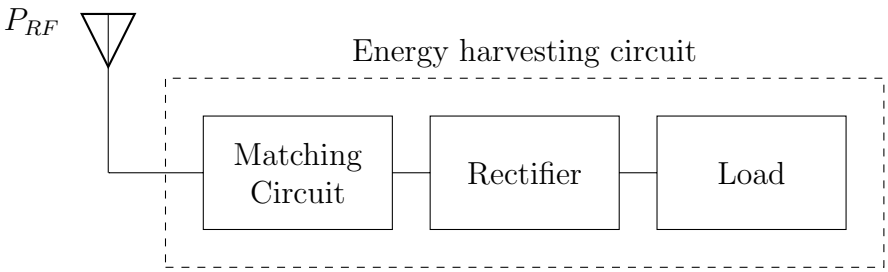

Figure 2.1: Rectenna structure

In an optic of low power level, all the circuit losses impact strongly on the system funcionality. For this reason the matching circuit is not considered in this case, since even with a matching net with lossless elements, in order to get a perfect matching of impedance a lot of power must be despoiled by the matching circuit [2]. The rectenna is supposed to work for frequencies of 915 MHz and 860 MHz, according to the US and EU normative respectively.

2.1 Antenna

For this project the idea is to use a patch antenna, since it is quite easy to build and in can be integrated in an electronic circuit with the other devices. Two kinds of patch antenna may be used:

- microstrip-fed patch, by means of a stripline;

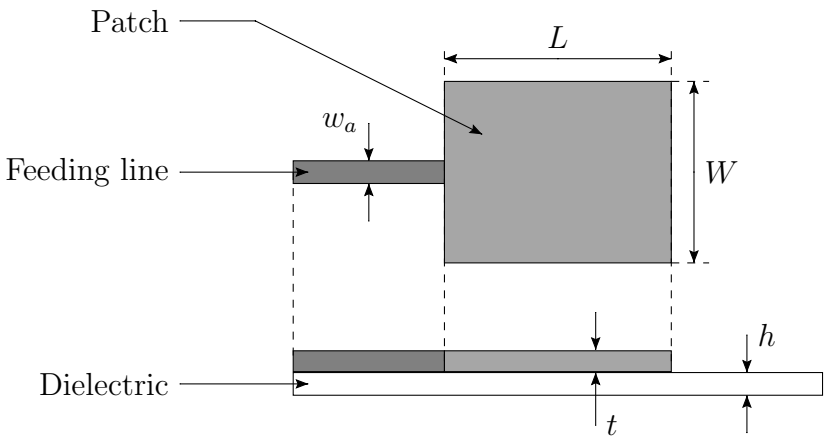

Figure 2.2: Patch antenna - microstrip feed

- probe-fed patch with a coaxial cable;

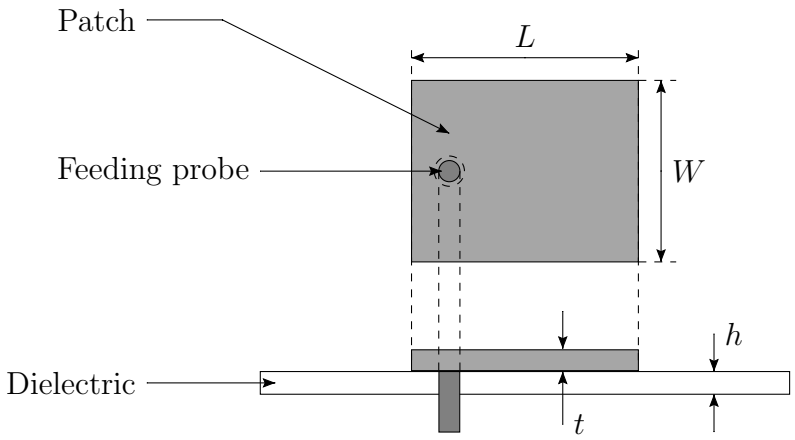

Figure 2.3: Patch antenna - probe feed

The focus point is to get an equivalent circuit of the structure. As first approximation the antenna can be modeled as a voltage generator in series to a generic impedance (figure 2.4):

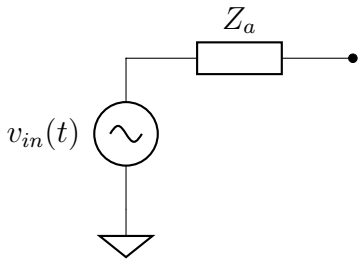

Figure 2.4: Antenna equivalent circuit

2.1.1 Input voltage

The first step consist to determine the input voltage. An important parameter for the antenna is the *effective height* $\bar{h}_e$ that relates the induced voltage to the incident electric field [3]:

$$V_{in} = \vec{h}_e \cdot \vec{E} = |h_e||E_{inc}|\hat{h}_e \cdot \vec{E}_{inc} \tag{2.1}$$

Assuming the antenna oriented in the direction of the maximum reception, the expression 2.1 can be simplified as:

$$V_{in} = |h_e||E_{inc}| \tag{2.2}$$

The effective height is related to the physical dimensions of the antenna and the frequency:

$$|h_e(\theta,\phi)|^2 = \lambda^2 G\frac{R_{rad}}{\pi Z_0} \quad \rightarrow \quad |h_e(\theta,\phi)| = \lambda\sqrt{G\frac{R_{rad}}{\pi Z_0}} \tag{2.3}$$

where:

- G is the (maximum) gain of the antenna in linear unit;
- R_{rad} is radiation resistance;
- $\lambda = \dfrac{\lambda_0}{\sqrt{\varepsilon_r}}$ is the wavelength in the patch medium.

EIRP considerations

The maximum value of the incident electric field on the antenna can be evaluated starting from the limitations on the maximum power density that can be radiated. The first consideration is related to the *Effective Isotropic Radiated Power* (or EIRP) that is the power density radiated by an ideal isotropic antenna. It refers

the effective power transmitted in a radio system. The EIRP (in dBm) is calculated using this formula:

$$EIRP = P_{tx} - C_t + G_t \quad [dB] \tag{2.4}$$

where:

- P_{tx} is the transmitter power output (dBm)[1];
- C_t is the signal loss in cable (dB);
- G_t gain of the antenna (dBi)[2].

Since in this case the reciver side is considered, it is possible to neglect the cable losses. In this case the EIRP can be simplified in linear unit as:

$$EIRP = P_{tx} \cdot G_t \tag{2.5}$$

The normative ETS 300-328 fixes a limit on the maximum transmitted power with an EIRP of 100 mW (20 dBm) for the frequency range involved on this project (and the harmonics). The power density can be expressed as:

$$S(r, \theta, \phi) = \left(\frac{\mathrm{d}P}{\mathrm{d}\Sigma}\right)_{inc} = \frac{P_{inc}}{4\pi r^2} = \frac{|E_{inc}|^2}{2Z_0} \tag{2.6}$$

Where Z_0 is the free space impedance and r is the distance. Since:

$$P_{inc} = P_{out} \cdot G_t = EIRP$$

it is possible express the incident field in terms of EIRP:

$$|E_{inc}| = \frac{1}{r}\sqrt{\frac{EIRP\ Z_0}{2\pi}} \tag{2.7}$$

Supposing to place the receiver at distance $r = 1.5$ m from the radiating source, the corresponding maximum incident field is:

$$|E_{inc}| = 1.633 \text{ V/m}$$

From this result it is possible to get an order of magnitude of the voltage at the antenna terminal, that can be used for the successive simulations.

[1] Power ratio in decibels (dB) of the measured power referenced to one milliwatt (mW).

[2] Power ratio in decibels relative to an isotropic radiator.

Gain

The gain is defined to relate the power density to the input power:

$$g(\theta,\phi) = \frac{\left(\frac{\mathrm{d}P}{\mathrm{d}\Sigma}\right)_{r,\theta,\phi}}{\frac{P_{in}}{4\pi r^2}} \tag{2.8}$$

where the input power P_{in} may be obtained from the radiated power P_{rad} through the efficiency ν:

$$P_{rad} = \nu P_{in}$$

By making some calculation it is possible to evaluate the maximum gain as:

$$G = \frac{4\pi\nu}{\int_0^{2\pi} d\phi \int_0^{\pi} d\theta \sin\theta |\vec{e}(\theta,\phi)|^2} \tag{2.9}$$

where $\vec{e}(\theta,\phi)$[3] is the specific radiation vector of the antenna. In the case of a patch antenna:

$$\vec{e}(\theta,\phi) \propto \hat{\phi} \sin\theta \,\mathrm{sinc}\left(\pi \cos\theta \frac{W}{\lambda_0}\right) \cos\left(\pi \frac{L}{\lambda_0} \sin\theta \sin\phi\right)$$

A plot of the gain in function of the ratios W/λ_0 and L/λ_0 is shown in figure 2.5:

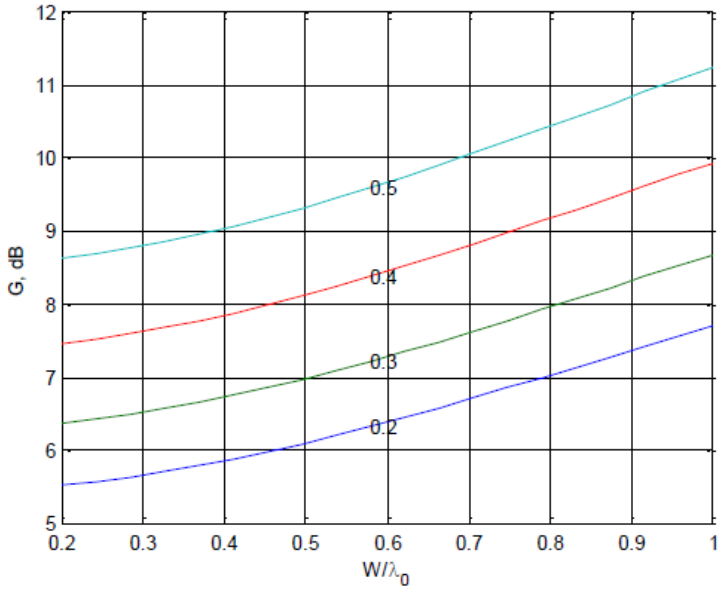

Figure 2.5: Maximum patch gain at resonance [4] (the parameter is L/λ_0)

[3]The polarization is linear;

A practical value of the gain of 6 dB was used, independently on the size ratio, in order to take into account possible losses and non-idealities.

Radiation resistance

The radiation resistance can be evaluated starting from the definition of input power:

$$P_{in} = \frac{1}{2} G_{rad} |V_{in}|^2 \tag{2.10}$$

Considering a lossless case:

$$\nu = 1 \quad \rightarrow \quad P_{in} = P_{rad}$$

it is possible rewrite the expression 2.10 as:

$$P_{rad} = \frac{1}{2} G_{rad} |V_{in}|^2 = \frac{|\vec{E}_{inc}|^2}{2Z_0} \tag{2.11}$$

the incident field can be expressed in function of the specific radiation vector of the antenna $\vec{e}(\theta, \phi)$:

$$\vec{E}_{inc}(r, \theta, \phi) = \frac{1}{4\pi r^2} \int\int \sin\theta \vec{e}(\theta, \phi) d\Sigma \quad \rightarrow \quad d\Sigma = r^2 \sin\theta d\phi d\theta \tag{2.12}$$

In the case of a patch antenna, $\vec{e}(\theta, \phi)$ can be expressed as:

$$\vec{e}(\theta, \phi) = \begin{cases} e_0 \sin\theta \operatorname{sinc}\left(\pi \cos\theta \frac{W}{\lambda_0}\right) \cos\left(\pi \frac{L}{\lambda_0} \sin\theta \sin\phi\right) \hat{\phi} & \text{for } -\pi/2 < \phi < \pi/2 \\ 0 & \text{for } -\pi/2 < \phi \vee \phi > \pi/2 \end{cases}$$

where

$$e_0 = -jV_{in} 4\pi \frac{W}{\lambda_0}$$

So the radiation conductance can be derived as:

$$G_{rad} = \frac{4}{Z_0} \left(\frac{W}{\lambda_0}\right)^2 \int_0^{\pi} \sin^3\theta \left[\operatorname{sinc}\left(\pi \cos\theta \frac{W}{\lambda_0}\right)\right]^2 d\theta \int_{-\pi/2}^{\pi/2} \cos^2\left(\pi \frac{L}{\lambda_0} \sin\theta \sin\phi\right) d\phi \tag{2.13}$$

At resonance, since $\Im\{Y_a\} = 0$, it is possible to write:

$$R_{rad}(\omega_r) = \Re\{Z_a(\omega_r)\} = \Re\left\{\frac{1}{Y_a(\omega_r)}\right\} = \frac{1}{G_{rad}(\omega_r)}$$

In particular it is possible to notice that the radiation resistance depends on the physical dimensions W and L of the patch as it is shown in figure 2.6:

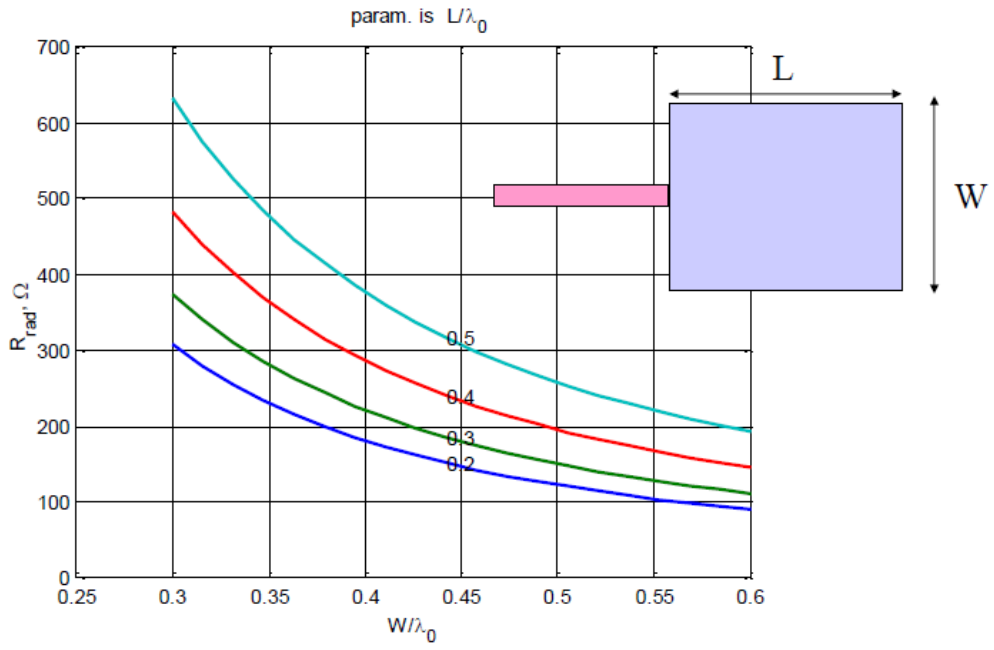

Figure 2.6: R_{rad} at resonance [4]

From these considerations it is possible to represent the patch impedance: assuming the radiation produced just to two magnetic currents localized at the edges of the patch and separated by a transmission line, it is possible to get the *two radiating edges* model (figure 2.7). In this case:

$$G_{edge}(\omega) \simeq \frac{1}{2} G_{rad}(\omega_r)$$

In reality this approximation that is valid at resonance frequency only.

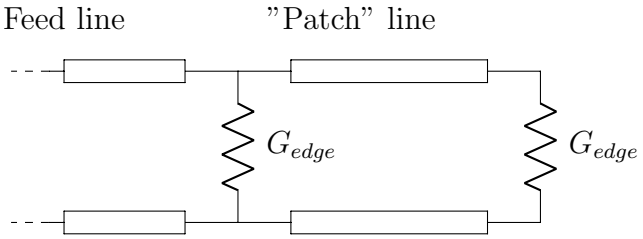

Figure 2.7: Two radiating edges model

By looking at the termination of the patch a strong field variation is present. This electric field is called *fringing field* and it corresponds to a charge accumulation:

$$\nabla \cdot \vec{E} = -j\omega\rho$$

This effect can be represented in the circuit by adding a pair of capacitances, the so called *fringing capacitances* C_F, in parallel to the conductances (figure 2.8):

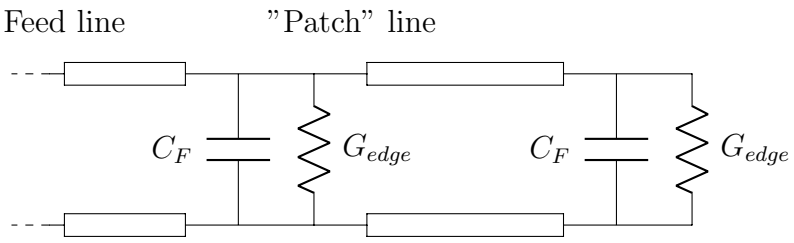

Figure 2.8: Model with finging capacitances

The effect of these capacitances can be interpreted as a pair of increments ΔL of the patch electrical length:

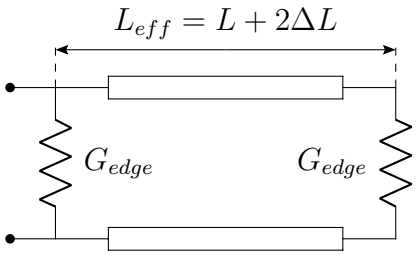

Figure 2.9: Patch model (edge feeding)

Assuming G_{edge} constant for all the frequencies, the equivalent impedance shows a frequency behaviour as figure 2.10:

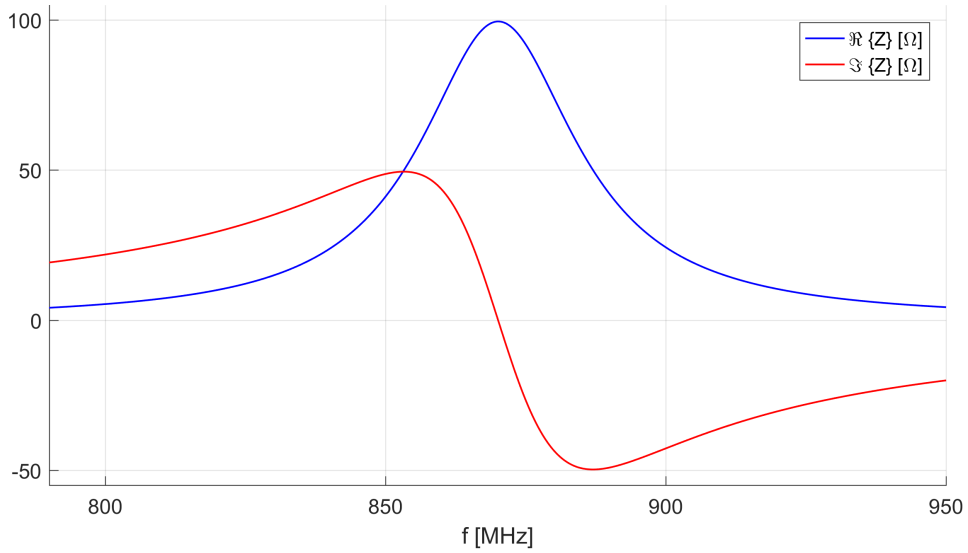

Figure 2.10: Example of patch frequemcy response

All the previous discussions were based on the assumption that the patch has been feed at one of the edges, that is the case in which the radiating resistance is the maximum. It is possible to change the antenna impedance by changing the feeding point. Supposing to put the probe position at a distance x from the edge:

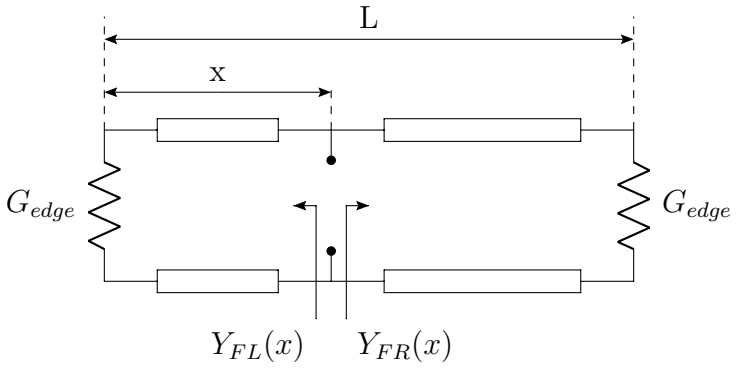

Figure 2.11: Patch model (recessed feeding)

$$Y_{in}(x) = Y_{FL}(x) + Y_{FR}(x)$$

So it is possible to get many value of impedance by properly choosing the tap point:

- the impedance gets a high value when the patch is feed from one edge ($R_{rad}(0)$);

- when the tap point is at center,a very small resistance is present ($r_{1/2}$).

Neglecting the center resistance, it is possible to express the variation of the radiation resistance in function of the position of the feeding point by the following relation:

$$\frac{R_{rad}(x)}{R_{rad}(0)} \approx \cos^2\left(\pi\frac{x}{L}\right) \tag{2.14}$$

In figure 2.12 is present graphical representation of this behaviour:

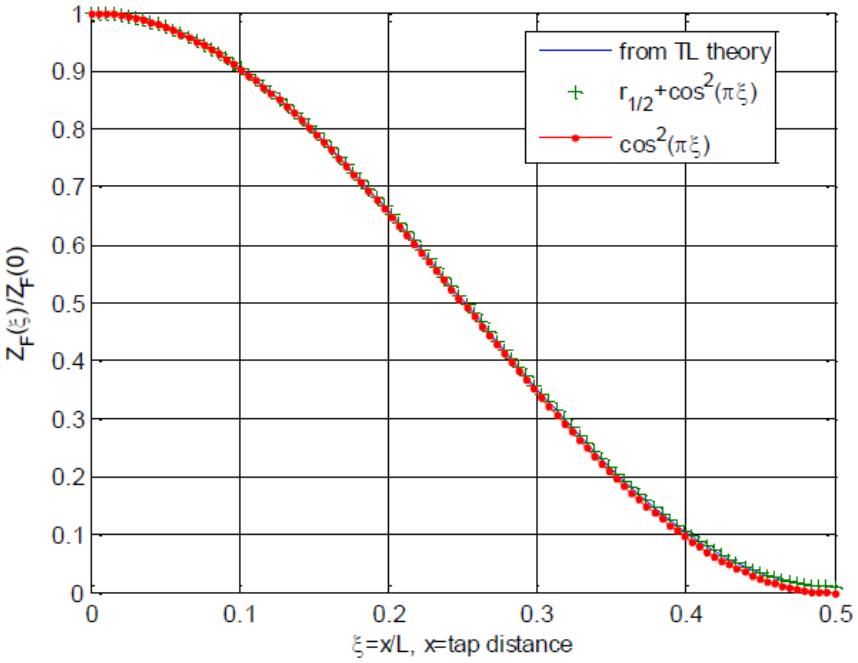

Figure 2.12: Impedance variation along x of different models [4]

In this way it is possible to rewrite the effective height in function of the feeding point:

$$|h_e(x)| = \lambda\sqrt{G\frac{R_{rad}(x)}{\pi Z_0}} = |h_e(0)|\cos\left(\pi\frac{x}{L}\right) \tag{2.15}$$

where $h_e(0)$ is the maximum value evaluated at the edge:

$$|h_e(0)| = \lambda\sqrt{G\frac{R_{rad}(0)}{\pi Z_0}}$$

Numerical results

Starting from all the considerations of chapter 2.1.1, it is well evident that the input voltage depends on the dimensions of the antenna, so each project must be considered stand alone. To get an order of magnitude of the input voltage for the simulations, the following values are considered:

- $f_0 = 868$ MHz $\rightarrow$ $\lambda_0 = \dfrac{c}{f_0} = 345.6$ mm
- $\varepsilon_r = 1$ (air) $\rightarrow$ $\lambda = \lambda_0 = 345.6$ mm
- $R_{rad}(0) = R_{rad}(x) = 200\ \Omega$ (supposing to feed the patch at the edge);
- $G_{dB} = 6\ dB \rightarrow$ $G = 3.98$;

it points out an effective height:

$$|h_e| = 283.3 \text{ mm}$$

So the maximum input voltage has an order of magnitude of:

$$V_{in} \approx 0.5 \text{ V}$$

2.1.2 Antenna impedance

As already discussed, the frequency response of the patch is shown figure 2.10. This behaviour is the same of a parallel RLC resonator in the frequency range around the resonance frequency.

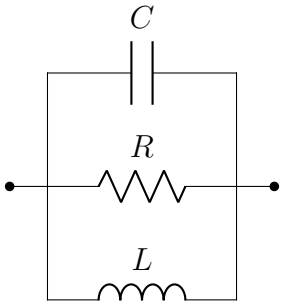

Figure 2.13: Parallel RLC resonator

The impedance can be written in the Fourier domain as:

$$Z_{res}(j\omega) = \frac{j\omega RL}{j\omega L - \omega^2 RLC + R}$$

or alternatively the admittance:

$$Y_{res}(j\omega) = \frac{1}{R} - j\frac{1}{\omega L} + j\omega C$$

In order to simplify the computation it is needed to pass from the equivalent circuit of the transmission line to an approximate resonator. Considering the circuit already discussed in figure 2.14:

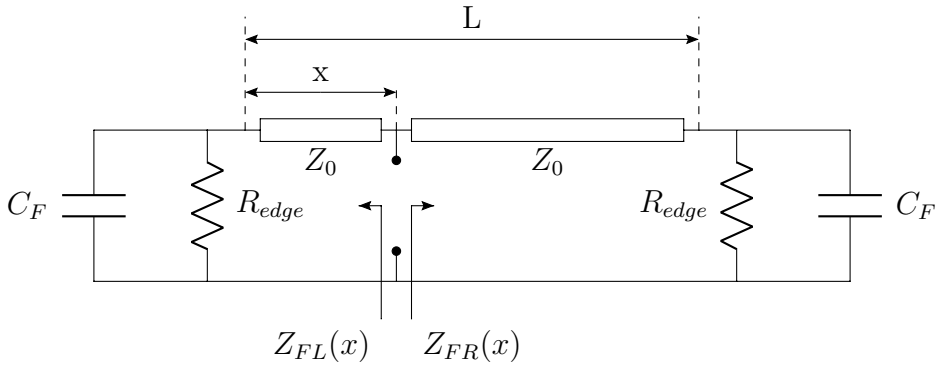

Figure 2.14: Patch circuit

The impedance that can be seen from each side, neglecting all the line losses, can be written as:

$$Z_{Fi}(l) = Z_0 \left[\frac{Z_L + Z_0 \tan(kl)}{Z_0 + Z_L \tan(kl)}\right] \tag{2.16}$$

where:

- Z_0 is the characteristic impedance of the patch;
- Z_L is the termination impedance:

$$Z_L = Z_L(j\omega) = R_{edge}//\frac{1}{j\omega C_F} = \frac{R_{edge}}{1 + j\omega R_{edge} C_F} \tag{2.17}$$

- k is the wavenumber:

$$k = \frac{2\pi}{\lambda} \tag{2.18}$$

The equivalent impedance that can be seen from the feeding point can be evaluated as:

$$Z_{FL} = Z_0 \left[\frac{Z_L + Z_0 \tan(kx)}{Z_0 + Z_L \tan(kx)}\right]$$
$$Z_{FR} = Z_0 \left[\frac{Z_L + Z_0 \tan\left[k(L-x)\right]}{Z_0 + Z_L \tan\left[k(L-x)\right]}\right]$$
$$Z_{in} = Z_{FL}//Z_{FR}$$

In order to get the equivalent resonator, it is useful to consider also the input admittance:

$$Y_{in} = \frac{1}{Z_{in}}$$

The graphical representation is shown in figure 2.15:

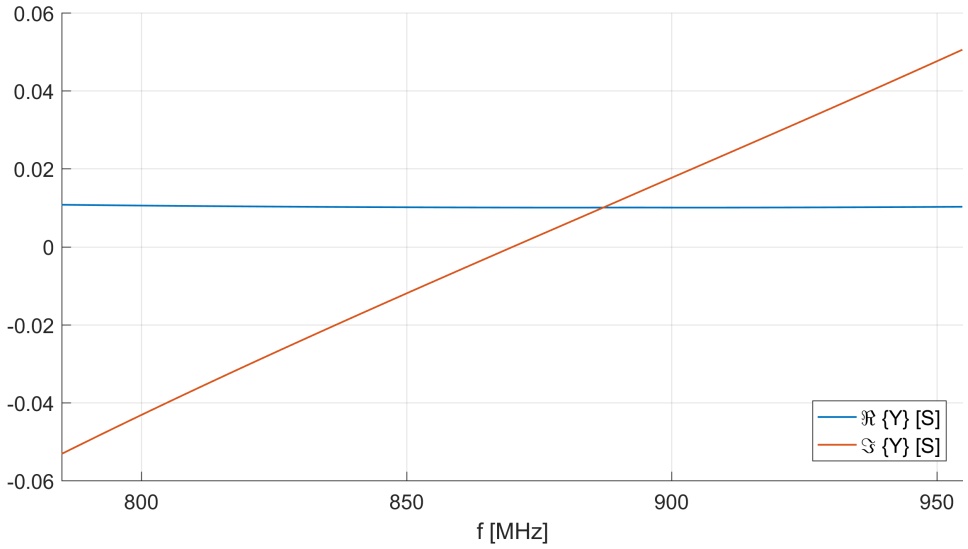

Figure 2.15: Input admittance of the patch

From this result it is possible to get R, L ans C starting from the following considerations:

- the real part is almost constant and it coincides with the reciprocal of the resonator resistance:

  $$\Re\{Y_{in}\} = \frac{1}{R}$$

  It is important to notice that also the resonator resistance is similar to the radiation resistance, previously computed, if the feeding point is sufficiently far from the center of the patch (where it is null).

  $$R \simeq R_{rad}$$

- the resonance frequency can be approximated as:

  $$\omega_0 = \frac{1}{\sqrt{LC}} \;\rightarrow\; L = \frac{1}{\omega_0^2 C}$$

- the imaginary part of the input admittance can be written as:

  $$Im\{Y_{in}\} = \omega C - \frac{1}{\omega L} = C\left(\omega - \frac{\omega_0^2}{\omega}\right)$$

So starting from some data obtained with Matlab it is possible to get all the parameters of the equivalent resonator. In conclusion the equivalent circuit for the antenna is shown in figure 2.16:

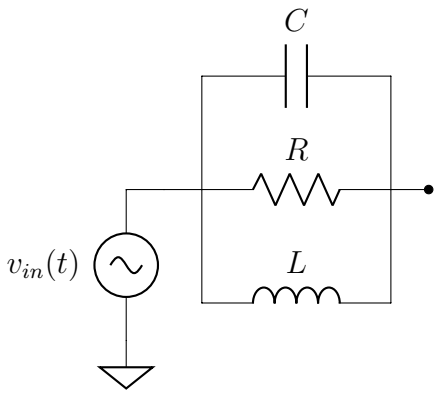

Figure 2.16: Antenna equilvaent circuit

It is important to underline that this approximation is valid just for a small range around the resonance frequency.

2.1.3 Simulations

The *Istituto superiore Mario Boella* (ISMB) provided a Matlab code to design patch antennas: it allows to get the physical dimensions and the transmission line parameters of a patch providing as input:

- the central frequency f_0;
- the dielectric height h;
- the dielectric constant ε_r.

Furthermore it allowed to choose the kind of feeding (microstrip or probe) and the design metrics (squared patch or fixed W).
The results obtained from this code were used to get the equivalent circuit discussed in chapters 2.1.1 and 2.1.2. To this aim, two additional parameters must be used:

- antenna gain G;
- distance from the antenna r;

The first step was the choice of the substrate that is quite important, since the correct value of the dielectric coefficient allows to get the resonance matching and the circuit may work. Several metrics may be used for the choice of the most

appropriate substrate, depending on the costs and the availability of the material. For the project it was opted for the substrate ROHACELL. In the the table 2.1 the main electric characteristics are reported:

Propriety	Frequency [GHz]	ROHACELL 31 HF	ROHACELL 51 HF	ROHACELL 71 HF
Dielectric Constant	2.5	1.050	1.057	1.075
	5	1.043	1.065	1.106
	10	1.046	1.067	1.093
	26.5	1.041	1.048	1.093
Loss Tangent	2.5	<0.0002	<0.0002	<0.0002
	5	0.0016	0.0008	0.0016
	10	0.0017	0.0041	0.0038
	26.5	0.0106	0.0135	0.0155

Table 2.1: Electrical Properties of ROHACELL HF

Two squared patch probe feed were realized. The design data are reported in the following list:

- a ROHACELL HF 31 substrate with
  - $h = 0.508$ mm
  - $\varepsilon_r = 1.050$
- $f_0 = 868,915$ MHz
- $G = 6$ dB
- $r = 1.5$ mm

In table 2.2 are reported all the transmission line of the patches:

Squared patch (W=L)						
Frequency [MHz]	Width [mm]	Length [mm]	$\varepsilon_{r_{eff}}$	R_{edge} [Ω]	C_F [µF]	Z_∞ [Ω]
868	163.185	163.185	1.0474	201.583	1.0506	8.2433
915	154.530	154.530	1.0473	202.294	0.9942	8.6704

Table 2.2: Patches - transmission line parameterss

For each patch, two versions were realized changing the feeding point (using the edges as reference coordinate) in order to obtain two different input impedances:

- a 50 Ω input impedance, in order to be attached to others rectenna kit already presents on the market;

- a maximum radiation resistance. In this case the feeding was placed at a small distance from the edge for feasibility reasons. The frequency responses are shown in figure 2.17 and 2.18 in which there is the comparison between the transmission line and the equivalent circuit frequency responses:

In table 2.3 are reported the circuit parameters of each patch antenna:

Square patch (W=L)				
Frequency [MHz]	Feeding position [mm]	R_{res} [Ω]	L_{res} [pH]	C_{res} [pF]
868	54	50.152	245.153	137.140
	2	200.010	980.075	34.304
915	50	51.856	253.097	119.540
	2	200.804	982.662	30.789

Table 2.3: Patches - circuit parameters

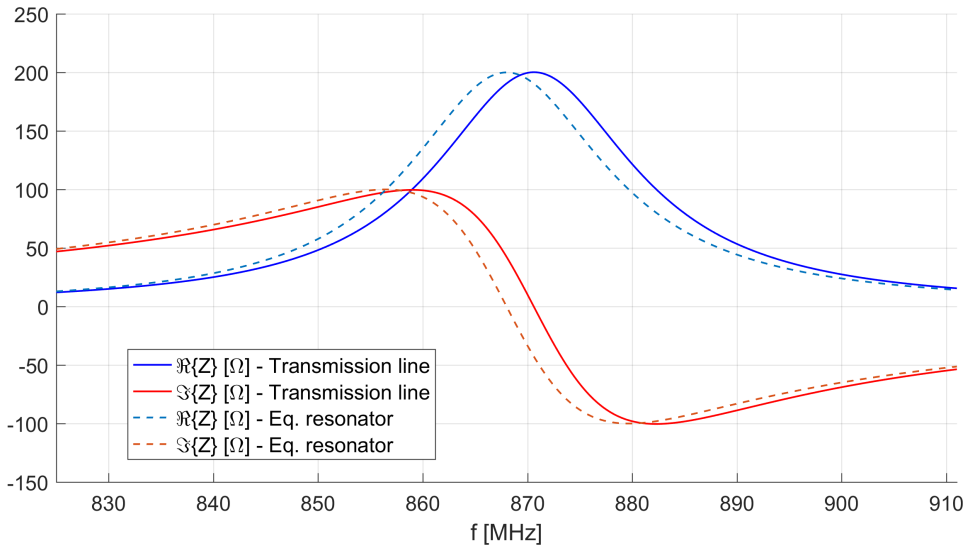

Figure 2.17: 868 MHz patch frequency response comparison

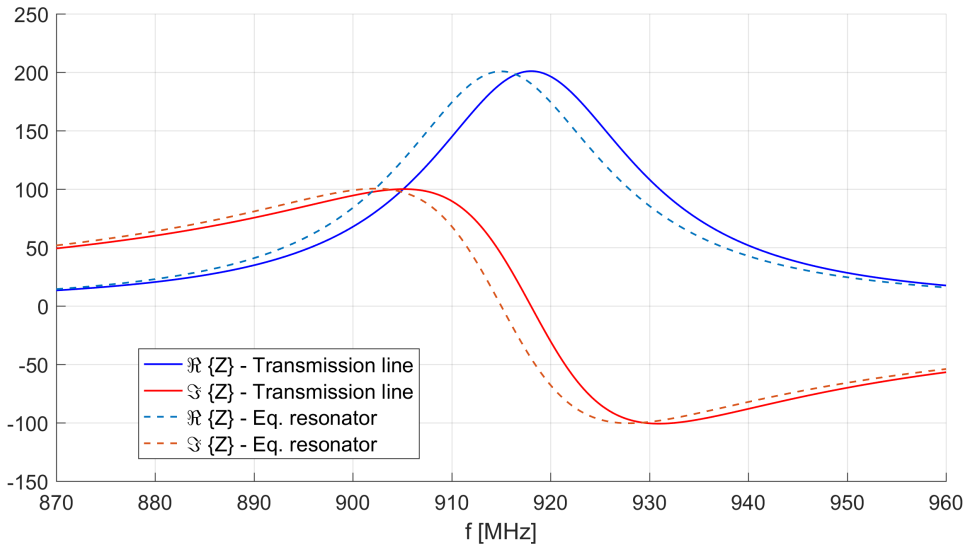

Figure 2.18: 915 MHz patch frequency response comparison

2.2 Rectifier

Electronics circuits require to be supplied a constant voltage. So the received power from the antenna must be converted from AC to DC. The circuits that perform this conversion are called *rectifiers*. These devices are based on diodes, that are nonlinear devices, and capacitors, that are storage elements, in order to demodulate the AC input voltage.
The first step is is the topology choice. There are many circuits that can be used as rectifiers rectifiers. The simplest example is the half-wave rectifier (figure 2.19). Moreover, since the power involved are quite low, there are circuits that performs the rectification plus a little boost of the input voltage (figure 2.20, 2.21 and 2.22).

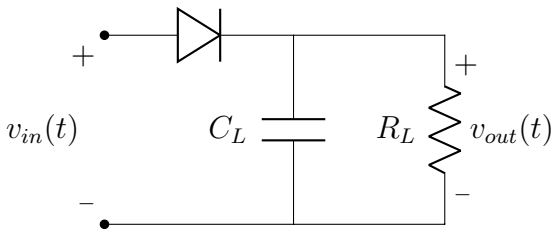

Figure 2.19: Half-wave rectifier

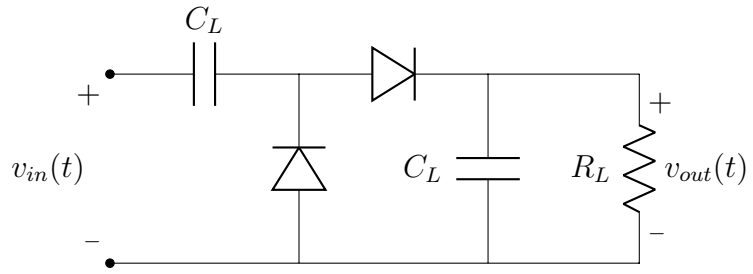

Figure 2.20: Single-stage voltage multiplier

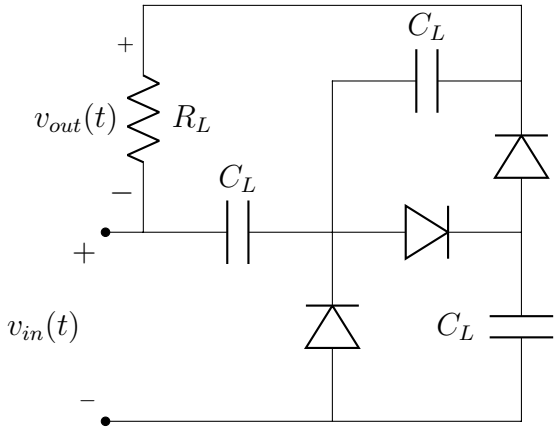

Figure 2.21: Greinacher charge pump

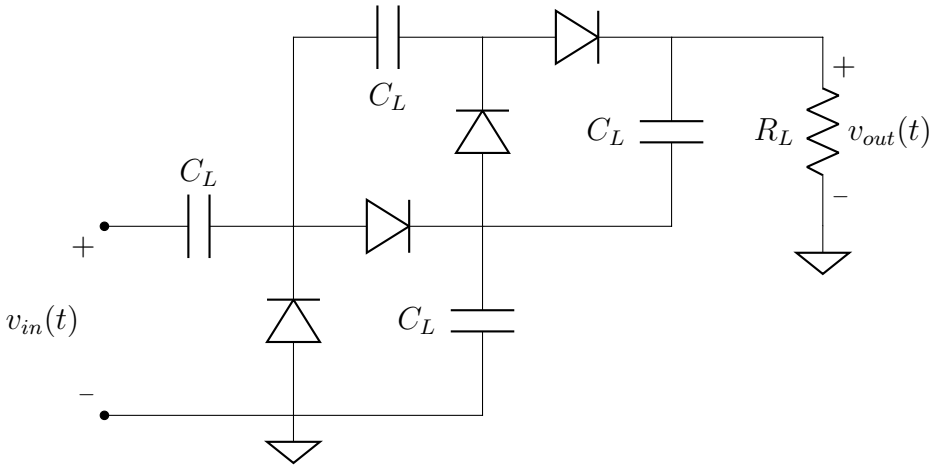

Figure 2.22: Dickson charge pump

The power conversion efficiency is defined as:

$$\nu = \frac{P_{dc}}{P_{in}}$$

where:

- P_{in} is the RF input power collected by the antenna;
- P_{dc} is the DC power of the load resistor.

Once $v_{out}(t)$ is solved numerically, P_{dc} can be evaluated as:

$$P_{dc} = \frac{\left(\frac{1}{T}\int_0^T v_{out}(t)\,dt\right)^2}{R_L}$$

In [2] it was been analyzed that all the multiple-stages rectifiers produces a higher output voltage but the power conversion efficiency is maximum in the half-wave rectifier, independently on the frequency, due to the fact that the losses due to the voltage are minimized since just many components are presents. For this reason this topology will be used for this point on. The second step is the components choice:

- the diode must have a very fast switching time due to the high frequency operation and small device parasitics, especially the junction resistance R_j that dissipates power in the semiconductor witch consequently reduction on the conversion efficiency. Another important aspect that must be considered is the harmonic generation: the non-linearity of the diode will generates harmonics from the incident power, that corresponds to less DC power generated. The best choice, accordingly on this kind of project, are the Schottky diodes because the metal-semiconductor junctions allows fast operations and limited voltage drops. In particular the choice for this design falls upon the HSMS-286x diode by Avago Technologies. The main parameters are reported in table 2.4:

Parameter	Units	Value
BV	[V]	7.0
C_{J0}	[pF]	0.18
E_G	[eV]	$1 \cdot 10^{-5}$
I_{BV}	[A]	$5 \cdot 10^{-8}$
N		1.08
R_S	[Ω]	6
$P_B(VJ)$	[V]	0.65
$P_T(XTI)$		2
M		0.5

Table 2.4: SPICE parameters of HSMS-286x diode

Considering the current range, from the datasheet, the threshold voltage assumes values from 1.5 V to 2.5V;

- the rectifier capacitor is a AQ series of AVX, that is optimized for RF/ Microwave applications typically ranging from 10 MHz to 4.2 GHz;

Chapter 3

Theoretical analysis

Starting from all the discussion done in chapter 2, it is possible to get the rectenna connecting the antenna equivalent circuit to the half wave rectifier. The result is shown in figure 3.1.

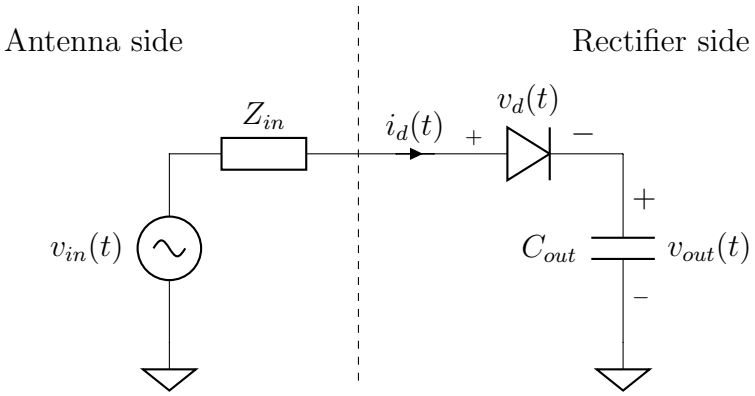

Figure 3.1: Rectenna generic circuit

- the antenna is modeled as a single tone voltage generator with amplitude $\hat{V}_{in}$ and frequency f connected in series to the antenna impedance Z_{in};
- the rectifier circuit consists in a diode in series to a capacitor C, both of them assumed ideals;
- the load is a capacitor. Since it assumed to be much bigger than the one present in the rectifier, just a single capacitor is considered in the schematic.

Initially the antenna impedance is modeled just as a resistance and successively by a parallel RLC resonator. The purpose is to evaluate the impact of the antenna impedance in the charge of the output capacitor. The most difficult element to

treat in the analysis is the diode, since it is a non-linear device. So the fist point consists to define a proper characteristic to model the diode.

Piece-wise linear characteristic

A possible way to represent the diode is through a linear piece-wise (PWL) characteristic (figure 3.2):

$$\begin{cases} v_d > V_{on} \text{ (diode ON)} \;\rightarrow\; i_d = \dfrac{v_d - V_{on}}{R_{on}} \\ \\ v_d < V_{on} \text{ (diode OFF)} \;\rightarrow\; i_d = \dfrac{v_d}{R_{off}} \end{cases} \tag{3.1}$$

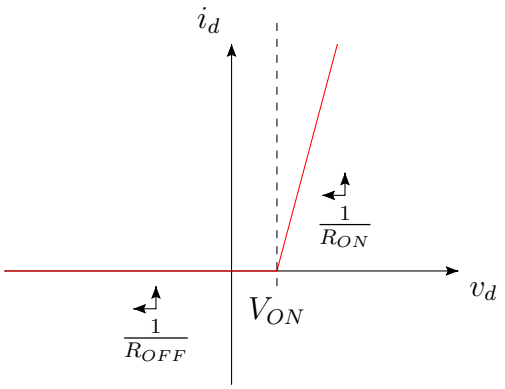

Figure 3.2: Diode piece-wise characteristic

In this case in each region the device can be considered as a combination of linear components and so a closed analytic solution can be obtained [7].

Shockley characteristic

Another way to model the diode, more realistic, is through a Shockley equation, in which the voltage-current relation is exponential (figure 3.3):

$$i_d(t) = I_s \left(e^{\frac{v_d(t)}{\eta V_t}} - 1 \right) \tag{3.2}$$

where:

- I_s is the reverse saturation current;
- $V_t = \dfrac{k_b T}{q}$ is the equivalent thermal voltage:

  - k_b is the Boltzmann's constant;
  - q is the charge of an electron;
  - T is the absolute temperature;
- η is the diode emission coefficient.

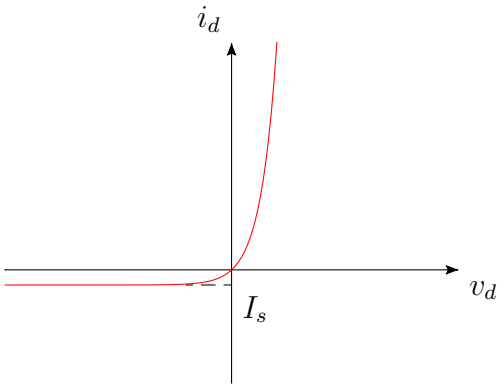

Figure 3.3: Diode exponential characteristic

With this relation the element is non-linear consequently an analytic closed solution cannot be found.

3.1 Simplified circuit

As first approximation, the antenna impedance is assumed purely resistive (figure 3.4).

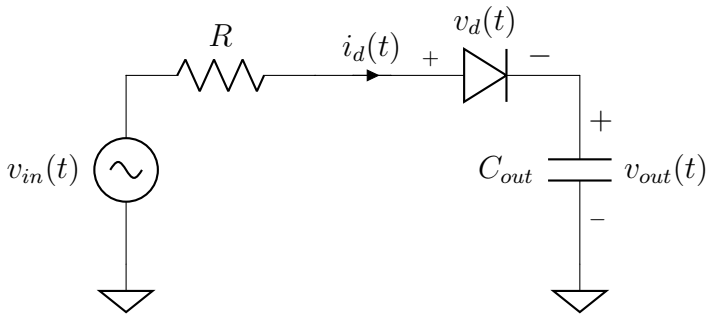

Figure 3.4: Rectenna simplified circuit

This circuit is a first order circuit since there is just an element with memory. In the following, it is analyzed modeling the diode with both diode characteristics.

3.1.1 PWL diode

The circuit must be analyzed during each phase:

- during the ON-phase the diode can be considered as a small resistance connected in series to a DC voltage source (figure 3.5);
- during the OFF-phase the diode can be considered just as a big resistance (figure 3.6).

In both cases the system is a first order system. Then the solution will be a combination of the two solutions.

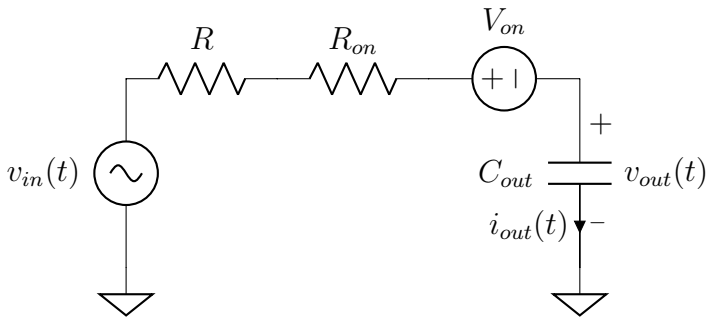

Figure 3.5: ON-phase circuit

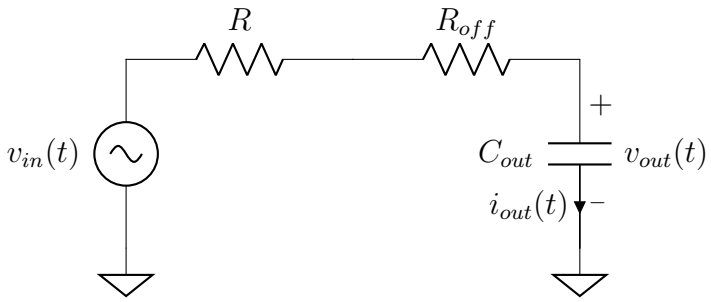

Figure 3.6: OFF-phase circuit

ON-Phase

The mesh circuit equations are the followings:

$$\begin{cases} v_{in}(t) = (R + R_{on}) \cdot i_{out}(t) + V_{on} + v_{out}(t) \\ \\ i_{out}(t) = C_{out} \dfrac{\mathrm{d}v_{out}(t)}{\mathrm{d}t} \end{cases} \tag{3.3}$$

For a more simple formulation, by calling:

$$\frac{\mathrm{d}v_{out}(t)}{\mathrm{d}t} = \dot{v_{out}}(t)$$
$$\tau_{on} = (R + R_{on}) \cdot C_{out}$$

the expression 3.3 can be rewritten as:

$$\dot{v_{out}}(t) + \frac{v_{out}(t)}{\tau_{on}} = \frac{v_{in}(t) - V_{on}}{\tau_{on}} \tag{3.4}$$

The solution of this differential equation, considering $v_{in}(t) = \hat{V}_{in}\sin(2\omega t)$, is:

$$v_{out_{on}}(t) = v_{tran}(t) + v_{\infty}(t) \tag{3.5}$$

where:

$$v_{tran}(t) = \left\{ v_{out}(t_0) + \frac{\hat{V}_{in}}{\omega^2 + 1/\tau_{on}^2}\left[\omega\cos(\omega t_0) + \frac{\sin(\omega t_0)}{\tau_{on}}\right] + V_{on} \right\} \cdot e^{\frac{t_0 - t}{\tau_{on}}} - V_{on}$$

$$v_{\infty}(t) = -\frac{\hat{V}_{in}}{\omega^2 + 1/\tau_{on}^2} \cdot \left[\omega\cos(\omega t) + \frac{\sin(\omega t)}{\tau_{on}}\right]$$

OFF-Phase

In this case, the mesh circuit equations are the followings:

$$\begin{cases} v_{in}(t) = (R + R_{off}) \cdot i_{out}(t) + v_{out}(t) \\ \\ i_{out}(t) = C_{out}\dfrac{\mathrm{d}v_{out}(t)}{\mathrm{d}t} \end{cases} \tag{3.6}$$

Similarly to the previous case, by calling:

$$\frac{\mathrm{d}v_{out}(t)}{\mathrm{d}t} = \dot{v_{out}}(t)$$
$$\tau_{off} = (R + R_{off}) \cdot C_{out}$$

the previous expression can be rewritten as:

$$\dot{v_{out}}(t) + \frac{v_{out}(t)}{\tau_{off}} = \frac{v_{in}(t)}{\tau_{off}} \tag{3.7}$$

Again, the solution of this differential equation gives out this result:

$$v_{out_{off}}(t) = v_{tran}(t) + v_{\infty}(t) \tag{3.8}$$

where:

$$v_{tran}(t) = v_{out}(t_0) \cdot e^{\frac{t_0 - t}{\tau_{off}}} + \frac{\hat{V}_{in}}{\omega^2 + 1/\tau_{off}^2} \cdot e^{\frac{t_0 - t}{\tau_{off}}}\left[\omega\cos(\omega t_0) + \frac{\sin(\omega t_0)}{\tau_{off}}\right]$$

$$v_{\infty}(t) = -\frac{\hat{V}_{in}}{\omega^2 + 1/\tau_{off}^2} \cdot \left[\omega\cos(\omega t) + \frac{\sin(\omega t)}{\tau_{off}}\right]$$

Algorithm

Once that all the equations for each phase are known it is possible to evaluate the charge of the output capacitor through a Matlab code: assuming the capacitor initially discharged, the diode is initially OFF and the corresponding equation is used. Than v_d can be written as:

$$v_{d_{off}}(t) = [v_{in}(t) - v_{out}(t)] \cdot \frac{R_{off}}{R + R_{off}}$$

During the first half of a period $v_{in}(t)$ increases while $v_{out}(t)$ stays quite constant. It is possible to evaluate numerically the time instant t_0 in which $v_d(t) = V_{on}$. From this time on the diode switched-ON and so both the diode equivalent model and the output voltage's equation changes:

$$v_{d_{on}}(t) = [v_{in}(t) - v_{out}(t)] \cdot \frac{R_{on}}{R + R_{on}} + V_{on} \cdot \frac{R}{R + R_{on}}$$

The new initial condition corresponds to the final voltage reached in the previous phase $v_{start} = v_{out}(t_0)$. Again it is possible to evaluate the time in which $v_d(t)$ intercept V_{on} and consequently the diode switched-OFF and so the process continue until the capacitor completely charges. The pseudocode is reported as following (appendix A.1):

Pseudocode for PWL diode (simplified)		
1:	set initial condition:	$v_{start} = 0$
2:	set initial time:	$t_{start} = 0$
3:	start a cycle	for $t = 0$ to T_{sim} do:
4:	use OFF-Phase equations:	$v_{out}(t) = v_{out_{OFF}}(t)$
5:	solve the equation:	$v_{d_{off}} = V_{on} \ \rightarrow \ t = t_0$
6:	set new initial time:	$t_{start} = t_0$
7:	set new initial condition:	$v_{start} = v_{out}(t_0)$
8:	use ON-Phase equations:	$v_{out}(t) = v_{out_{ON}}(t)$
9:	solve the equation:	$v_{d_{on}}(t) = V_{on} \ \rightarrow \ t = t_0$
10:	simulation end	end for

3.1.2 Shockley diode

In this case the circuit cannot be subdivided anymore in two sub-circuits. The Kirchhoff's laws are:

$$\begin{cases} v_{in}(t) = Ri_d(t) + v_d(t) + v_{out}(t) \\ i_d(t) = i_{out}(t) \end{cases} \tag{3.9}$$

and the following constitutive relations are valid:

$$i_d(t) = I_s \left(e^{\frac{v_d(t)}{\eta V_t}} - 1 \right) \tag{3.10}$$

$$i_{out}(t) = C_{out} \frac{\mathrm{d}v_{out}(t)}{\mathrm{d}t} \tag{3.11}$$

Euler's Method

It possible to study the circuit through a time discrete simulation:

- the fist step consists to subdivide the continuous time in in many time instants ΔT:

  $$t \ \rightarrow \ k \cdot \Delta T \quad k = 1,2,3...$$

  Where ΔT is a fraction of the period T:

  $$\Delta T = \frac{T}{N_{points}}$$

- the second step consists to replace replace the derivative with the incremental ratio:

  $$\frac{\mathrm{d}x(t)}{\mathrm{d}t} \simeq \frac{x(t) - x(t - \Delta T)}{\Delta T}$$

This approach is called *inverse Euler's Method* [8]. It can be demonstrated that this method prevent numeric instability, differently form a *direct Euler's Method*, and for this reason it gives a more accurate solution, moreover if the system is stable, the error is kept limited even increasing the value of k. This method is particularly useful when it is needed to deal with time dependent generators, as in this case. Calling:

$$\begin{aligned} v_{in_k} &= v_{in}(k\Delta T) \\ v_{out_k} &= v_{out}(k\Delta T) \\ v_{d_k} &= v_d(k\Delta T) \end{aligned}$$

It is possible tho write the current equation as:

$$i_{d_k} = \frac{v_{in_k} - v_{d_k} - v_{out_k}}{R} = I_s \left(e^{\frac{v_{d_k}}{\eta V_t}} - 1 \right) \tag{3.12}$$

In each time instant, it is possible to define the increment of $v_d(t)$ and $v_{out}(t)$ as

$$\begin{aligned} \Delta v_d &= v_{d_k} - v_{d_{k-1}} \\ \Delta v_{out} &= v_{out_k} - v_{out_{k-1}} \end{aligned}$$

The equation 3.12 can be rewritten as:

$$\frac{v_{in_k} - (v_{d_{k-1}} + \Delta v_d) - (v_{out_{k-1}} + \Delta v_{out})}{R} = I_s \left(e^{\frac{v_{d_{k-1}}}{\eta V_t}} e^{\frac{\Delta v_d}{\eta V_t}} - 1 \right)$$

By choosing $\Delta T \to 0 \;\Rightarrow\; \Delta V_D \to 0$ it is possible to express the exponential term with a Taylor expansion stopping at the first order:

$$e^{\frac{\Delta v_d}{\eta V_t}} \simeq \left(1 + \frac{\Delta v_d}{\eta V_t} \right)$$

In this way it is possible to write the increment Δv_d in a closed form:

$$\Delta v_d = \frac{v_{in_k} - v_{d_{k-1}} - v_{out_{k-1}} - \Delta v_{out} - RI_s \left(e^{\frac{v_{d_{k-1}}}{\eta V_t}} - 1 \right)}{1 + \frac{I_s R}{\eta V_t} e^{\frac{v_{d_{k-1}}}{\eta V_t}}} \tag{3.13}$$

The next step is to obtain the other increment Δv_{out}:

$$\frac{v_{in_k} - (v_{d_{k-1}} + \Delta v_d) - (v_{out_{k-1}} + \Delta v_{out})}{R} = C_{out} \frac{\Delta v_{out}}{\Delta T}$$

Replacing Δv_d with the previous expression it is possible to get also a closed form of Δv_{out}:

$$\Delta v_{out} = \frac{\left(\frac{v_{in_k} - v_{d_{k-1}} - v_{out_{k-1}}}{\eta V_t} + 1 \right) e^{\frac{v_{d_{k-1}}}{\eta V_t}} - 1}{1 + \frac{I_s R}{\eta V_t} \left(1 + \frac{\Delta T}{R C_{out}} \right) e^{\frac{v_{d_{k-1}}}{\eta V_t}}} \frac{I_s \Delta T}{C_{out}} \tag{3.14}$$

It is possible to notice that for all the time instants:

$$v_{out_k}, v_{d_k} = f(v_{in_k}, v_{out_{k-1}}, v_{d_{k-1}})$$

So the resulting system is the following:

$$\begin{cases} \Delta v_{out} = \dfrac{\left(\frac{v_{in_k} - v_{d_{k-1}} - v_{out_{k-1}}}{\eta V_t} + 1 \right) e^{\frac{v_{d_{k-1}}}{\eta V_t}} - 1}{1 + \frac{I_s R}{\eta V_t} \left(1 + \frac{\Delta T}{R C_{out}} \right) e^{\frac{v_{d_{k-1}}}{\eta V_t}}} \frac{I_s \Delta T}{C_{out}} \\ \Delta v_d = \dfrac{v_{in_k} - v_{d_{k-1}} - v_{out_{k-1}} - \Delta v_{out} - RI_s \left(e^{\frac{v_{d_{k-1}}}{\eta V_t}} - 1 \right)}{1 + \frac{I_s R}{\eta V_t} e^{\frac{v_{d_{k-1}}}{\eta V_t}}} \\ v_{out_k} = v_{out_{k-1}} + \Delta v_{out} \\ v_{d_k} = v_{d_{k-1}} + \Delta v_d \end{cases} \tag{3.15}$$

If $\Delta T \rightarrow 0$ the series of v_{out_k} and v_{d_k} converges to the exact solution of the equation 3.11. A Matlab code can be implemented to solve the system 3.15 (appendix A.2:

Pseudocode for Shockley diode (simplified)		
1:	set initial condition:	$v_{out_{k-1}} = 0$ $v_{d_{k-1}} = 0$
2:	start a cycle:	for $k = 0$ to k_{max} do:
3:	evaluate the increments :	$\Delta v_{out} = f(v_{in_k}, v_{out_{k-1}}, v_{d_{k-1}})$ $\Delta v_d = f(v_{in_k}, v_{out_{k-1}}, v_{d_{k-1}}, \Delta v_{out})$
4:	evaluate the nonlinear variables:	$v_{out_k} = v_{out_{k-1}} + \Delta v_{out}$ $v_{d_k} = v_{d_{k-1}} + \Delta v_d$
5:	simulation end:	end for

3.2 Complete circuit analysis

The next step consist to replace the resistance by the resonator derived in chapter 2.1.2. The circuit is shown in figure 3.7.

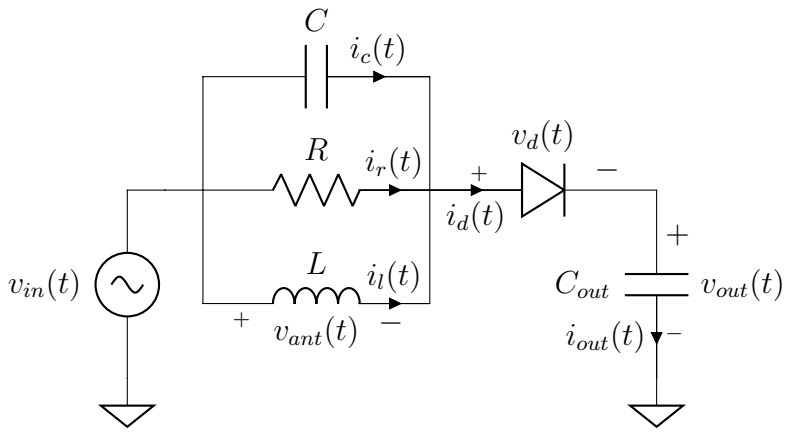

Figure 3.7: Rectenna complete circuit

The resonator that adds two new state variables as consequence the circuit becomes a third order circuit. In this case Kirchhoff's laws are:

$$\begin{cases} v_{in}(t) & = v_{ant}(t) + v_d(t) + v_{out}(t) \\ i_d(t) & = i_r(t) + i_c(t) + i_l(t) \end{cases} \tag{3.16}$$

and the constitutive relations are:

$$i_{out}(t) = C_{out}\frac{\mathrm{d}v_{out}(t)}{\mathrm{d}t} \tag{3.17}$$

$$i_r(t) = \frac{v_{ant}(t)}{R} \tag{3.18}$$

$$i_c(t) = C\frac{\mathrm{d}v_{ant}(t)}{\mathrm{d}t} \tag{3.19}$$

$$i_l(t) = \int_0^t \frac{v_{ant}(t)}{L}\mathrm{d}t \tag{3.20}$$

Again the circuit is solved by modeling the diode by both piece-wise linear and exponential equation.

3.2.1 PWL diode

Similarly to the simplified version, the circuit was analyzed during each phase:

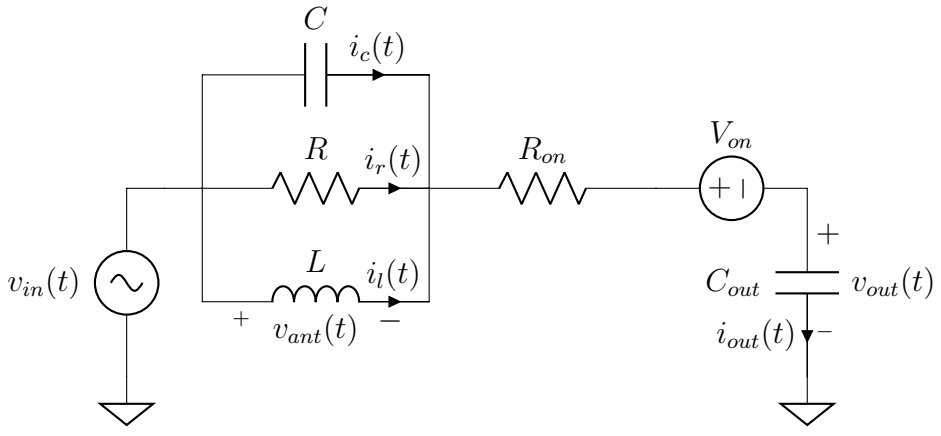

Figure 3.8: ON-Phase circuit

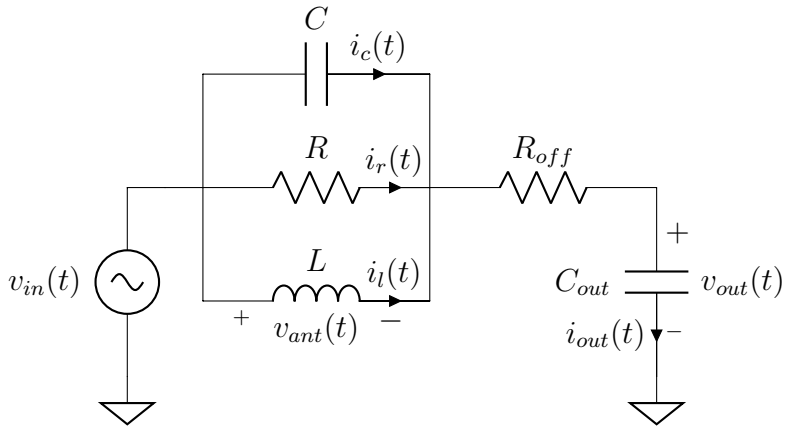

Figure 3.9: OFF-Phase circuit

ON-phase

All the equations of the circuit can be rewritten in a more compact matrix form:

$$\dot{\mathbf{x}}(t) = \mathbf{A_{on}}\mathbf{x}(t) + \mathbf{b_{on}}u_{on}(t) \tag{3.21}$$

where:

$$\mathbf{x}(t) = \begin{bmatrix} v_c(t) \\ v_{out}(t) \\ i_l(t) \end{bmatrix} \quad \Rightarrow \quad \dot{\mathbf{x}}(t) = \begin{bmatrix} \dot{v_c}(t) \\ \dot{v_{out}}(t) \\ \dot{i_l}(t) \end{bmatrix}$$

$$\mathbf{A_{on}} = \begin{bmatrix} -\frac{1}{C}\left(\frac{1}{R} + \frac{1}{R_{on}}\right) & -\frac{1}{CR_{on}} & -\frac{1}{C} \\ -\frac{1}{C_{out}R_{on}} & -\frac{1}{C_{out}R_{on}} & 0 \\ \frac{1}{L} & 0 & 0 \end{bmatrix}$$

$$\mathbf{b_{on}} = \begin{bmatrix} -\frac{1}{CR_{on}} \\ -\frac{1}{C_{out}R_{on}} \\ 0 \end{bmatrix}$$

$$u_{on}(t) = \hat{V}_{in}\sin(\omega t) - V_{on}$$

This system can be transformed in a diagonal system in order to be solved more simply.

$$\mathbf{V^T A_{on} V} = \mathbf{\Lambda_{on}} \quad \rightarrow \quad \mathbf{\Lambda_{on}} = \begin{bmatrix} s_{11}^{on} & 0 & 0 \\ 0 & s_{22}^{on} & 0 \\ 0 & 0 & s_{33}^{on} \end{bmatrix}$$

where s_{ii}^{on} are the eigenvalues of the matrix $\mathbf{A_{on}}$. Then multiplying both terms of the equation 3.21 by $\mathbf{V^T}$:

$$\underbrace{\mathbf{V^T}\dot{\mathbf{x}}(t)}_{\dot{\boldsymbol{\xi}}(t)} = \mathbf{\Lambda_{on}}\underbrace{\mathbf{V^T}\mathbf{x}(t)}_{\boldsymbol{\xi}(t)} + \underbrace{\mathbf{V^T b_{on}}}_{\boldsymbol{\beta_{on}}}u_{on}(t)$$

it is possible to get an equivalent diagonal system that is easier to solve:

$$\dot{\boldsymbol{\xi}}(t) = \boldsymbol{\Lambda}_{\mathbf{on}}\boldsymbol{\xi}(t) + \boldsymbol{\beta}_{\boldsymbol{on}} u_{on}(t) \tag{3.22}$$

Each row of this system is a first order linear differential equation that can be solved as:

$$\xi_{ii}^{on}(t) = \underbrace{\xi_0 e^{s_{ii}^{on}(t-t_0)}}_{\xi_h(t)} + \underbrace{e^{s_{ii}^{on}t}\int_{t_0}^{t} e^{s_{ii}^{on}\tau}\beta_i u_{on_i}\mathrm{d}\tau}_{\xi_f(t)} \tag{3.23}$$

that is composed by a homogeneous solution $\xi_f(t)$, that depends on the initial conditions

$$\boldsymbol{\xi_0} = \mathbf{V^T x_0}$$

plus a forced solution $\xi_f(t)$ that depends on the input signal. In this case the input is:

$$u_{on}(t) = v_{in}(t) + V_{on}$$

so the corresponding forced solution becomes:

$$\xi_f(t) = \xi_f^{v_{in}}(t) + \xi_f^{V_{on}}(t)$$

where

$$\xi_f^{v_{in}}(t) = \hat{V}_{in} K\left[(\omega\cos(\omega t_0) + s_{ii}^{on}\sin(\omega t_0))\, e^{s_{ii}^{on}(t-t_0)} - (\omega\cos(\omega t) + s_{ii}^{on}\sin(\omega t))\right]$$
$$\xi_f^{V_{on}}(t) = V_{on}\frac{\beta_i}{s_{ii}^{on}}\left[1 - e^{s_{ii}^{on}(t-t_0)}\right]$$

with:

$$K = \frac{\beta_i\omega}{\omega^2 + s_{ii}^{on2}}$$

Then it is needed to move back to the original state variables:

$$x_k(t) = \sum_{j=1}^{3} V_{jk}\xi_j^{on}((t) \quad k = 1{,}2{,}3$$

$$\begin{cases} v_{ant_{ON}}(t) & = V_{11}\xi_1^{on}(t) + V_{12}\xi_2^{on}(t) + V_{13}\xi_3^{on}(t) \\ v_{out_{ON}}(t) & = V_{21}\xi_1^{on}(t) + V_{22}\xi_2^{on}(t) + V_{23}\xi_3^{on}(t) \\ i_{l_{ON}}(t) & = V_{31}\xi_1^{on}(t) + V_{32}\xi_2^{on}(t) + V_{33}\xi_3^{on}(t) \end{cases} \tag{3.24}$$

OFF-phase

Similarly a matrix form of the circuit equation is defined:

$$\dot{\mathbf{x}}(t) = \mathbf{A_{off}}\mathbf{x}(t) + \mathbf{b_{off}}u_{off}(t) \tag{3.25}$$

where:

$$\mathbf{x}(t) = \begin{bmatrix} v_c(t) \\ v_{out}(t) \\ i_l(t) \end{bmatrix} \quad \Rightarrow \quad \dot{\mathbf{x}}(t) = \begin{bmatrix} \dot{v_c}(t) \\ \dot{v_{out}}(t) \\ \dot{i_l}(t) \end{bmatrix}$$

$$\mathbf{A_{off}} = \begin{bmatrix} -\frac{1}{C}\left(\frac{1}{R} + \frac{1}{R_{off}}\right) & -\frac{1}{CR_{off}} & -\frac{1}{C} \\ -\frac{1}{C_{out}R_{off}} & -\frac{1}{C_{out}R_{off}} & 0 \\ \frac{1}{L} & 0 & 0 \end{bmatrix}$$

$$\mathbf{b_{off}} = \begin{bmatrix} -\frac{1}{CR_{off}} \\ -\frac{1}{C_{out}R_{off}} \\ 0 \end{bmatrix}$$

$$u_{off}(t) = \hat{V}_{in}\sin(\omega t)$$

Again the system is transformed in a diagonal system in order to be solved more simply.

$$\mathbf{V^T A_{off} V} = \mathbf{\Lambda_{off}} \quad \rightarrow \quad \mathbf{\Lambda_{off}} = \begin{bmatrix} s_{11}^{off} & 0 & 0 \\ 0 & s_{22}^{off} & 0 \\ 0 & 0 & s_{33}^{off} \end{bmatrix}$$

where s_{ii}^{off} are the eigenvalues of the matrix $\mathbf{A_{off}}$. Then it is possible to get an equivalent diagonal system that is easier to solve:

$$\dot{\boldsymbol{\xi}}(t) = \mathbf{\Lambda_{off}}\boldsymbol{\xi}(t) + \boldsymbol{\beta_{off}}u_{off}(t) \tag{3.26}$$

Each row of this system is a first order linear differential equation that can be solved as:

$$\xi_{ii}^{off}(t) = \underbrace{\xi_0 e^{s_{ii}^{off}(t-t_0)}}_{\xi_h(t)} + \underbrace{e^{s_{ii}^{off}t}\int_{t_0}^{t} e^{s_{ii}^{off}\tau}\beta_i u_{off_i}\mathrm{d}\tau}_{\xi_f(t)} \tag{3.27}$$

The solution is almost equal to the on-phase with the only difference of the forced solution since in this case the input is just:

$$u_{off}(t) = \hat{V}_{in}\sin(\omega\tau)$$

so the corresponding forced solution becomes:

$$\xi_f(t) = \hat{V}_{in}Q\left[\left(\omega\cos(\omega t_0) + s_{ii}^{off}\sin(\omega t_0)\right)e^{s_{ii}^{off}(t-t_0)} - \left(\omega\cos(\omega t) + s_{ii}^{off}\sin(\omega t)\right)\right]$$

with:

$$Q = \frac{\beta_i \omega}{\omega^2 + s_{ii}^{off\,2}}$$

Then it is needed to move back to the original state variables:

$$x_k(t) = \sum_{j=1}^{3} V_{jk} \xi_j^{off}(t) \quad k = 1,2,3$$

$$\begin{cases} v_{out_{OFF}}(t) & = V_{11}\xi_1^{off}(t) + V_{12}\xi_2^{off}(t) + V_{13}\xi_3^{off}(t) \\ v_{out_{OFF}} & = V_{21}\xi_1^{off}(t) + V_{22}\xi_2^{off}(t) + V_{23}\xi_3^{off}(t) \\ i_{l_{OFF}}(t) & = V_{31}\xi_1^{off}(t) + V_{32}\xi_2^{off}(t) + V_{33}\xi_3^{off}(t) \end{cases} \tag{3.28}$$

Algorithm

It is possible to evaluate the charge of the output capacitor through a Matlab code similarly to the simplified circuit: assuming the capacitor initially discharged, the diode is initially OFF and the corresponding equation is used. The main difference with respect the simplified circuit is that the expression of $v_d(t)$ is the same for both phases:

$$v_d(t) = v_{in}(t) - v_{ant}(t) - v_{out}(t)$$

The difference is in the evolution of $v_{ant}(t)$,v_{out} and $i_l(t)$ during each of them. Again it is possible to evaluate numerically the time instant t_0 in which $v_d(t) = V_{on}$ so all the state variable at this time instant becomes the new initial conditions for the next phase:

$$\begin{aligned} v_{ant_{start}} &= v_{ant}(t_0) \\ v_{out_{start}} &= v_{out}(t_0) \\ i_{l_{start}} &= i_l(t_0) \end{aligned}$$

From this time on the diode switched-ON and the process continue until the capacitor completely charges. The pseudocode is reported as following (appendix A.3:

Pseudocode for PWL diode (complete)		
1:	set initial condition:	$\begin{cases} v_{ant_{start}} & = 0 \\ v_{out_{start}} & = 0 \\ i_{l_{start}} & = 0 \end{cases}$
2:	set initial time:	$t_{start} = 0$
3:	start a cycle	for $t = 0$ to T_{sim} do:
4:	use OFF-Phase equations:	$\begin{cases} v_{ant_{start}} & = v_{ant_{OFF}} \\ v_{out_{start}} & = v_{out_{OFF}} \\ i_{l_{start}} & = i_{l_{OFF}} \end{cases}$
5:	solve the equation:	$v_d(t) = V_{on} \rightarrow t = t_0$
6:	set new initial time:	$t_{start} = t_0$
7:	set new initial condition:	$\begin{cases} v_{ant_{start}} & = v_{ant}(t_0) \\ v_{out_{start}} & = v_{out}(t_0) \\ i_{l_{start}} & = i_l(t_0) \end{cases}$
8:	use ON-Phase equations:	$\begin{cases} v_{ant_{start}} & = v_{ant_{ON}} \\ v_{out_{start}} & = v_{out_{ON}} \\ i_{l_{start}} & = i_{l_{ON}} \end{cases}$
9:	solve the equation:	$v_d(t) = V_{on} \rightarrow t = t_0$
10:	simulation end	end for

3.2.2 Shockley diode

Again, it is possible to use the Euler approach. The first step consists to define the discrete voltages:

$$\begin{aligned} v_{in_k} &= v_{in}(k\Delta T) \\ v_{out_k} &= v_{out}(k\Delta T) \\ v_{d_k} &= v_d(k\Delta T) \end{aligned}$$

and defining the voltage increments as:

$$\begin{aligned} \Delta v_{in} &= v_{in_k} - v_{in_{k-1}} \\ \Delta v_{out} &= v_{out_k} - v_{out_{k-1}} \\ \Delta v_d &= v_{d_k} - v_{d_{k-1}} \end{aligned}$$

where Δv_{in} is notice and Δv_{out} and Δv_d are unknown. All the current are considered constant during each time step, so starting from the equation 3.16:

$$i_{d_k} = i_{r_k} + i_{c_k} + i_{l_k} \tag{3.29}$$

The left hand side can be written as:

$$i_{d_k} = I_s \left(e^{\frac{v_{d_{k-1}} + \Delta v_d}{\eta V_t}} - 1 \right) \simeq I_s \left[e^{\frac{v_{d_{k-1}}}{\eta V_t}} \left(1 + \frac{\Delta v_d}{\eta V_t} \right) - 1 \right]$$

The right hand side becomes:

$$\begin{aligned} i_{r_k} &= \frac{v_{ant_{k-1}}}{R} + \frac{\Delta v_{in} - \Delta v_{out} - \Delta v_d}{R} \\ i_{c_k} &= \frac{C}{\Delta T} \left(\Delta v_{in} - \Delta v_{out} - \Delta v_d \right) \\ i_{l_k} &= i_{l_{k-1}} \end{aligned}$$

where $v_{ant_{k-1}}$ is:

$$v_{ant_{k-1}} = v_{in_{k-1}} - v_{d_{k-1}} - v_{out_{k-1}}$$

The expression 3.29 can be rewritten as:

$$I_s \left[e^{\frac{v_{d_{k-1}}}{\eta V_t}} \left(1 + \frac{\Delta v_d}{\eta V_t} \right) - 1 \right] = \frac{v_{ant_{k-1}}}{R} + \left(\frac{1}{R} + \frac{C}{\Delta T} \right) \left(\Delta v_{in} - \Delta v_{out} - \Delta v_d \right) + i_{l_{k-1}}$$

This result can be rewritten in order to get the increment Δv_d:

$$\Delta v_d = \frac{\frac{v_{ant_{k-1}}}{R} + \left(\frac{1}{R} + \frac{C}{\Delta T} \right) \left(\Delta v_{in} - \Delta v_{out} \right) + i_{l_{k-1}} - I_s \left(e^{\frac{v_{d_{k-1}}}{\eta V_t}} - 1 \right)}{\frac{1}{R} + \frac{C}{\Delta T} + \frac{I_s}{\eta V_t} e^{\frac{v_{d_{k-1}}}{\eta V_t}}} \tag{3.30}$$

Calling:

$$\begin{aligned} Y &= \frac{1}{R} + \frac{C}{\Delta T} \\ Y_d &= \frac{1}{R} + \frac{C}{\Delta T} + \frac{I_s}{\eta V_t} e^{\frac{v_{d_{k-1}}}{\eta V_t}} \\ i_{d_{k-1}} &= I_s \left(e^{\frac{v_{d_{k-1}}}{\eta V_t}} - 1 \right) \end{aligned}$$

it is possible to rewrite the expression 3.30 in the more compact form:

$$\Delta v_d = \frac{1}{Y_d} \left[\frac{v_{ant_{k-1}}}{R} + Y \left(\Delta v_{in} - \Delta v_{out} \right) + i_{l_{k-1}} - i_{d_{k-1}} \right] \tag{3.31}$$

The next step consists to consider the output voltage variation variation:

$$\frac{v_{ant_{k-1}}}{R} + Y \left(\Delta v_{in} - \Delta v_{out} - \Delta v_d \right) + i_{l_{k-1}} = C_{out} \frac{\Delta v_{out}}{\Delta T}$$

By replacing the result 3.31 in this expression it is possible to get:

$$\Delta v_{out} = \frac{\left(\frac{v_{ant_{k-1}}}{R} + Y\Delta v_{in} + i_{l_{k-1}}\right)\left(1 - \frac{Y}{Y_d}\right) - i_{d_{k-1}}\frac{Y}{Y_d}}{\frac{C_{out}}{\Delta T} + Y\left(1 - \frac{Y}{Y_d}\right)} \tag{3.32}$$

Then, once both increments are evaluated, it is possible to compute the new value of v_{ant_k}:

$$v_{ant_k} = v_{in_k} - v_{out_k} - v_{d_k} = v_{ant_{k-1}} + \Delta v_{in} - \Delta v_{out} - \Delta v_d$$

so it is possible to evaluate also the new value of i_{l_k}:

$$i_{l_k} = i_{l_{k-1}} + \frac{\Delta T}{L} v_{ant_k} \tag{3.33}$$

So the resulting system is the following:

$$\begin{cases} \Delta v_{in} & = v_{in_k} - v_{in_{k-1}} \\ \Delta v_{out} & = \dfrac{\left(\frac{v_{ant_{k-1}}}{R} + Y\Delta v_{in} + i_{l_{k-1}}\right)\left(1 - \frac{Y}{Y_d}\right) - i_{d_{k-1}}\frac{Y}{Y_d}}{\frac{C_{out}}{\Delta T} + Y\left(1 - \frac{Y}{Y_d}\right)} \\ \Delta v_d & = \dfrac{1}{Y_d}\left[\dfrac{v_{ant_{k-1}}}{R} + Y\left(\Delta v_{in} - \Delta v_{out}\right) + i_{l_{k-1}} - i_{d_{k-1}}\right] \\ v_{out_k} & = v_{out_{k-1}} + \Delta v_{out} \\ v_{d_k} & = v_{d_{k-1}} + \Delta v_d \\ v_{ant_k} & = v_{in_k} - v_{out_k} - v_{d_k} \\ i_{l_k} & = i_{l_{k-1}} + \dfrac{\Delta T}{L} v_{ant_k} \end{cases} \tag{3.34}$$

Again a Matlab code can be implemented to solve the system 3.34 (appendix A.4:

Pseudocode for Shockley diode (complete)		
1:	set initial condition:	$v_{out_{k-1}} = 0$ $v_{c_{k-1}} = 0$ $i_{l_{k-1}} = 0$ $v_{d_{k-1}} = 0$
2:	start a cycle:	for $k = 0$ to k_{max} do:
3:	evaluate the increments:	$\Delta v_{out} = f(v_{in_k}, v_{out_{k-1}}, v_{d_{k-1}})$ $\Delta v_d = f(v_{in_k}, v_{out_{k-1}}, v_{d_{k-1}}, \Delta v_{out})$
4:	evaluate the nonlinear variables:	$v_{out_k} = v_{out_{k-1}} + \Delta v_{out}$ $v_{d_k} = v_{d_{k-1}} + \Delta v_d$ $v_{ant_k} = v_{in_k} - v_{out_k} - v_{d_k}$
5:	evaluate the inductor current:	$i_{l_k} = f(i_{l_{k-1}}, v_{ant_k})$
6:	simulation end:	end for

3.3 Transient simulations

All the algorithms were implemented on Matlab and tested ford for many impedances. An output capacitor not so big is used to get fast simulations. All the settings are reported as following:

- single tone input voltage:

$$v_{in}(t) = \hat{V}_{in} \sin(2\pi f t)$$

  with:

  - $\hat{V}_{in} = 1$ V
  - $f = 868$ MHz;

- $R = 50,\ 100,\ 150,\ 200\ \Omega$
- $C_{out} = 10$ nF
- PWL diode with:
  - $V_{on} = 0.25$ V
  - $R_{on} = 6\ \Omega$
  - $R_{off} = 1\ \text{M}\Omega$
- exponential diode with:
  - $T = 27\ ^\circ\text{C} \quad \rightarrow \quad V_t = 25.8$ mV;
  - $I_s = 80$ nA;

– $\eta = 1.08$.

The patches used are reported in table 3.1:

Squared patch (W=L)			
Design R [Ω]	R_{res} [Ω]	L_{res} [pH]	C_{res} [pF]
50	50.152	245.153	137.140
100	100.341	490.152	68.592
150	150.719	736.685	45.637
200	200.010	980.075	34.304

Table 3.1: Patches parameters

Successively a simulator for analog circuit was used as confront for the proposed algorithms. Many simulators are available. In this case the choice drops on LTspice,va high performance simulation software produced by Linear Technology based on a SPICE (*Simulation Program with Integrated Circuit Emphasis*) simulation engine. This software provides useful and free design simulation tools for analog circuit as well as device models (appendix B.1 and B.2). In figure are reported the circuit schematics:

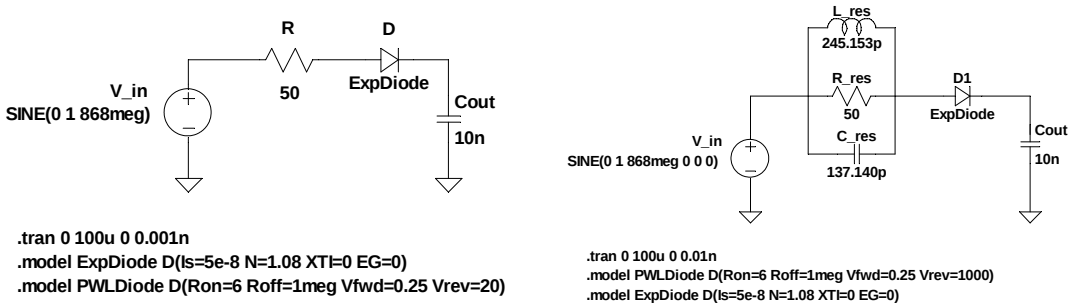

(a) Simplified circuit

(b) Complete circuit

Figure 3.10: LTspice schematic

The simulator allows to choose as integration methods to solve the net equations the modified trapezoidal and the Gear methods. Both of them were used with an absolute tolerance of 10^{-10} and a relative tolerance of 10^{-8}.

3.3.1 PWL diode

In the following section are reported the transients for 50 µs of both circuit versions evaluated by Matlab. The only uncertainty introduced is due to the precision by which the software evaluates numerically the commutation time from a phase to the another. It is possible to estimate the stead-state voltage:

$$v_{out_\infty} \simeq \hat{V}_{in} - V_{on} = 0.75 \text{ V}$$

Simplified circuit

As expected, the higher is the resistance value, the slower will be the capacitor charge.

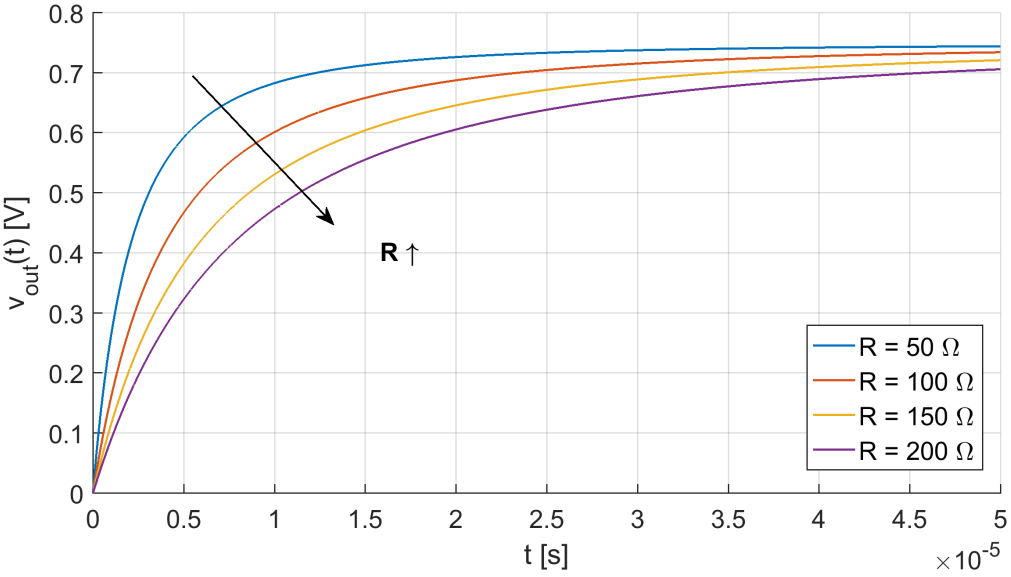

Figure 3.11: Transient simulation for PWL diode

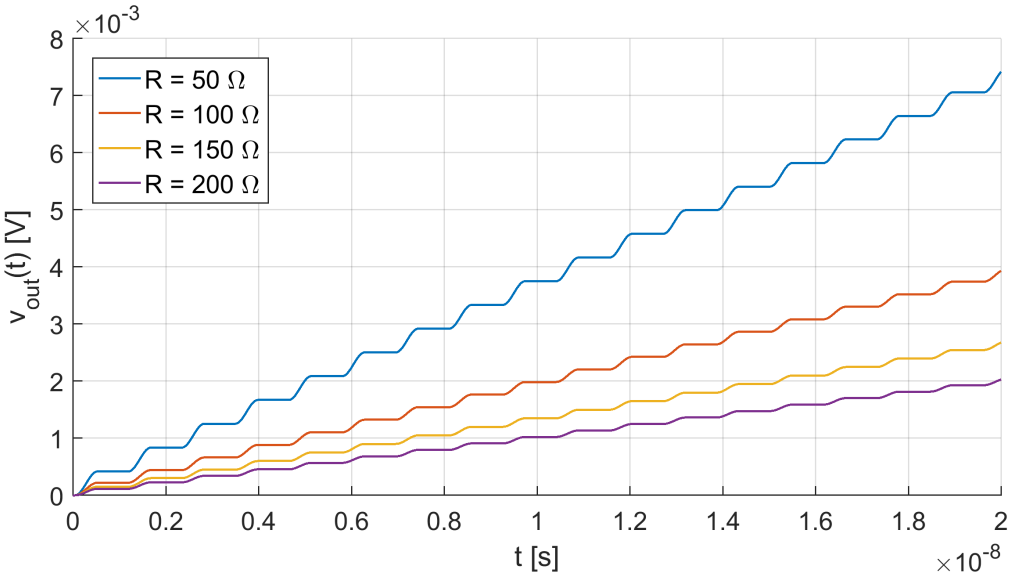

Figure 3.12: Trnsient in detail for the first 20 ns

In figure **??** it is possible to observe the difference in the charge from phase-ON to phase-OFF in the case of $R = 50\ \Omega$:

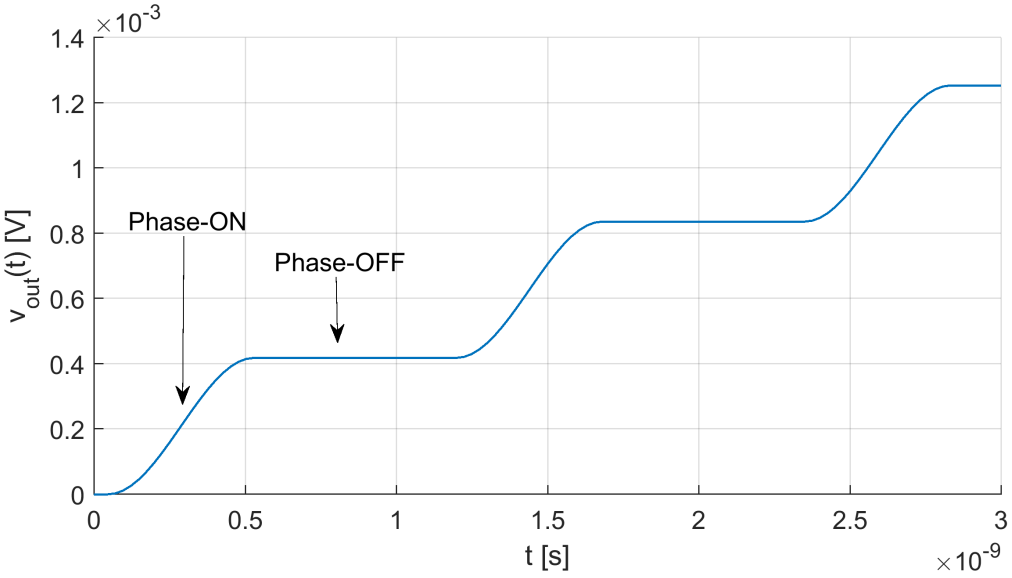

Figure 3.13: Difference between phase-ON and phase-OFF

Complete circuit

Also in this case the bigger is the resistance, the slower is the transient. In figure 3.15 is shown the behaviour during the first time of the transient.

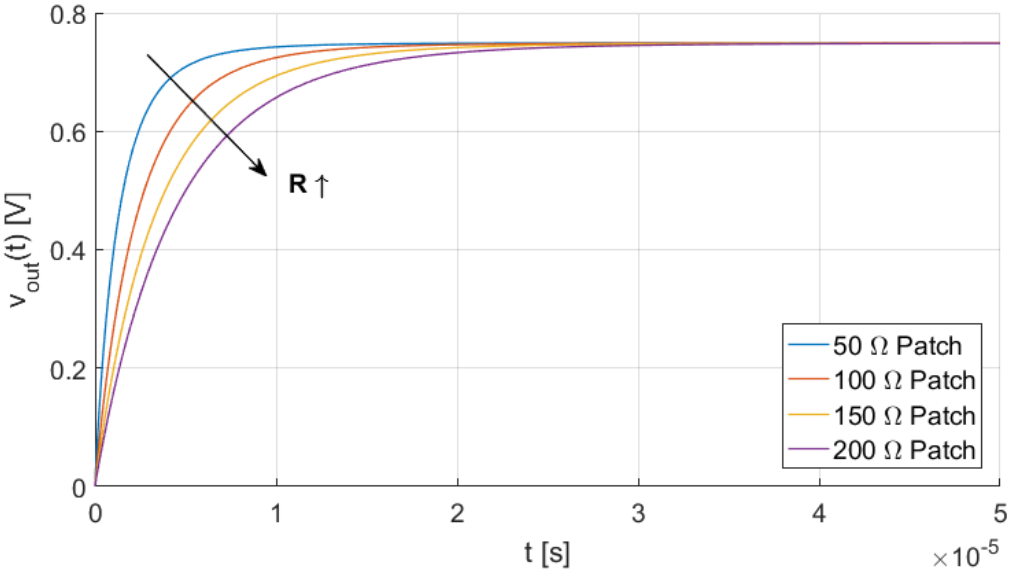

Figure 3.14: Simulation comparison

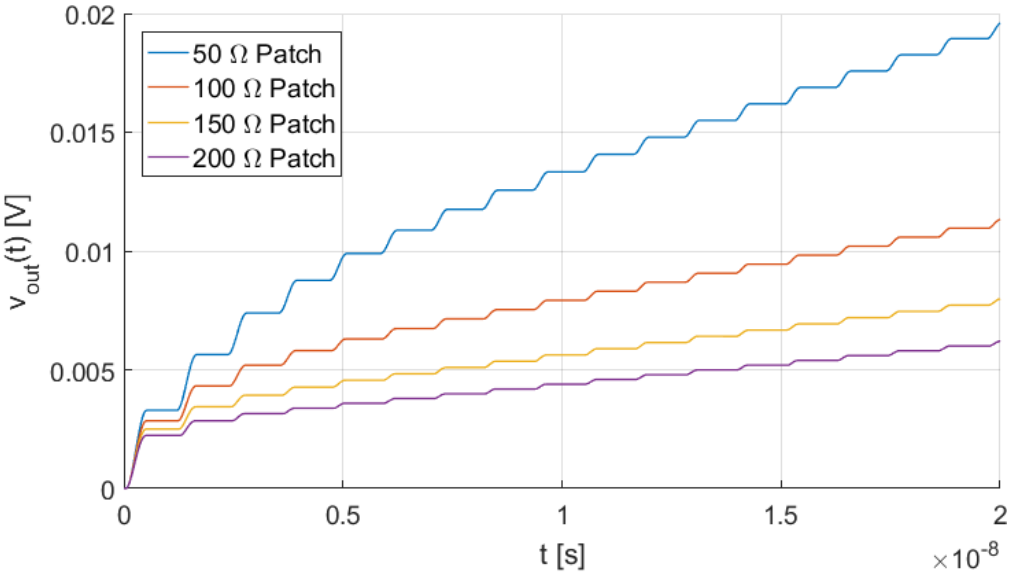

Figure 3.15: Simulation comparison in detail for the first 20 ns

An interesting observation: fixing the resistance value and the input voltage, the circuit with the resonator shows the faster transient (figure 3.16 and 3.17).

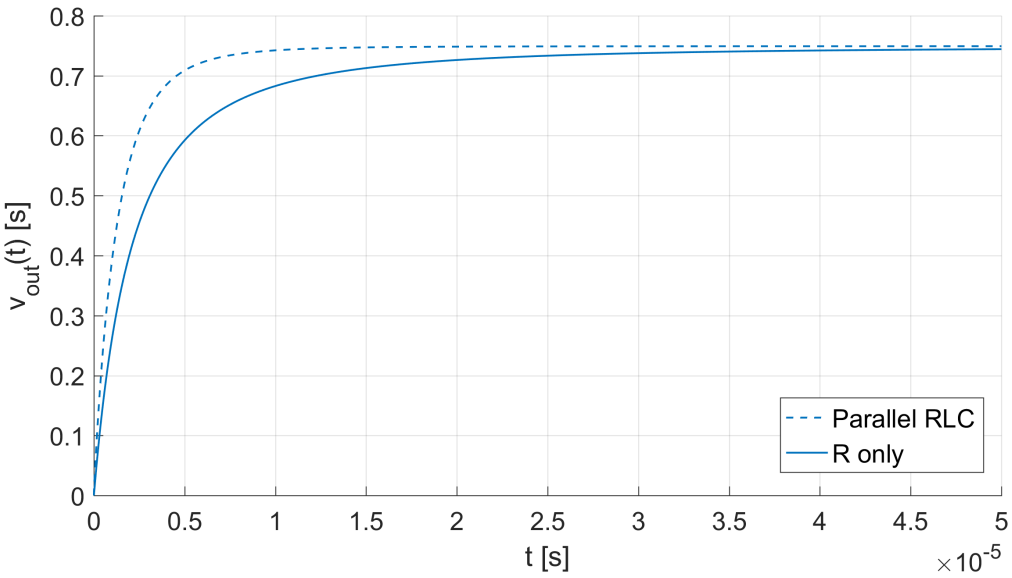

Figure 3.16: Responce differences - $R = 50\ \Omega$

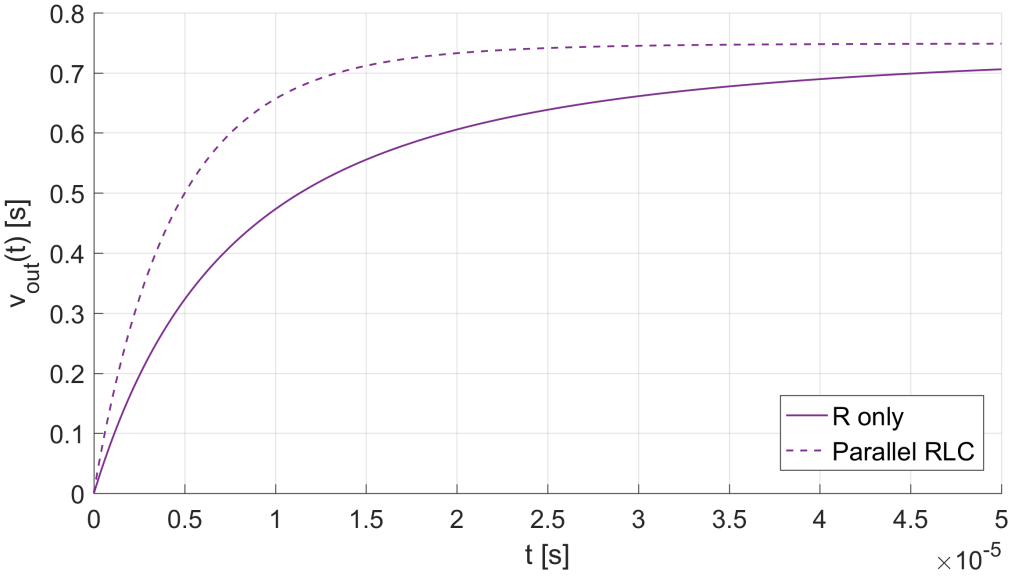

Figure 3.17: Responce differences - $R = 200\ \Omega$

3.3.2 Shockley diode

In the following section are reported the transient for 100 µs of both circuit version evaluated with Matlab, using $N_{points} = 1000$. The results are successively confronted to LTspice simulations.

Simplified circuit

As expected, the bigger is the resistance, the slower is the voltage transient. Moreover, it is interesting to notice that the transient is slower than the case of a piecewise linear diode by using the same parameters and the same simulation time, but it allows to reach a higher voltage.

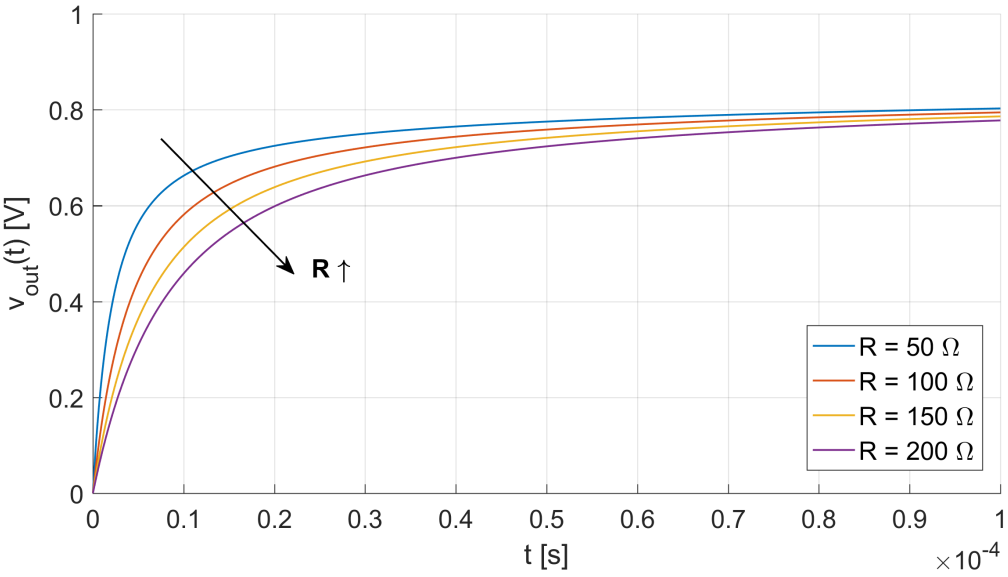

Figure 3.18: Transient simulation for exponential diode

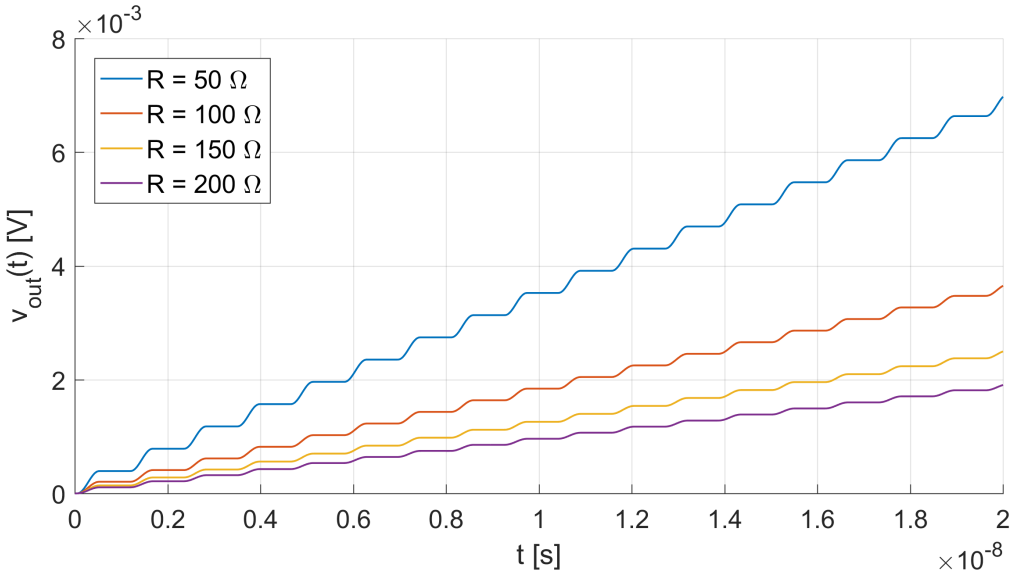

Figure 3.19: Transient simulation for exponential diode in detail for the first 20 ns

Similarly to the piece-wise linear diode, the transient shows some steps due to the non linearity introduced by the diode, as can be seen in figure 3.20:

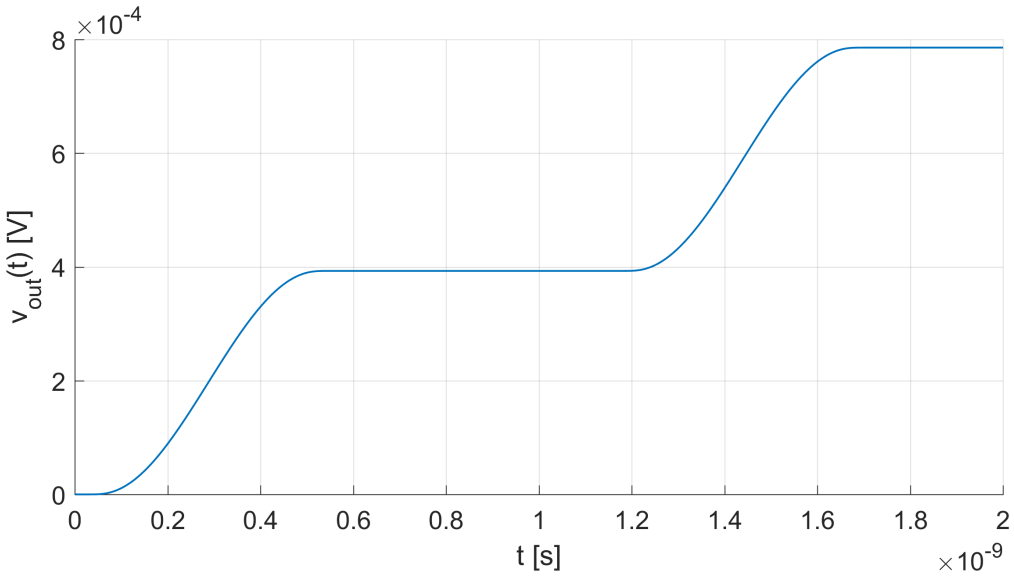

Figure 3.20: Non-linearity effect on the output voltage introduced by the diode

A comment on the number of points for the simulation (N_{points}) must be done:

choosing N_{points} small implies a ΔT not so small, and so the approximation will be inaccurate, on the contrary a N_{points} too big implies a very small ΔT and so the number of steps required to get the solution increases, so the truncation error increases and the solution can be perturbed. In figure 3.21 is shown the variation on the output voltage due to the different time step used. For more than 1000 points the results are almost the same. For this reason this value was used to get a trade-off between precision an simulation time.

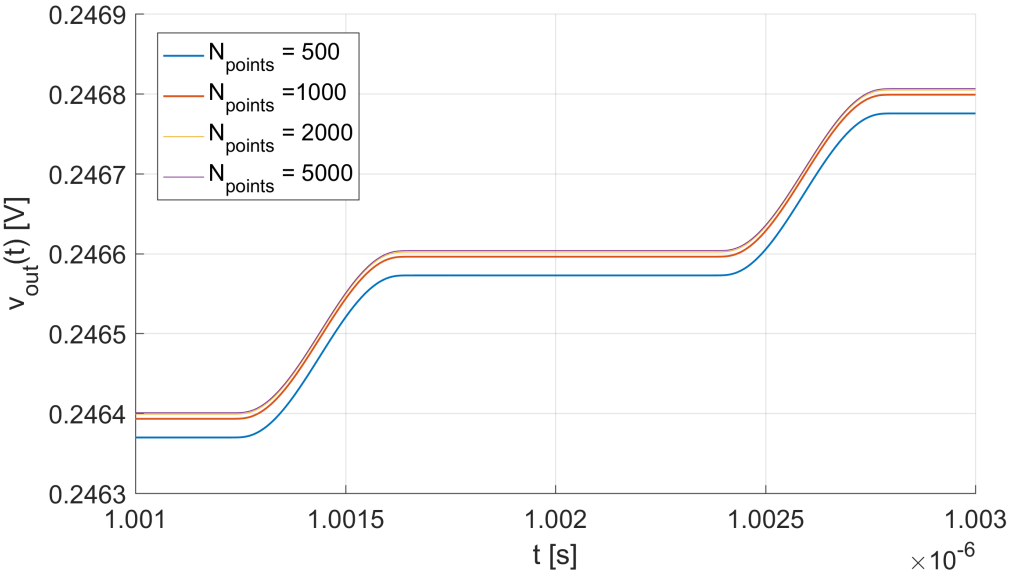

Figure 3.21: Variable number of points

In figure 3.22 is shown a comparison between Matlab and LTspice in which ϵ_1 (red curve) is the difference with respect the modified trapezoidal method, while ϵ_2 with respect the Gear method (blue curve). The maximum errors are reported in table 3.2:

R	ϵ_1 [mV]	ϵ_2 [mV]
50 Ω	1.031	2.642
100 Ω	1.193	2.577
150 Ω	1.319	2.616
200 Ω	1.432	2.757

Table 3.2: Difference simplified circuit

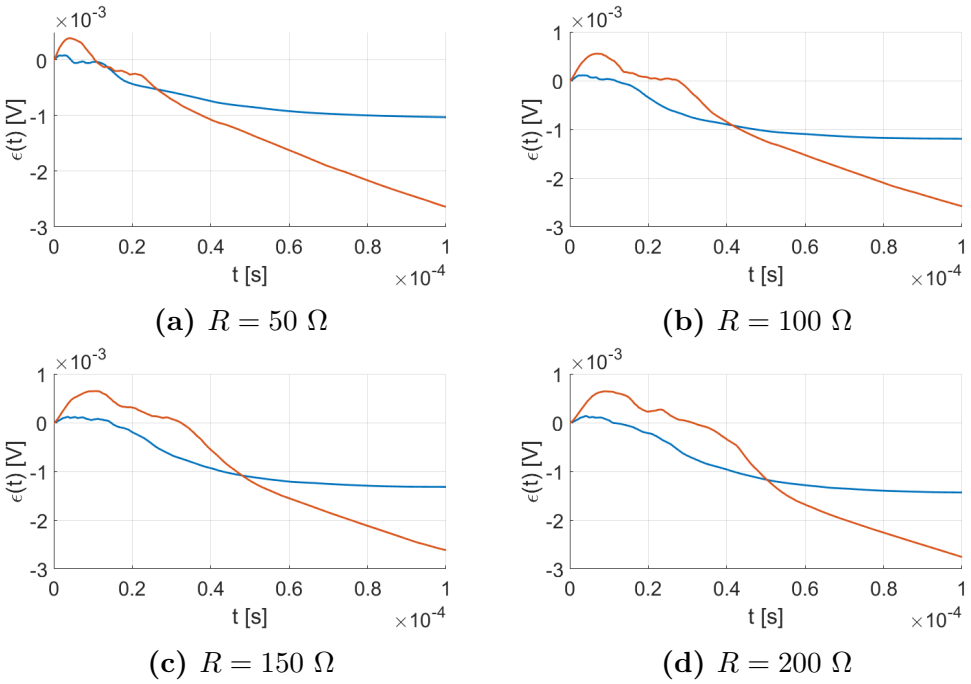

(a) $R = 50\ \Omega$ **(b)** $R = 100\ \Omega$

(c) $R = 150\ \Omega$ **(d)** $R = 200\ \Omega$

Figure 3.22: Differences between Matlab and LTspice

It is possible to notice that there is a consistent difference between the results obtained by LTspice depending on the integration method used but this problem is mainly due to the absolute and relative tolerances of the simulation. Increasing the resolution reduces this problem but the simulation takes a longer time. The situation is shown in figure 3.23, taking as example the case $R = 50\ \Omega$:

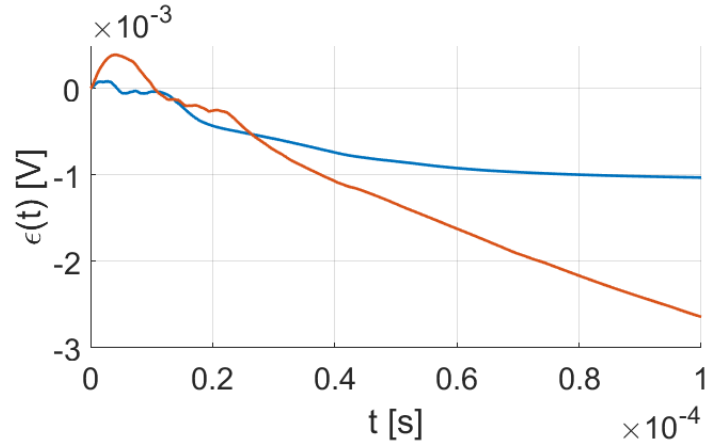

(a) Relative tolerance of 10^{-8}

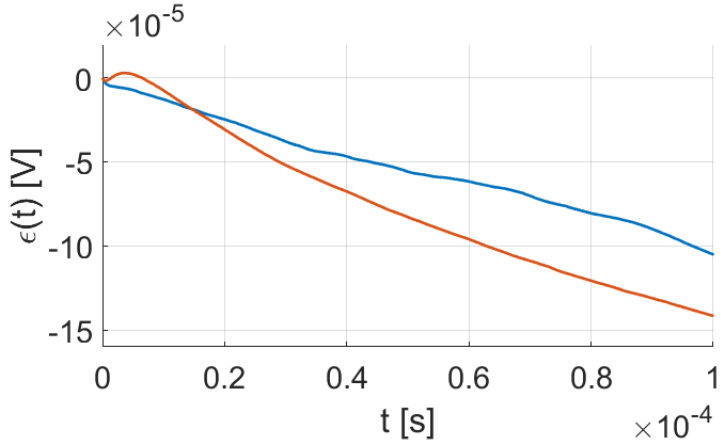

(b) Relative tolerance of 10^{-10}

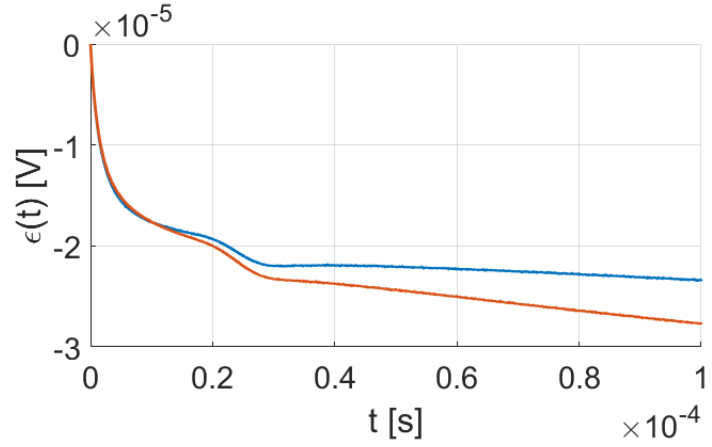

(c) Relative tolerance of 10^{-12}

Figure 3.23: Relative tolerance impact

RToll	ϵ_1 [mV]	ϵ_2 [mV]
10^{-8}	1.031	2.642
10^{-10}	0.105	0.142
10^{-12}	0.023	0.028

Table 3.3: Difference simplified circuit

Complete circuit

Again the higher is the resistance, the slower is the voltage transient. Moreover it is possible to notice that the resistance contribution can be seen in the first part of the transient and then all the curves assumes almost the same slope.

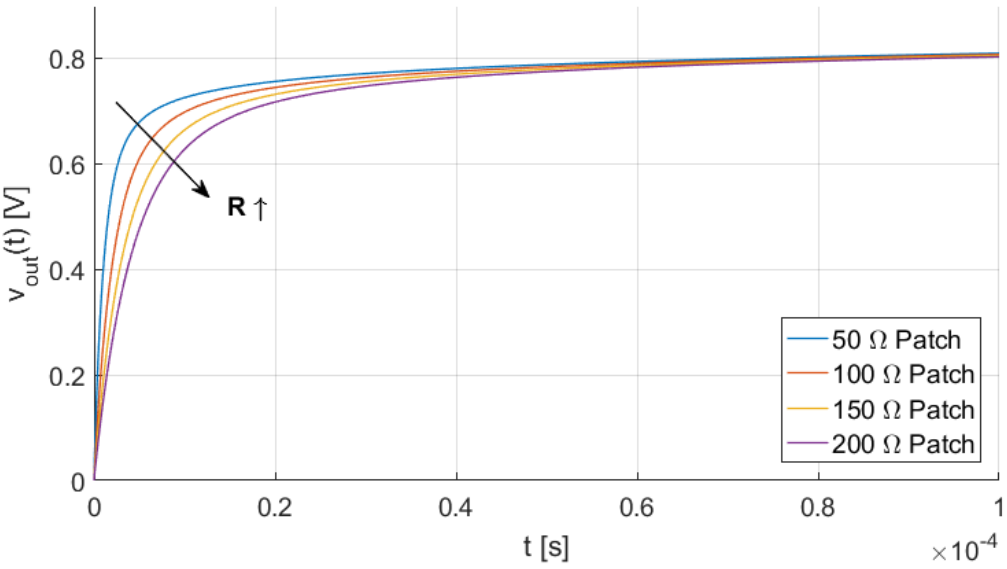

Figure 3.24: Simulation comparison - Matlab

In figure 3.25 it is possible to see more in detail the transient for the first 20 ns. Two followings steps int this case can have a decreasing amplitude due to the oscillation in the voltage over the resonator. This effect is well evident at the beginning of the transient and then it reduces.

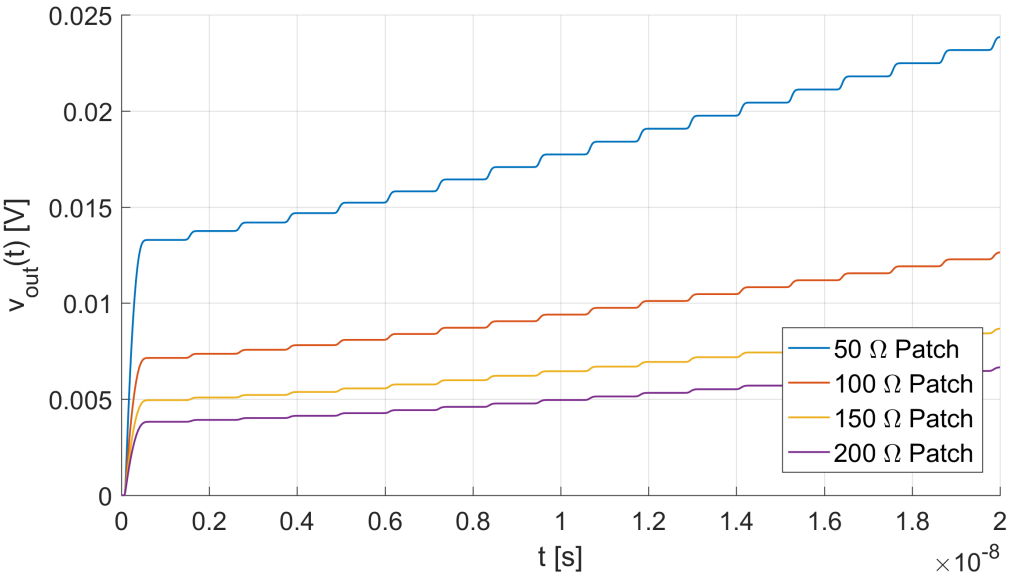

Figure 3.25: Simulation comparison in detail for the first 20 ns

In figure 3.26 are reported the difference between Matlab and LTspice simulations in which ϵ_1 (red curve) is the difference with respect the modified trapezoidal method, while ϵ_2 with respect the Gear method (blue curve). From the figure it is possible to notice that the maximum difference stands at the beginning of the transient and then it assumes a value almost constant. The maximum differences are reported in the table 3.4:

Patch	ϵ_1 [µV]	ϵ_2 [µV]
50 Ω	53.117	92.513
100 Ω	53.437	94.491
150 Ω	53.381	94.779
200 Ω	53.730	94.998

Table 3.4: Difference complete circuit

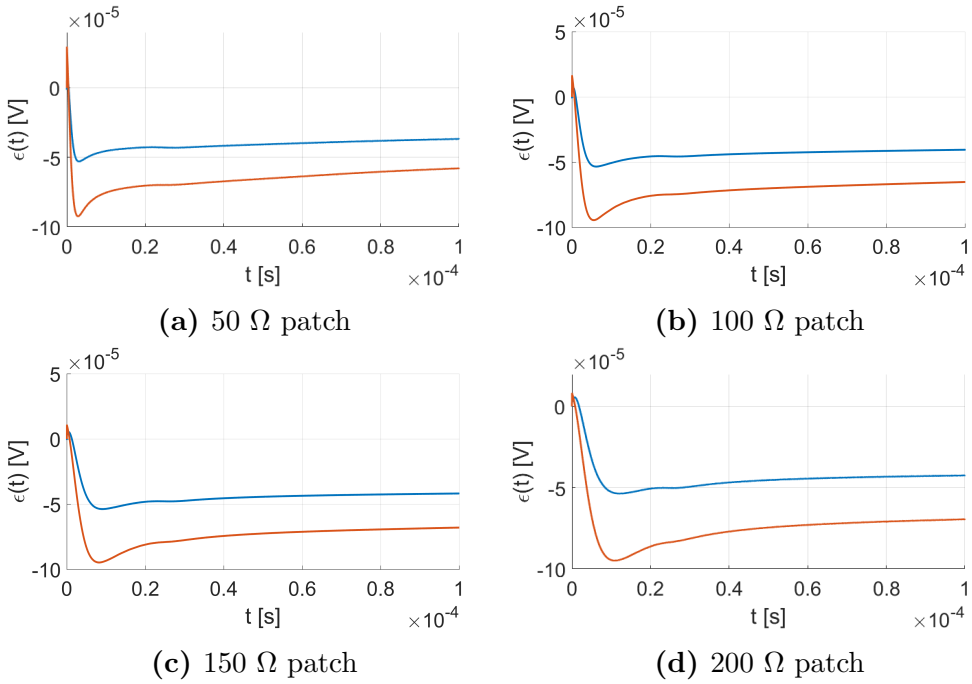

(a) 50 Ω patch **(b)** 100 Ω patch

(c) 150 Ω patch **(d)** 200 Ω patch

Figure 3.26: Differences between Matlab and LTspice

There are still small differences on the results obtained by LTspice, depending on the integration method evaluated by Matlab.
Also in this case, fixing the resistance value, the voltage shows a faster transient with a resonator instead of a resistance only, as can be seen in figure 3.27 and 3.28.

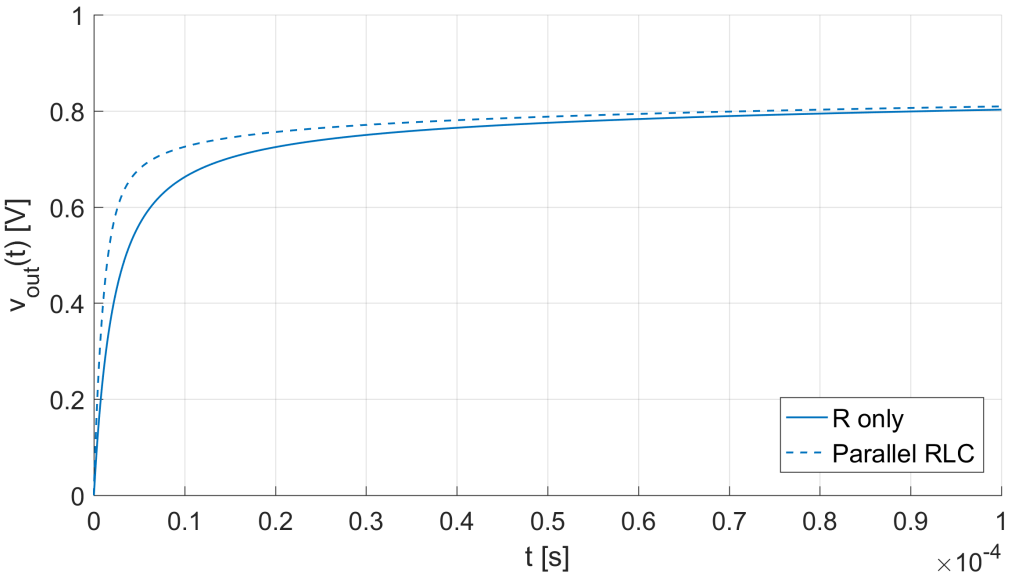

Figure 3.27: Responce differences - $R = 50\ \Omega$

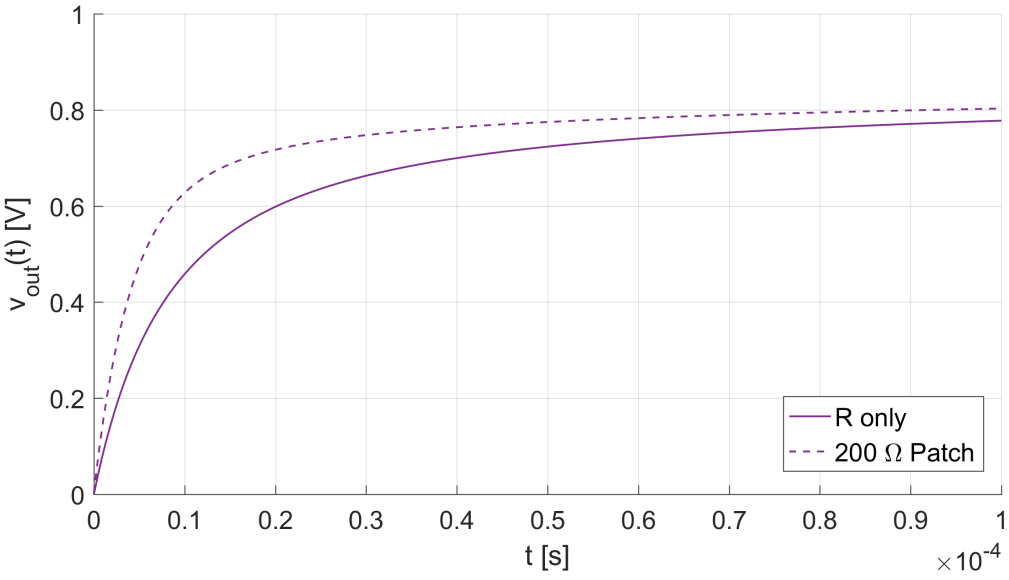

Figure 3.28: Responce differences - $R = 200\ \Omega$

3.3.3 Q variation

The *quality factor* defines the qualitative behaviour of a simple damped oscillators. Phisycally speaking it is proportional to the total energy stored divided by the

energy lost in a single cycle:

$$Q = 2\pi \cdot \frac{\text{Energy stored}}{\text{Energy dissipated per cycle}} \tag{3.35}$$

In the case of a parallel RLC resonator it can be expressed as:

$$Q = R \cdot \sqrt{\frac{C}{L}} = \frac{R}{\omega_0 L} = \omega_0 RC \tag{3.36}$$

The quality factors of the used patches are reported in table 3.5. It is important to underline that they are evaluated considering the resonator only and not the rest of the circuit.

Design R [Ω]	Q
50	37.5103
100	37.5361
150	37.5134
200	37.4191

Table 3.5: Patches quality factor

To better understand how the quality factor impact on the charge a resistance value of 200 Ω was fixed and then the quality factor swept from 10 to 50 (varying L and C), accordingly on the order of magnitude of the results. It points out that the higher is the quality factor, the faster is the charge. The main difference can be noticed mainly during the step of the first period (figure 3.29). The limit case of a resistance only shows the slowest charge.

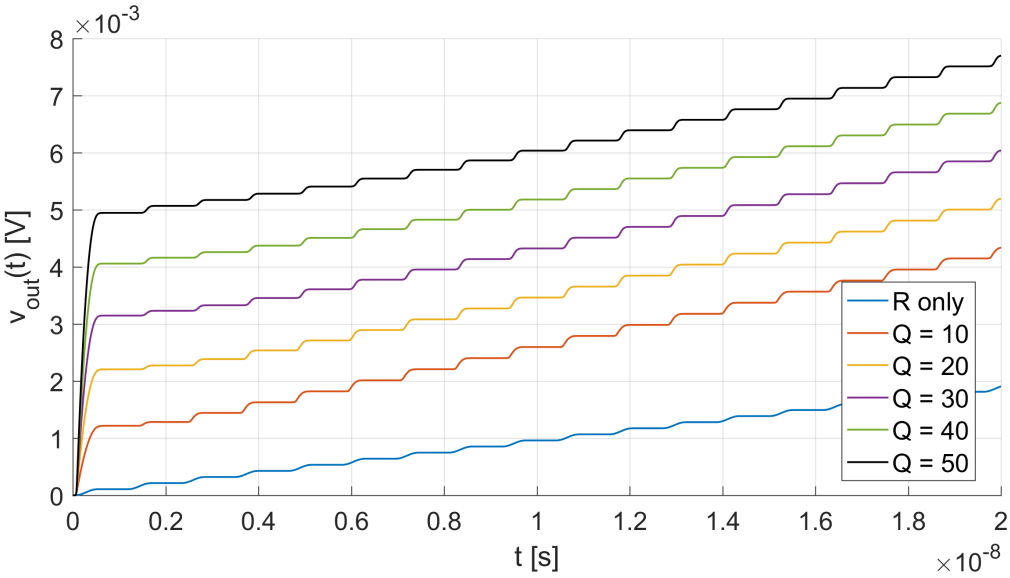

Figure 3.29: Quality factor impact on $v_{out}(t)$ ($R = 200\ \Omega$)

An interesting fact is that except for the first steps, the all the responses with a resonator have almost the same time constant and they increase in the same way, while the case with the resistance only is quite slower, as can be seen better in figure 3.30.

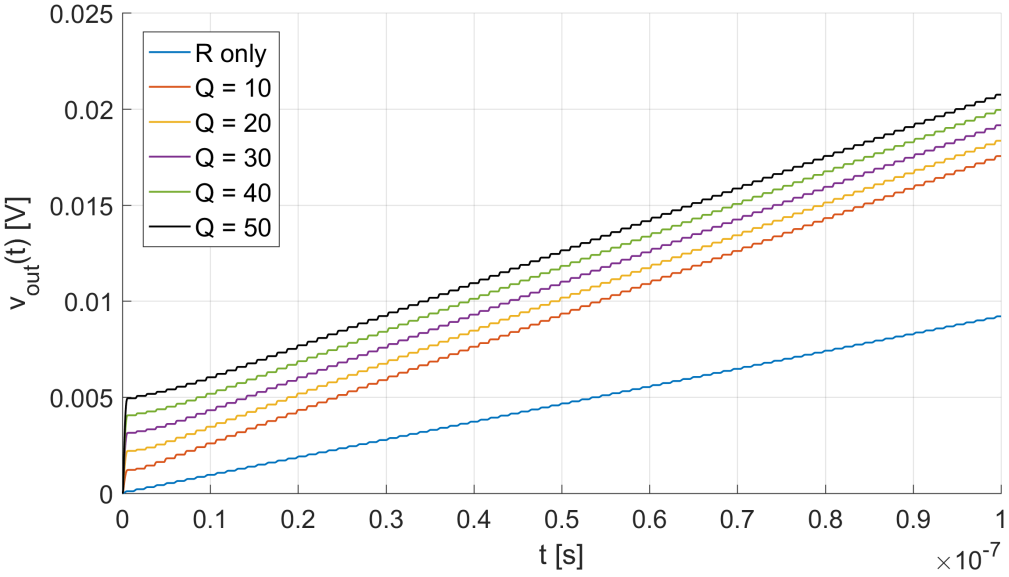

Figure 3.30: Transient for the first 100 ns ($R = 200\ \Omega$)

3.4 Steady state conditions

In the case of the diode with a Shockley characteristic it is possible to estimate the output voltage in steady state starting by making some simplifications starting from the system 3.15:

1. at the end of the transient $v_{out}(t)$ can be considered almost constant, so: In this way the system can be simplified as:
$$v_{out_k} \simeq v_{out_{k-1}} = v_{out}^{\infty} \ \forall \ k$$
2. since $v_{out}(t)$ is almost constant the current $i_d(t)$ becomes negligible;
3. starting from the previous assumptions it is possible to simplify the expression of v_{d_k}:
$$v_{d_k} \simeq v_{in_k} - v_{out}^{\infty} \ \Rightarrow \ v_{d_{k-1}} = v_{in_{k-1}} - v_{out}^{\infty}$$
4. v_{out}^{∞} becomes comparable to the amplitude $\hat{V}_{in}$ so $v_{d_k} < 0$ for most of the period T and during the positive time it has a negligible amplitude. In this way it is possible to simplify all the exponential terms:
$$e^{\frac{v_{d_{k-1}}}{\eta V_t}} \simeq 0$$

Consequently it is possible to rewrite the expression 3.14 as:

$$\Delta v_{out} \simeq \left[\left(\frac{v_{in_k} - v_{in_{k-1}}}{\eta V_t} + 1 \right) e^{\frac{v_{in_{k-1}} - v_{out}^{\infty}}{\eta V_t}} - 1 \right] \frac{I_s \Delta T}{C_{out}} \tag{3.37}$$

Considering that during each period the initial and the final value assumed by v_{out_k} are equal means that:

$$\sum_{i=1}^{N_p} \Delta v_{out_k} = 0$$

So the expression 3.37 can be rewritten as:

$$\frac{I_s \Delta T}{C_{out}} \cdot \sum_{k=1}^{N_p} \left[\left(\frac{v_{in_k} - v_{in_{i-1}}}{\eta V_t} + 1 \right) e^{\frac{v_{in_{k-1}} - v_{out}^{\infty}}{\eta V_t}} - 1 \right] = 0$$

This step means that during each period the voltage over the capacitor increases due to the input signal, but this increment is equal and opposite to the discharge due to the reverse current saturation I_s of the diode. In the transient the charging phase is higher and so the voltage increases. Simplifying this result:

$$e^{-\frac{v_{out}^{\infty}}{\eta V_t}} \sum_{k=1}^{N_p} \left(\frac{v_{in_k} - v_{in_{i-1}}}{\eta V_t} + 1 \right) e^{\frac{v_{in_{i-1}}}{\eta V_t}} = N_p$$

By solving this equation it is possible to get the following result:

$$v_{out}^{\infty} = \eta V_t \ln \left[\frac{1}{N_p} \sum_{k=1}^{N_p} \left(\frac{v_{in_k} - v_{in_{i-1}}}{\eta V_t} + 1 \right) e^{\frac{v_{in_{i-1}}}{\eta V_t}} \right] \tag{3.38}$$

It immediately points out that, at first approximation, the voltage in steady state v_{out}^{∞} depends just on the diode and the amplitude on the input signal. This result is an upper limit of the maximum voltage that can be reached. The real value will be less because of the strong approximation used. In figure 3.31 is reported the value of v_{out}^{∞} evaluated by Matlab starting from the result 3.38 for a variable number of points N_p:

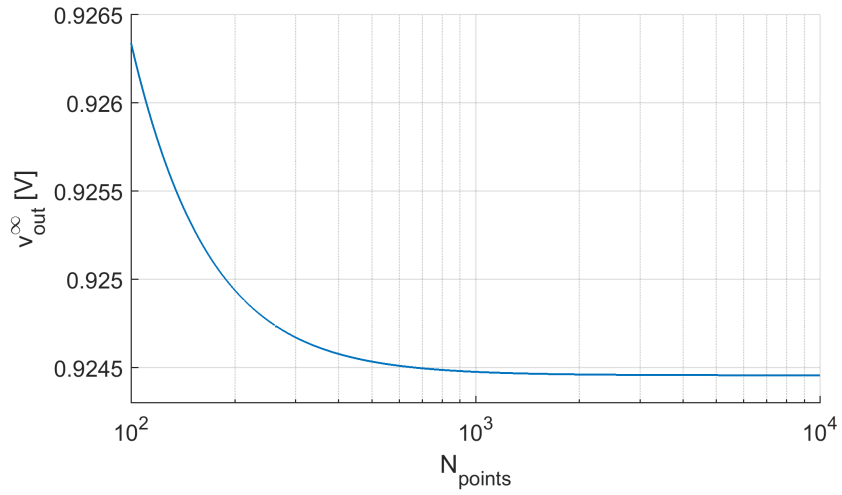

Figure 3.31: Relation between v_{out}^{∞} and N_p - Case $\hat{V}_{in} = 1$ V

It points out that for $N_p > 1000$ the value of v_{out}^{∞} is almost constant. In particular for, taking as reference $N_p = 1000$:

$$v_{out}^{\infty} = 924.476 \text{ mV}$$

In order to check this result, the algorithm previously used has been tested for 5 periods for $R = 50\ \Omega$ and by using as initial conditions:

$$v_{out_{k-1}} = v_{out}^{\infty}$$
$$v_{d_{k-1}} = -v_{out}^{\infty}$$

The result is shown if figure 3.32:

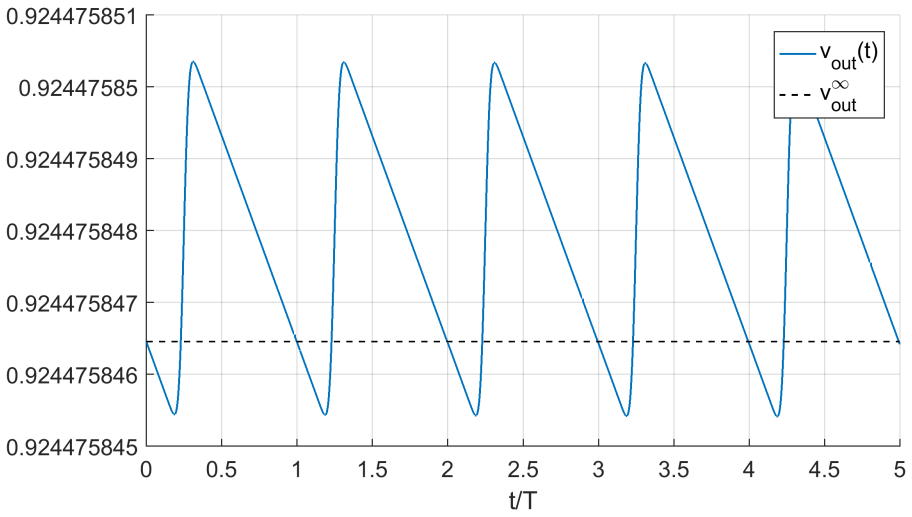

Figure 3.32: Steady state results obtained with Matlab

In order to evaluate the correctness of the results, the difference between the initial value, that is v_{out}^{∞}, and the final value at each period was computed. As expected this error is different from zero and it has a monotonic behaviour (figure 3.33). This means that the voltage considered is too high and so in the output capacitor the discharging phase prevails with respect the charging one. On the contrary, by using a smaller v_{out}^{∞}, this error increases since the capacitor charges.

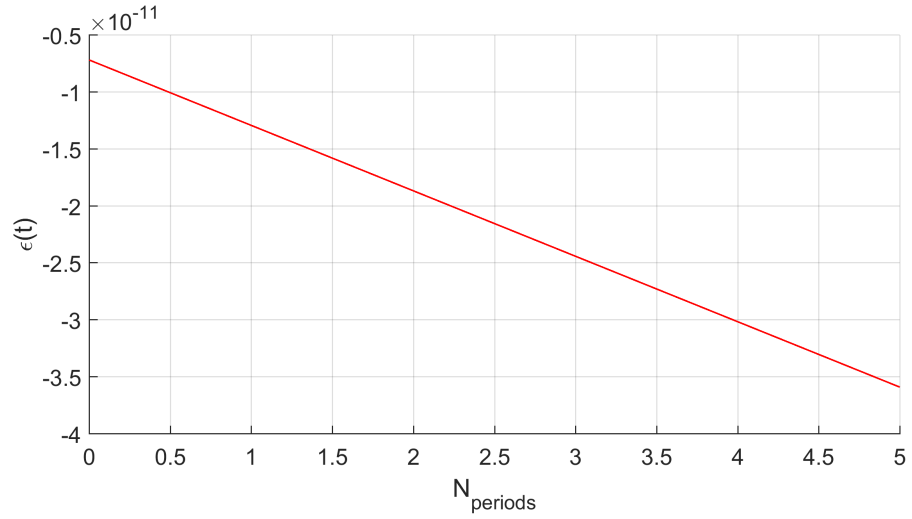

Figure 3.33: $v_{out}^{\infty} - v_{out}(N \cdot T)$

After many iterations it points out that the correct value of v_{out}^{∞} that gives a null

error is:

$$v_{out}^{\infty} = 924.441 \text{ mV}$$

In the table 3.6 are reported the different values of the steady state voltage in function of the resistance. As expected the higher is the resistance, the smaller is the output voltage since less current can pass.

R [Ω]	v_{out}^{∞} [mV]
50	924.441
100	924.417
150	924.393
200	924.369

Table 3.6: v_{out}^{∞} for different values of R

making similar approximations also in the circuit completed leads to the same result.

3.4.1 AWR comparison

LTspice performs time domain simulations and it is not able to detect the circuit steady state conditions. To this purpose a software that perform a frequency domain simulation for the circuit analysis must be used. A good choice is AWR Microwave Office, a software that can be used to create integrated systems, RF or analog circuits. Microwave office is the environment used to design circuits composed of schematics and electromagnetic structures taken from a database. A feature of this software particularly useful for this kind of simulation is the possibility to simulate the circuit by using as simulation engine the APLAC Harmonic Balance, that is a frequency domain method used to detect the steady state conditions. The circuit is reported in figure 3.34:

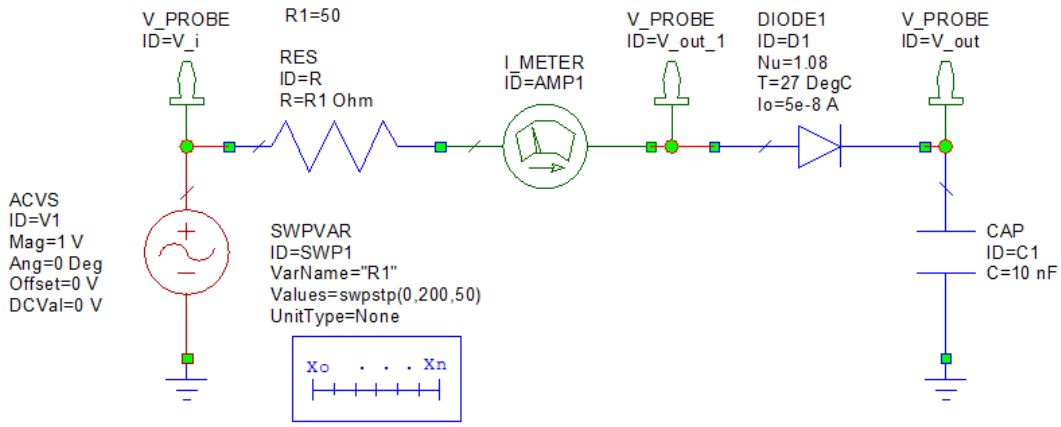

Figure 3.34: Circuit with resistance sweep

For the simulation the following settings has been used:

- Tone 1 Harmonics: 100;
- TAUDC : 0;
- HB Matrix Solver: Sparse;
- Integration Method: Euler;
- Small Resistor Limit R0 : 0;
- Relative Error: 10^{-8};
- Absolute Error: 10^{-10};
- Maximum Relative Truncation Error: 10^{-8}.

For the simulations the same resistances already considered was used plus $R = 0\ \Omega$, that simulates a short circuit. The results are reported in figure 3.35:

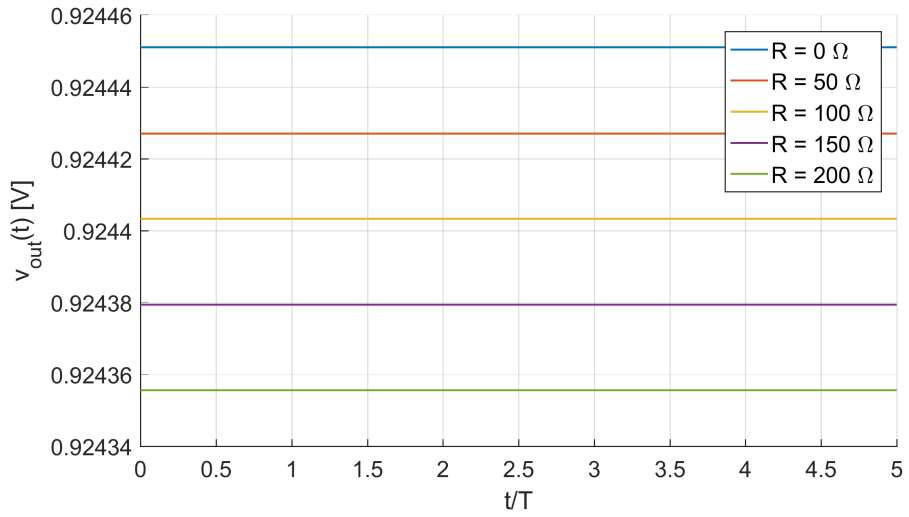

Figure 3.35: AWR results

In the table 3.7 are reported the voltage estimated by Matlab and AWR, the absolute error ϵ_{abs} and the relative error ϵ_{rel} (in percentage) defined as:

$$\epsilon_{abs} = |v^{\infty}_{out_{Matlab}} - v^{\infty}_{out_{AWR}}|$$
$$\epsilon_{rel} = \frac{|v^{\infty}_{out_{Matlab}} - v^{\infty}_{out_{AWR}}|}{|v^{\infty}_{out_{Matlab}}|} \cdot 100$$

It is possible to notice that the absolute error is almost constant ($\simeq$ 13 µV) for each resistance. So the solution is almost the same but shifted and this difference may be due to the numerical methods used by AWR, different model, particular settings, finite precision of computation and so on.

R [Ω]	$v^{\infty}_{out_{Matlab}}$ [mV]	$v^{\infty}_{out_{AWR}}$ [mV]	ϵ_{abs} [µV]	ϵ_{rel} [%]
50	924.441	924.427	13.767	$1.489229 \cdot 10^{-3}$
100	924.417	924.403	13.629	$1.473991 \cdot 10^{-3}$
150	924.393	924.379	13.473	$1.457495 \cdot 10^{-3}$
200	924.369	924.356	13.309	$1.439745 \cdot 10^{-3}$

Table 3.7: Comparison between Matlab and AWR

In conclusion, the value of v^{∞}_{out} obtained with Matlab script is used as reference for the following discussions.

3.5 Analytic approximation

Another step consists to find an approximate analytic solution for the exponential case in order to roughly estimate the charge time required to reach percentage of v_{out}^{∞}. By looking at the simulations, it is possible to notice that the contribution of the resistance in the transients act just at the beginning, while, for long times, in which $v_{out}(t)$ increases very slow, and all the behaviours converge on the same curve, independently on the value of R. This means that for very long time the resistance acts a negligible effect. So the following hypotheses are valid in the time discrete domain:

- $R \to 0 \quad \Rightarrow \quad v_{d_k} \simeq v_{in_k} - v_{out_k}$
- $\Delta v_{out} \to 0 \quad \Rightarrow \quad v_{out_k} \simeq v_{out_{k-1}} = v_{out}$

So starting from the discrete result 3.14, by using the previous assumption and neglecting the denominator, it is possible to get the following result:

$$\Delta v_{out_k} = \left[\left(\frac{v_{in_k} - v_{in_{k-1}}}{\eta V_t} + 1 \right) e^{\frac{v_{in_{k-1}} - v_{out}}{\eta V_t}} - 1 \right] \frac{I_s \Delta T}{C_{out}}$$

The next step consist to consider the sum over a period in order to simplify the term that depends on the on the index k:

$$\sum_{k=1}^{N_p} \Delta v_{out_k} = \frac{I_s \Delta T}{C_{out}} \cdot \sum_{k=1}^{N_p} \left[\left(\frac{v_{in_k} - v_{in_{k-1}}}{\eta V_t} + 1 \right) e^{\frac{v_{in_{k-1}} - v_{out}}{\eta V_t}} - 1 \right]$$

Assuming $\Delta v_{out_k} \simeq \text{const} \ \to \Delta v_{out}$ this expression can be simplified as:

$$\Delta v_{out} = \frac{I_s \Delta T}{C_{out}} \cdot \left[e^{-\frac{v_{out}}{\eta V_t}} \frac{1}{N_p} \sum_{k=1}^{N_p} \left(\frac{v_{in_k} - v_{in_{k-1}}}{\eta V_t} + 1 \right) e^{\frac{v_{in_{k-1}}}{\eta V_t}} - 1 \right] \tag{3.39}$$

considering that:

$$\frac{1}{N_p} \sum_{k=1}^{N_p} \left(\frac{v_{in_k} - v_{in_{k-1}}}{\eta V_t} + 1 \right) e^{\frac{v_{in_{k-1}}}{\eta V_t}} = e^{\frac{v_{out}^{\infty}}{\eta V_t}}$$

so the result 3.39 can be rewritten as:

$$\Delta v_{out} = \frac{I_s \Delta T}{C_{out}} \cdot \left(e^{\frac{v_{out}^{\infty} - v_{out}}{\eta V_t}} - 1 \right) \tag{3.40}$$

Then, considering a sufficient small time step, both Δv_{out} and ΔT can be replaced by infinitesimal increments:

$$\Delta T \to \mathrm{d}t$$
$$\Delta v_{out} \to \mathrm{d}v_{out}$$

in this way the result 3.40 becomes a separable variables differential equation:

$$\int \frac{1}{e^{\frac{v_{out}^{\infty} - v_{out}}{\eta V_t}} - 1} \mathrm{d}v_{out} = \int \frac{I_s}{C_{out}} \mathrm{d}t \tag{3.41}$$

By solving this differential equation:

$$v_{out}(t) = v_{out}^{\infty} + \eta V_t \cdot \ln\left[1 - e^{-\frac{I_s}{\eta V_t C} t} \cdot A\right] \tag{3.42}$$

The particular solution of this differential equation may be found by imposing an initial condition:

$$\begin{cases} v_{out}(t) = v_{out}^{\infty} + \eta V_t \cdot \ln\left[1 - e^{-\frac{I_s}{\eta V_t C} t} \cdot A\right] \\ v_{out}(t_0) = v_{out_0} \end{cases} \tag{3.43}$$

By fixing $v_{out}(0) = 0$ it is possible to solve the Cauchy problem:

$$v_{out}(0) = v_{out}^{\infty} + \eta V_t \cdot \ln\left[1 - A\right] = 0 \quad \Rightarrow \quad A = 1 - e^{-\frac{v_{C\infty}}{\eta V_t}}$$

So the complete solution becomes:

$$v_{out}(t) = v_{out}^{\infty} + \eta V_t \cdot \ln\left[1 - e^{-\frac{I_s}{\eta V_t C} t} \cdot \left(1 - e^{-\frac{v_{out}^{\infty}}{\eta V_t}}\right)\right] \tag{3.44}$$

From this result it is possible to estimate the time t_p required to reach a percentage p of v_{out}^{∞}:

$$v_{out}(t_p) = p \cdot v_{out}^{\infty} = v_{out}^{\infty} + \eta V_t \ln\left[1 - e^{-\frac{I_s}{\eta V_t C_{out}} \cdot t_p} \cdot \left(1 - e^{-\frac{v_{out}^{\infty}}{\eta V_t}}\right)\right]$$

By solving this equation:

$$t_p = \frac{\eta V_t C_{out}}{I_s} \cdot \ln\left[\frac{1 - e^{-\frac{v_{out}^{\infty}}{\eta V_t}}}{1 - e^{-\frac{(1-p) \cdot v_{out}^{\infty}}{\eta V_t}}}\right] \tag{3.45}$$

In figure 3.36 it shown a comparison between the analytic solution and the discrete solution of the simplified circuit for 0.5 ms:

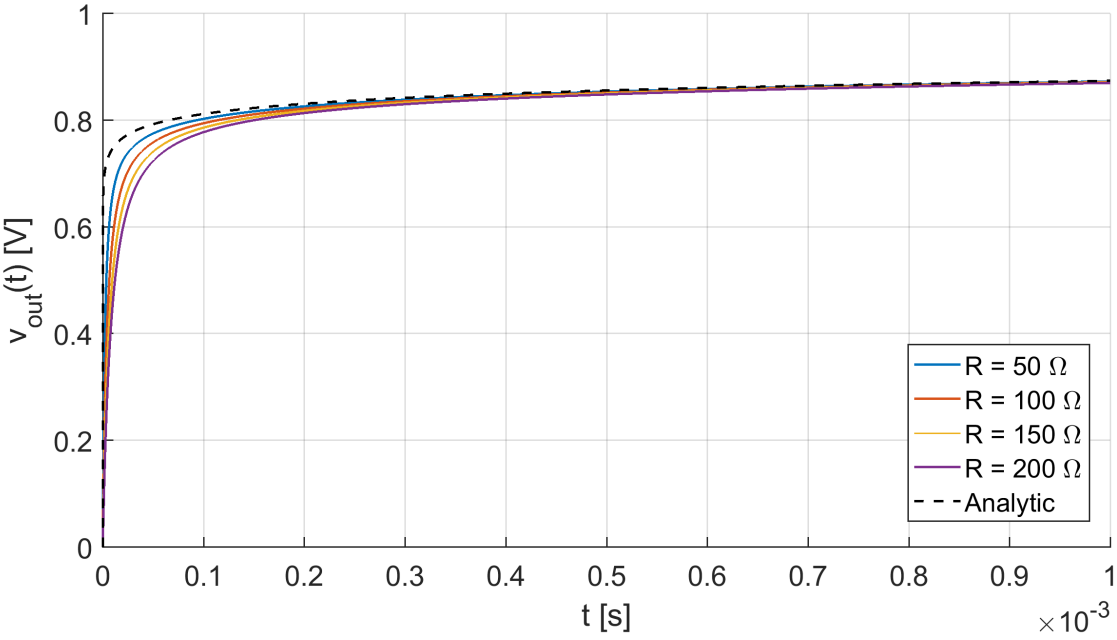

Figure 3.36: Comparison between Euler solution and Analytic solution

It is important to notice that this result is valid just for a time sufficiently high. At the beginning it well evident the difference due to the resistance.

From this result 2 considerations can be done:

- fixing the value of C_{out}, t_p depends on the value of $v_{out\infty}$ so on the amplitude of the input voltage $\hat{V}_{in}$. This relation is shown in figure 3.37:

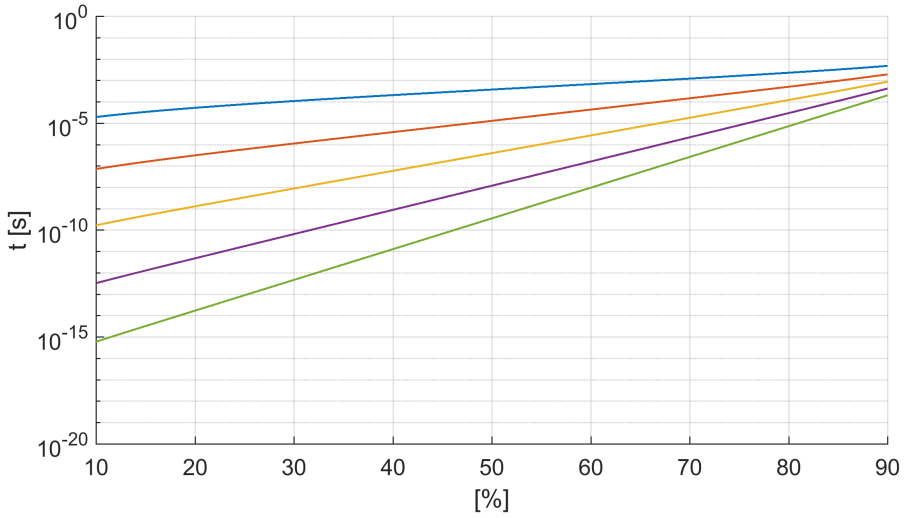

Figure 3.37: t_p for different values of $\hat{V}_{in}$ ($C_{out} = 10$ nF)

- with a fixed value of $\hat{V}_{in}$, t_p depends linearly on the value of C_{out} (figure 3.38).

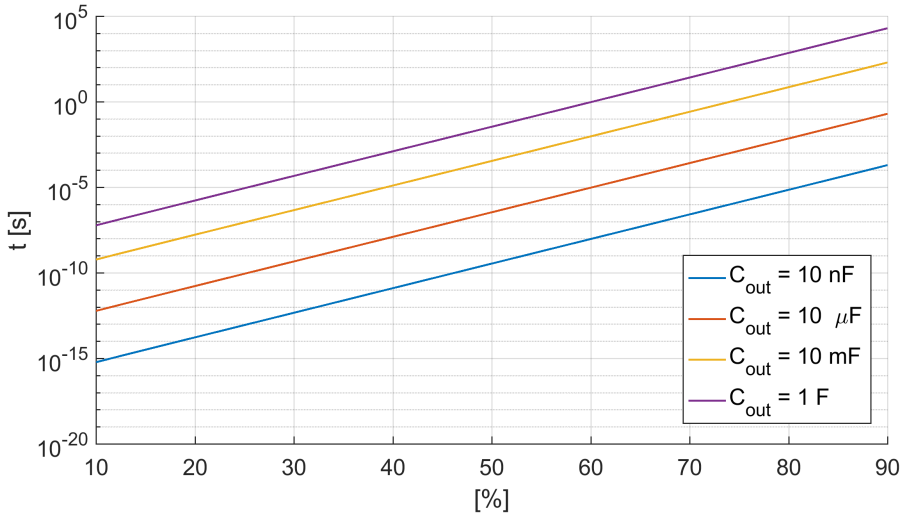

Figure 3.38: t_p for different values of C_{out} ($\hat{V}_{in} = 1$ V)

This result is more accurate for low values of the input voltage, since the approximation at the denominator is valid in that cases.

Chapter 4

Measurements

Two circuit were realized and tested together with an energy harvesting circuit already present on the market in the anechoic chamber of the Poitecnico di Torino. The anechoic chamber chamber is a laboratory environment that prevent the reflection. In this way it allows to recreate in a closed space a simulated open space of infinite size useful to perform high precision measurements. In figure 4.1 is reported the schematic used for the measurement:

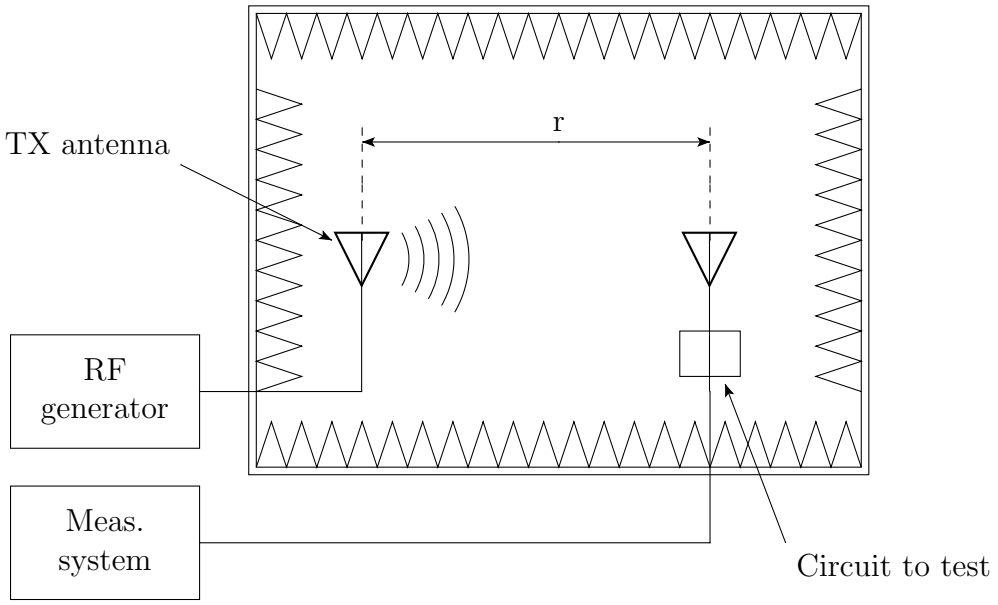

Figure 4.1: Measurement schematic

The main components are:

- the RF generator, a 83650L Synthesized Swept-CW Generator of HP (figure 4.3a);

- the measurements system, that consists in a computer connected throw a GPIB line to a digital multimeter, the Agilent 34401A (figure 4.3b). In this way the measurements could be controlled directly by the computer;

- the transmitting antenna, a horn antenna (figure 4.3c);

- the circuit to test, the powercast in this case (figure 4.3d).

The complete setup is reported in figure 4.2:

Figure 4.2: Measurement setup

(a) RF generator

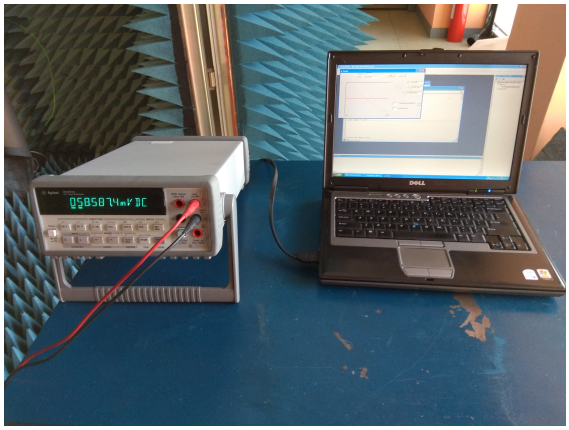

(b) Measurement system

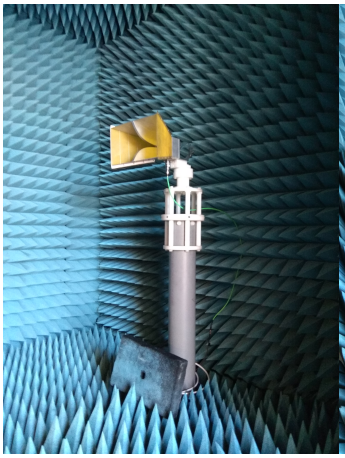

(c) Transmitting antenna

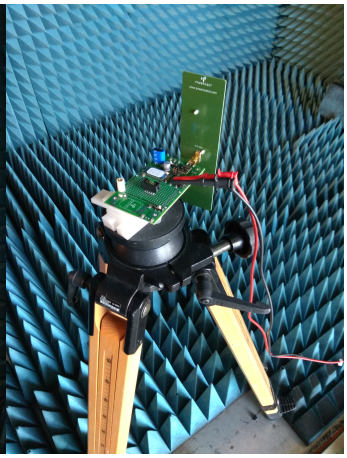

(d) Powercast

4.0.1 Powercast P2110B

The Lifetime Power® Energy Harvesting Development Kit for Wireless Sensors is a demonstrative platform for creating battery-free wireless sensor applications powered by RF energy (radio waves). It is designed and configured for extremely low power operation optimized for a RF energy at 915 MHz.

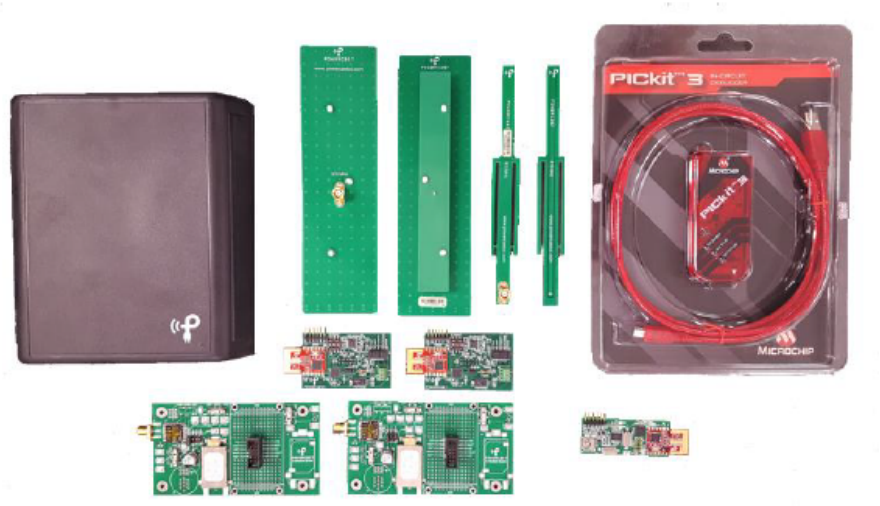

Figure 4.4: Lifetime Power® Energy Harvesting Development Kit

The kit (figure 4.4) includes an RF transmitter, RF energy harvesting receiver boards, two and antennas (a dipole and a patch of 50 Ω), a wireless sensor boards, a PIC® MCU-based development board and radio and a programming tool. Just the receiver board was used (figure 4.5).

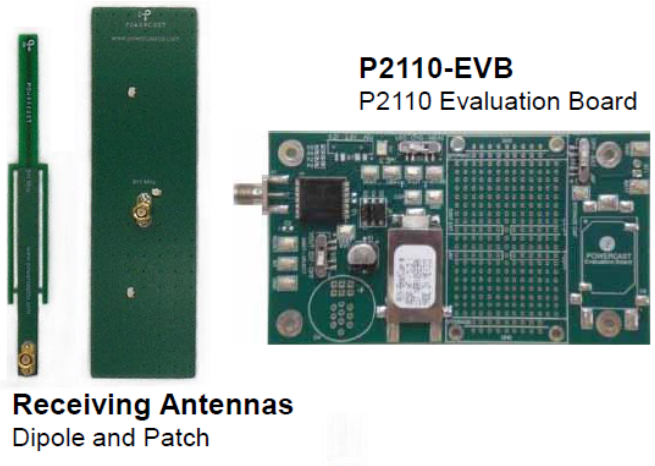

Figure 4.5: P2110B receiver

The receiver features are the following:

- receives power and data;
- converts RF to DC power and stores it in a capacitor;
- Charge / Power management unit;
- I/O interface.

The schematic is reported in figure 4.6.

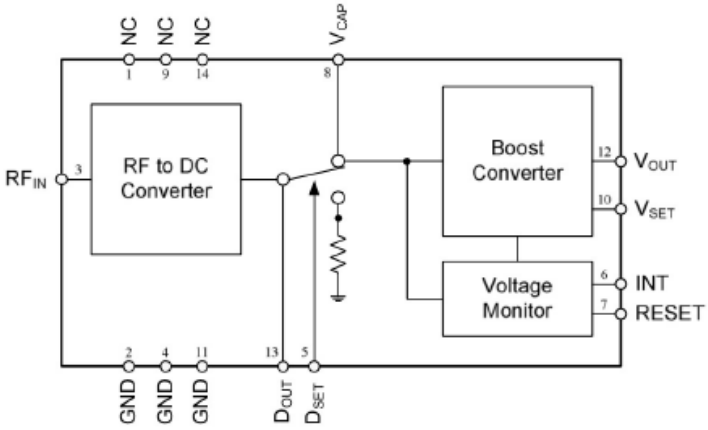

Figure 4.6: Powercast functional block diagram

The circuit offers the possibility to choose between 3 different capacitors by changing the position of a pin:

- $C_3 = 1$ mF
- $C_4 = 1$ F (supercap - user selectable)
- $C_5 = 50$ mF

When the capacitor voltage V_{CAP} reaches a threshold, the the P2110B boosts the voltage to the set output voltage level and enables the voltage output (V_{OUT}). In this phase the V_{CAP} decreases, and when it declines to the low voltage threshold the voltage output is turned off and so the capacitor charges again. The situation is explained is figure 4.7:

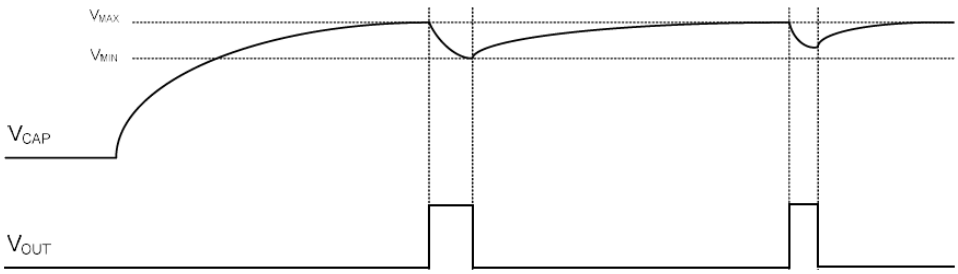

Figure 4.7: Powercast timing diagram

The datasheet states that V_{CAP} can reach values from 1.02 V to 1.25 V with a maximum input power of 23 dBm. The attention is focused on the time t_{charge} required to charge the capacitor up to V_{MAX} starting from 0 V, using both the antennas present in the kit.

4.0.2 Results

For the measurements the transmitting antenna was used to radiate a signal of 20 dBm with a frequency of 915 MHz to the powercast, placed a at a distance $r = 1.5$ m from it. The measurement system was set to measure the voltage from the proper terminal of the powercast every second. In the table 4.1 are reported the charge time for the different capacitance values, using the both antennas of the kit.

Capacitance	Patch	Dipole
$C = 1$ mF	9 s	31 s
$C = 50$ mF	5 min	15 min
$C = 1$ F	140 min	458 min

Table 4.1: Charge time

It was not possible to measure the steady state output voltage rectifier since the circuit stops the charge when the capacitor voltage reaches the threshold. Using the patch is is possible to reach the maximum voltage approximately in a third of the time it would take using the dipole, for all the output capacitor. This result can be expected since the patch has an higher gain and so a higher input voltage.

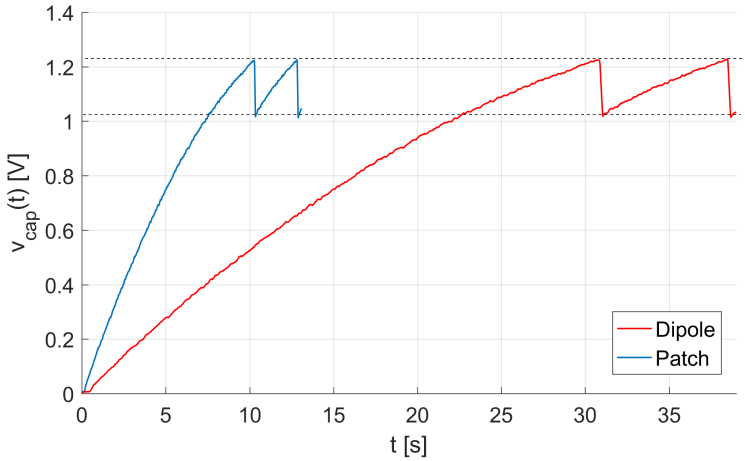

(a) Case $C = 1$ mF

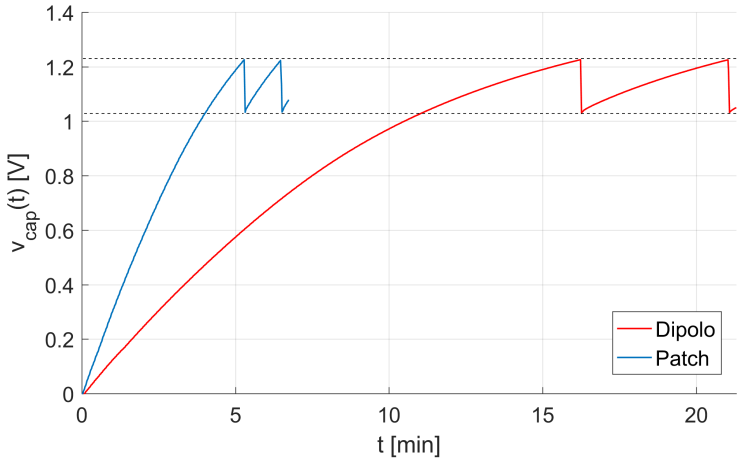

(b) Case $C = 50$ mF

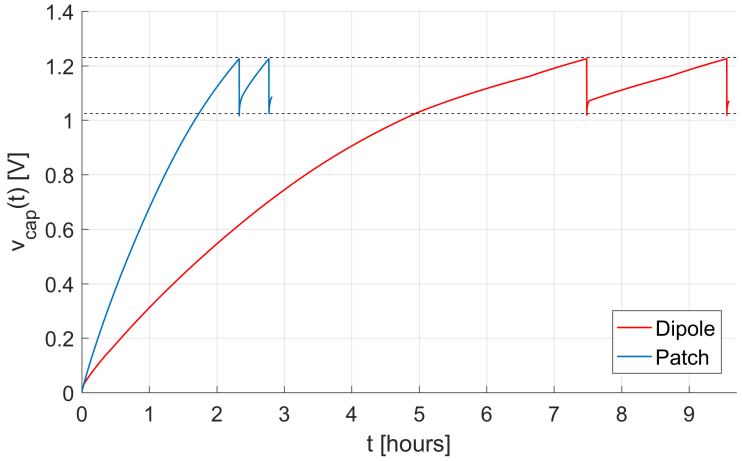

(c) Case $C = 1$ F

4.1 Circuit implementation

A half-wave rectifier and a single stage voltage multiplier were realized in the ISMB. The schematics with all the components are reported in figure 4.9 and 4.10:

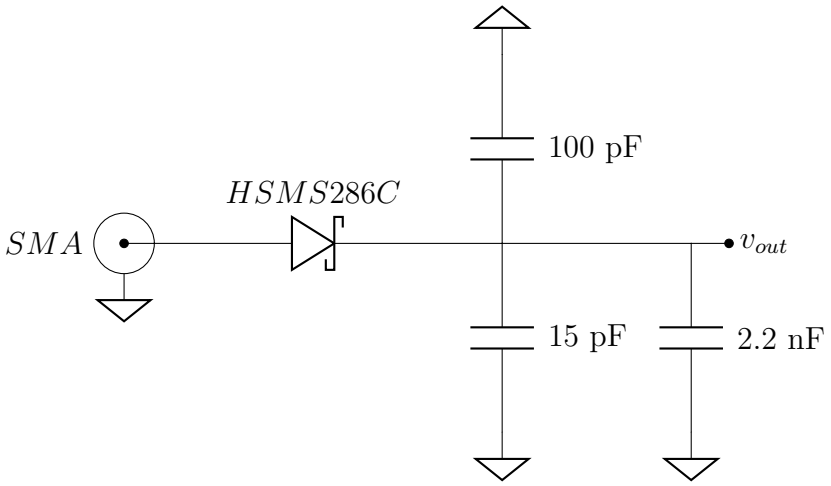

Figure 4.9: Half-wave rectifier schematic

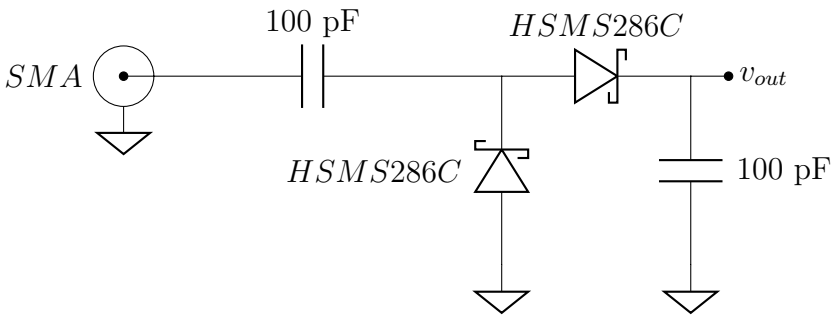

Figure 4.10: Single stage voltage multiplier schematic

The presence of 3 capacitors with different capacities in the first circuit is due to the fact that each capacitor must deal with different frequency components. The final results are shown in figure 4.11:

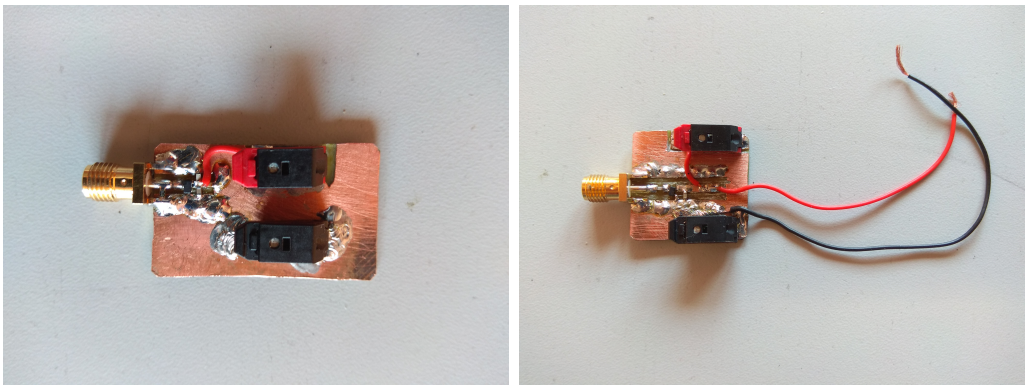

(a) Half wave rectifier **(b)** Single stage voltage multiplier

Figure 4.11: Circuit prototypes

Both circuits were tested with and without load, using a sinusoidal input voltage with an amplitude of 0.5 V and a frequency of 10 MHz (approximately two decades below the interested frequencies). All the measurements are reported in table 4.2:

Circuit	Load	v_{out} [mV]	i_{out} [µA]
Half wave rectifier	$R = 12\ \Omega$	270	22
	No load	450	0
Single stage voltage mult.	$R = 12\ \Omega$	500	41.6
	No load	930	0

Table 4.2: Prototypes meas

Successively they were connected the antennas of the powercast kit and placed inside the anechoic chamber to measure the output voltage in no load conditions placing the circuit at different distances from the transmitting antenna, that was used to radiate in the same conditions as the powercast (figure 4.12).

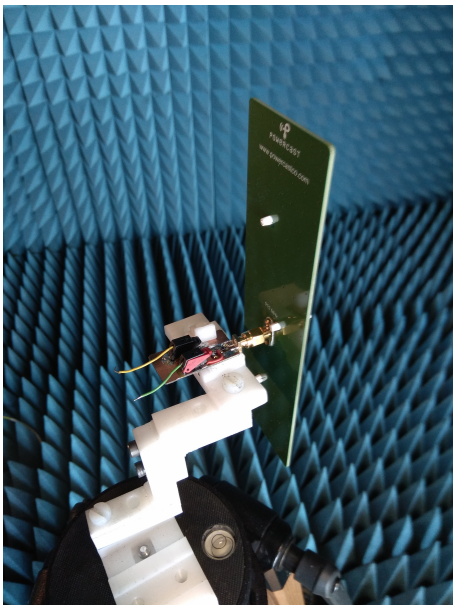

Figure 4.12: Half-wave rectifier connected to the patch antenna

The results are reported in table 4.3 and 4.4 and in figure 4.13b:

Distance [m]	Patch v_{out} [mV]	Dipole v_{out} [mV]
0.5	524.617	322.721
1	211.689	135.198
1.5	63.325	15.389
2	42.034	8.089

Table 4.3: v_{out} measurements - half-wave rectifier

Distance [m]	Patch v_{out} [mV]	Dipole v_{out} [mV]
0.5	221.054	117.511
1	52.270	6.401
1.5	7.332	0.144
2	2.153	0.102

Table 4.4: v_{out} measurements - single stage voltage multiplier

As expected, the half wave rectifier shows better performances with respect the single stage voltage multiplier. This can be imputed a lower reflected power and less voltage drop on the circuit components. The patch allows again the get a higher output voltage.
The datasheet of the powercast states that the patch has s resistance of 50 Ω. Knowing this value and using all the hypotheses of chapter 2.1.1 it was possible to estimate the maximum input voltage and so the steady state output voltage from the rectifier, using the expression 3.38. In figure 4.13a it is possible to confront the difference between the theoretical output voltage and the measured one. The real value is below the theoretical one due to losses in the circuit and reflections. This is more evident for higher distances.

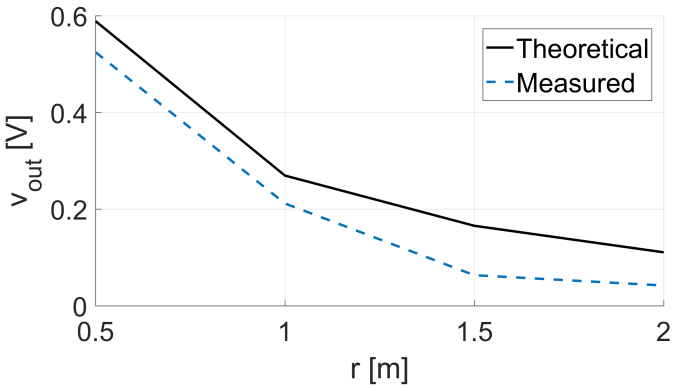

(a) Comparison between circuits

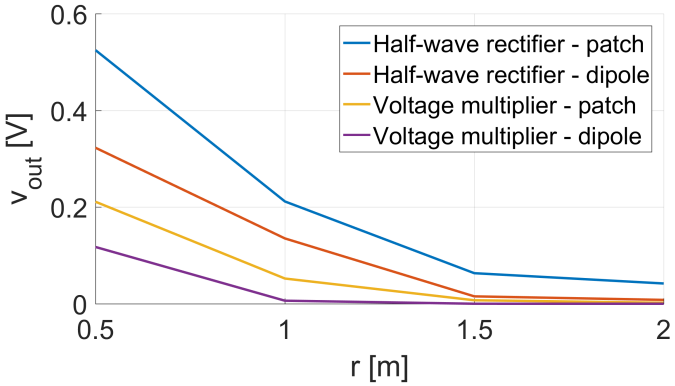

(b) Comparison between circuits

Successively the half-wave rectifier was connected to a signal generator and supplied with a sinusoidal input signal with an amplitude of 1 V and a frequency of 868 MHz. In this condition an output voltage of 0.8765 V mas measured from the output terminals,that is below the theoretical 0.924 V derived in similar conditions in chapter . Then the circuit was used to charge a capacitor of 470 µF.

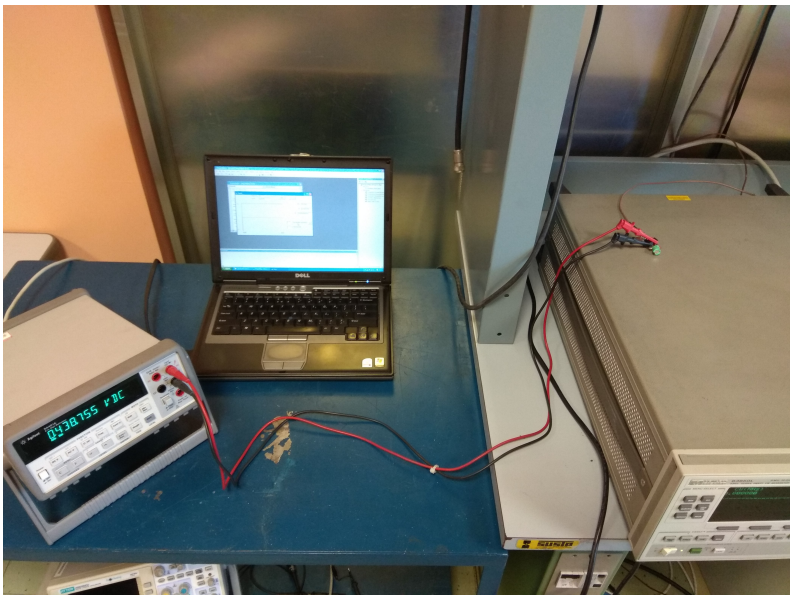

Figure 4.14: Measurements

In order to reach the 0.871 V ($\simeq$ 99% of the charge) it takes an hour. The transient is shown in figure 4.15:

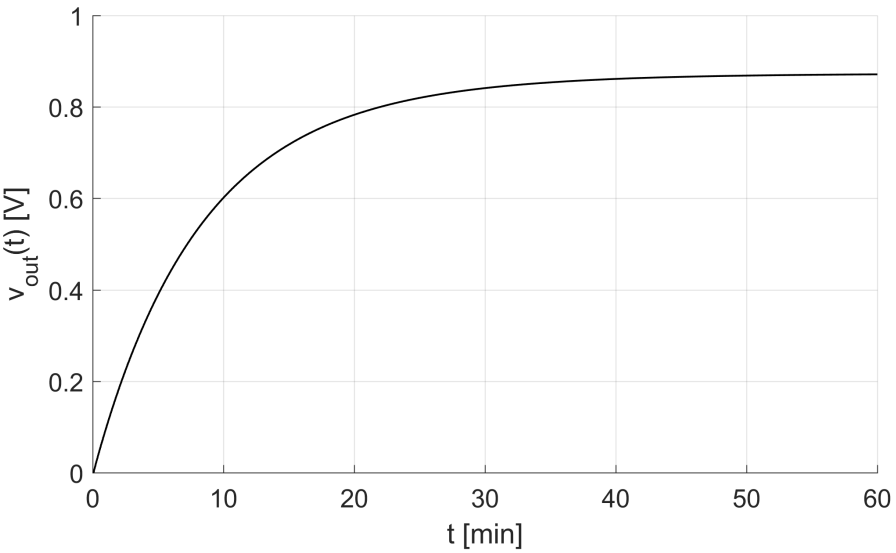

Figure 4.15: Output voltage transient

Chapter 5

Conclusions and perspectives

The purpose of this thesis was to understand the impact of the antenna impedance on the charge of the output capacitor of a rectenna.
In chapter 2.1 it was estimated an equivalent circuit of the patch antenna. It is discovered that the maximum input voltage depends on the distance from the source and the radiation resistance.
From the simulations of chapter 3.3 it can be notice that:

- the transient in the circuit with a resonator;
- considering many input impedances with the same quality factor, the charge is faster when the resistance is low;
- considering the same input resistance, the higher is the antenna quality factor the faster is the charge. The limit case of a resistance only shows the slowest charge;
- the steady state conditions depends mainly on the diode.

In general an antenna with an input impedance is a better choice since it allows to get a higher steady state voltage at the expense of greater charge time.
From the measurements of chapter 4.1 the following conclusions can be done:

- the half-wave rectifier shows a higher output voltage than the single stage voltage multiplier using both the patch and the dipole. This result is in agreement with the discussion of chapter 2.2;
- connecting the patch to the half-wave rectifier, the real output voltage is lower than the theoretical expectations since the model does not consider any losses. This is more evident for higher distances.

From these preliminary results the radiation resistance is able to affects the output voltage. Future work will focus on:

- a more complex model capable to take into account all the parameters present in the circuit, like the diode and the capacitor;
- the impact of a matching circuit on the output voltage;
- more analysis using different kind of antennas;
- use this rectenna to charge a big capacitor or other circuits in a energy harvesting environment.

Appendix A

Matlab Codes

A.1 Simplified circuit

Listing A.1: Algorithm 1

```
clear all
close all
clc
%
% Inputs
Vin   = 1;          % [V]   - input voltage amplitude
R     = 50;         % [ohm] - antenna resistance
Cout  = 10e-9;      % [F]   - output capacitor
f     = 868e6;      % [Hz]  - input frequency
T_sim = 1e-6;       % [s]   - simulation time
Ron   = 6;          % [ohm] - diode Phase-ON resistance
Roff  = 1e6;        % [ohm] - diode Phase-OFF resistance
Von   = 0.26;       % [V]   - Forward threshold voltage
%
% Initial settings
omega   = 2*pi*f;
T       = 1/f;
DT      = T/100;
tau_on  = Cout*(Ron+R);
tau_off = Cout*(Roff+R);
vout    = [];
t       = [];
t_prev  = 0;
t_next  = 0;
%
```

```
% Initial conditions
vout_0  = 0;
%
V_i     = @(t) Vin*sin(omega*t);
tSimul  = tic;
%
% Main code
while(t_next<T_sim)
    %
    % OFF-Phase
    t_prev  = t_next;
    Vout    = @(t) vout_0*exp((t_prev - t)/tau_off) + Vin
       /(tau_off*(omega^2 + 1/tau_off^2))*(exp((t_prev -
       t)/tau_off)*(omega*cos(omega*t_prev) + sin(omega*
       t_prev)/tau_off) - (omega*cos(omega*t) + sin(omega
       *t)/tau_off));
    V_d     = @(t) (V_i(t) - Vout(t))*Roff/(R+Roff) - Von
       ;
    %
    t_inf   = t_prev + DT;
    cond    = 1;
    t_sup   = t_inf;
    while cond >0
        t_sup   = t_sup + DT;
        cond    =  V_d(t_sup)*V_d(t_inf);
    end
    t_next  = fzero(V_d,[t_inf t_sup]);
    vout_0  = Vout(t_next);
    t_int   = linspace(t_prev,t_next,20);
    for ind1 = 1:length(t_int)
       v(ind1) = Vout(t_int(ind1));
    end
    vout    = [vout v];
    t       = [t t_int];
    %
    % ON-Phase
    t_prev  = t_next;
    Vout    = @(t) vout_0*exp((t_prev - t)/tau_on) + Von
       *(exp((t_prev - t)/tau_on) - 1) + Vin/(tau_on*(
       omega^2 + 1/tau_on^2))*(exp((t_prev - t)/tau_on)*(
       omega*cos(omega*t_prev) + sin(omega*t_prev)/tau_on
       ) - (omega*cos(omega*t) + sin(omega*t)/tau_on));
```

```
    V_d      = @(t) (V_i(t) - Vout(t)- Von)*Ron/(R+Ron);
    %
    t_inf    = t_prev + DT;
    cond     = 1;
    t_sup =  t_inf;
    while cond >0
        t_sup    = t_sup + DT;
        cond     =  V_d(t_sup)*V_d(t_inf);
    end
    t_next   = fzero(V_d,[t_inf t_sup]);
    vout_0   = Vout(t_next);
    t_int    = linspace(t_prev,t_next,20);
    for ind1 = 1:length(t_int)
       v(ind1) = Vout(t_int(ind1));
    end
    vout     = [vout v];
    t        = [t t_int];
end
%
tSimulTot = toc(tSimul);
%
% Picture
figure, hold on
plot(t,vout);
xlabel('t [s]');
ylabel('v_{out}(t) [V]');
grid on
```

Listing A.2: Algorithm 2

```
clear all
close all
clc
%
% Constants
kb     = 1.38064852e-23;      % [m^2 kg s^(-2) K^(-1)]
q      = 1.60217662e-19;      % [C]
%
% Inputs
v_i    = 1;           % [V]   - input voltage amplitude
R      = 50;          % [ohm] - antenna resistance
Cout   = 10e-9;       % [F]   - output capacitor
f      = 868e6;       % [Hz]  - input frequency
```

```
14 n      = 1.08;        % Diode emission coefficient
15 T_rel  = 27;          % [Celsius]  - temperature
16 Is     = 5e-8;        % [A]    - reverse saturation current
17 T_sim  = 1e-6;        % [s]    - simulation time
18 Npts   = 1000;        % Number of points per period
19 %
20 % Initial settings
21 T_abs        = 273.15 + T_rel;
22 vt           = kb*T_abs/q;
23 nvt          = n*vt;
24 T            = 1/f;
25 omega        = 2*pi*f;
26 N_periods    = floor(T_sim/T);
27 t            = linspace(0,N_periods,N_periods)*T;
28 DT           = T/Npts;
29 k1           = (Is*DT/Cout);
30 k2           = (Is*R/nvt);
31 k3           = DT/(R*Cout);
32 k4           = R*Is;
33 %
34 % Initial conditions
35 vout         = zeros(1,N_periods);
36 vd_new       = 0;
37 vout_new     = 0;
38 %
39 % Temporal variables
40 vd_old       = 0;
41 vout_old     = 0;
42 %
43 tSimul = tic;
44 %
45 % Main code
46 for ind2 = 2:N_periods
47   for ind1 = 1 : Npts
48      k5      = exp(vd_old/nvt);
49      vin     = v_i*sin(omega*DT*ind1);
50      %
51      Dvout       = k1*(((vin-vout_old-vd_old)/nvt+1)*k5-1)
          /(1+k2*k5*(1+k3));
52      Dvd         = (vin - vd_old - vout_old - Dvout-k4*(k5
          -1))/(1 + k2*k5);
53      vout_new    = vout_old + Dvout;
```

```
54      vd_new      = vd_old + Dvd;
55      %
56      vout_old    = vout_new;
57      vd_old      = vd_new;
58   end
59   vout(ind2) = vout_new;
60  end
61  %
62  tSimulTot = toc(tSimul);
63  %
64  % Picture
65  figure, hold on
66  plot(t,vout);
67  xlabel('t [s]');
68  ylabel('v_{out}(t) [V]');
69  grid on
```

A.1.1 Complete circuit

Listing A.3: Algorithm 3

```
1  clear all
2  close all
3  clc
4  %
5  % Inputs
6  Vin    = 1;           % [V]    - input voltage amplitude
7  R      = 50;          % [ohm]  - patch resistance
8  L      = 245.153e-12;% [H]    - patch inductance
9  C      = 137.140e-12;% [F]    - patch capacitance
10 Cout   = 10e-9;       % [F]    - output capacitor
11 f      = 868e6;       % [Hz]   - input frequency
12 T_sim  = 10e-9;       % [s]    - simulation time
13 Ron    = 6;           % [ohm]  - diode Phase-ON resistance
14 Roff   = 1e6;         % [ohm]  - diode Phase-OFF resistance
15 Von    = 0.26;        % [V]    - Forward threshold voltage
16 %
17 % Initial settings
18 omega   = 2*pi*f;
19 T = 1/f;
20 DT = T/100;
21 vout = [];
```

```
22 t = [];
23 t_0 = 0;
24 t_1 = 0;
25 %
26 % ON-Phase system
27 A_on    = [-1/C*(1/R + 1/Ron),-1/(C*Ron),-1/C;-1/(Cout*
      Ron),-1/(Cout*Ron),0;1/L 0 0] ;
28 b_on = [1/(C*Ron);1/(Cout*Ron);0];
29 [V_on, S_on] = eig(A_on);
30 s_on = diag(S_on);
31 beta_on = V_on\b_on;
32 %
33 % OFF-Phase system
34 A_off   = [-1/C*(1/R + 1/Roff),-1/(C*Roff),-1/C;-1/(Cout*
      Roff),-1/(Cout*Roff),0;1/L 0 0] ;
35 b_off = [1/(C*Roff);1/(Cout*Roff);0];
36 [V_off, S_off]=eig(A_off);
37 s_off = diag(S_off);
38 beta_off = V_off\b_off;
39 % Initial conditions
40 vc_0    = 0;
41 vout_0  = 0;
42 il_0    = 0;
43 x0 = [vc_0;vout_0;il_0];
44 %
45 V_i = @(t) Vin*sin(omega*t);
46 tSimul = tic;
47 %
48 % Main code
49 while(t_1<T_sim)
50     %
51     % OFF-Phase
52     t_0 = t_1;
53     x0 = [vc_0;vout_0;il_0];
54     xi0 = V_off\x0;
55     %
56     xi_1_forced = @(t) Vin*(beta_off(1)/(s_off(1)^2 +
          omega^2))*((omega*cos(omega*t_0)+ s_off(1)*sin(
          omega*t_0))*exp(s_off(1)*(t-t_0)) - omega*cos(
          omega*t)- s_off(1)*sin(omega*t));
```

```
57      xi_2_forced = @(t) Vin*(beta_off(2)/(s_off(2)^2 +
           omega^2))*((omega*cos(omega*t_0)+ s_off(2)*sin(
           omega*t_0))*exp(s_off(2)*(t-t_0)) - omega*cos(
           omega*t)- s_off(2)*sin(omega*t));
58      xi_3_forced = @(t) Vin*(beta_off(3)/(s_off(3)^2 +
           omega^2))*((omega*cos(omega*t_0)+ s_off(3)*sin(
           omega*t_0))*exp(s_off(3)*(t-t_0)) - omega*cos(
           omega*t)- s_off(3)*sin(omega*t));
59      %
60      xi_1_homo = @(t)(xi0(1))*exp(s_off(1)*(t-t_0));
61      xi_2_homo = @(t)(xi0(2))*exp(s_off(2)*(t-t_0));
62      xi_3_homo = @(t)(xi0(3))*exp(s_off(3)*(t-t_0));
63      %
64      xi_1 = @(t) xi_1_forced(t) + xi_1_homo(t);
65      xi_2 = @(t) xi_2_forced(t) + xi_2_homo(t);
66      xi_3 = @(t) xi_3_forced(t) + xi_3_homo(t);
67      %
68      x1   = @(t) real(V_off(1,1)*xi_1(t) + V_off(1,2)*xi_2
           (t) + V_off(1,3)*xi_3(t));
69      x2   = @(t) real(V_off(2,1)*xi_1(t) + V_off(2,2)*xi_2
           (t) + V_off(2,3)*xi_3(t));
70      x3   = @(t) real(V_off(3,1)*xi_1(t) + V_off(3,2)*xi_2
           (t) + V_off(3,3)*xi_3(t));
71      V_d     = @(t) V_i(t) - x1(t) - x2(t) - Von;
72      %
73      t_inf   = t_0 + DT;
74      cond    = 1;
75      t_sup = t_inf;
76      while cond >0
77          t_sup = t_sup + DT;
78          cond =  V_d(t_sup)*V_d(t_inf);
79      end
80      t_1 = fzero(V_d,[t_inf t_sup]);
81      vc_0    = x1(t_1);
82      vout_0  = x2(t_1);
83      il_0    = x3(t_1);
84      t_int = linspace(t_0,t_1,20);
85      for ind1 = 1:length(t_int)
86         v(ind1) = x2(t_int(ind1));
87      end
88      vout = [vout v];
89      t = [t t_int];
```

```
90      %
91      % ON-Phase
92      t_0 = t_1;
93      x0 = [vc_0;vout_0;il_0];
94      xi0 = V_on\x0;
95      %
96      xi_1_forced = @(t) Vin*(beta_on(1)/(s_on(1)^2 + omega
           ^2))*((omega*cos(omega*t_0)+ s_on(1)*sin(omega*t_0
           ))*exp(s_on(1)*(t-t_0)) - omega*cos(omega*t)- s_on
           (1)*sin(omega*t)) + Von*beta_on(1)*(1-exp(s_on(1)
           *(t-t_0)))/s_on(1);
97      xi_2_forced = @(t) Vin*(beta_on(2)/(s_on(2)^2 + omega
           ^2))*((omega*cos(omega*t_0)+ s_on(2)*sin(omega*t_0
           ))*exp(s_on(2)*(t-t_0)) - omega*cos(omega*t)- s_on
           (2)*sin(omega*t)) + Von*beta_on(2)*(1-exp(s_on(2)
           *(t-t_0)))/s_on(2);
98      xi_3_forced = @(t) Vin*(beta_on(3)/(s_on(3)^2 + omega
           ^2))*((omega*cos(omega*t_0)+ s_on(3)*sin(omega*t_0
           ))*exp(s_on(3)*(t-t_0)) - omega*cos(omega*t)- s_on
           (3)*sin(omega*t)) + Von*beta_on(3)*(1-exp(s_on(3)
           *(t-t_0)))/s_on(3);
99      %
100     xi_1_homo = @(t)(xi0(1))*exp(s_on(1)*(t-t_0));
101     xi_2_homo = @(t)(xi0(2))*exp(s_on(2)*(t-t_0));
102     xi_3_homo = @(t)(xi0(3))*exp(s_on(3)*(t-t_0));
103     %
104     xi_1 = @(t) xi_1_forced(t) + xi_1_homo(t);
105     xi_2 = @(t) xi_2_forced(t) + xi_2_homo(t);
106     xi_3 = @(t) xi_3_forced(t) + xi_3_homo(t);
107     %
108     x1   = @(t) real(V_on(1,1)*xi_1(t) + V_on(1,2)*xi_2(t
           ) + V_on(1,3)*xi_3(t));
109     x2   = @(t) real(V_on(2,1)*xi_1(t) + V_on(2,2)*xi_2(t
           ) + V_on(2,3)*xi_3(t));
110     x3   = @(t) real(V_on(3,1)*xi_1(t) + V_on(3,2)*xi_2(t
           ) + V_on(3,3)*xi_3(t));
111     %
112     V_d     = @(t) V_i(t) - x1(t) - x2(t) - Von;
113     t_inf   = t_0 + DT;
114     cond    = 1;
115     t_sup   = t_inf;
116     while cond >0
```

```
        t_sup = t_sup + DT;
        cond =  V_d(t_sup)*V_d(t_inf);
    end
    t_1 = fzero(V_d,[t_inf t_sup]);
    vc_0    = x1(t_1);
    vout_0  = x2(t_1);
    il_0    = x3(t_1);
    t_int = linspace(t_0,t_1,20);
    for ind1 = 1:length(t_int)
       v(ind1) = x2(t_int(ind1));
    end
    vout = [vout v];
    t = [t t_int];
end
tSimulTot = toc(tSimul);
%
% Picture
figure, hold on
plot(t,vout);
xlabel('t [s]');
ylabel('v_{out}(t) [V]');
grid on
```

Listing A.4: Algorithm 4

```
clear all
close all
clc
%
% Constants
kb    = 1.38064852e-23;      % [m^2 kg s^(-2) K^(-1)]
q     = 1.60217662e-19;      % [C]
%
% Inputs
v_i   = 1;           % [V]    - input voltage amplitude
R     = 50;          % [ohm]  - patch resistance
L     = 245.153e-12;% [H]    - patch inductance
C     = 137.140e-12;% [F]    - patch capacitance
Cout  = 10e-9;       % [F]    - output capacitor
f     = 868e6;       % [Hz]   - input frequency
n     = 1.08;        % Diode emission coefficient
T_rel = 27;          % [Celsius]  - temperature
Is    = 5e-8;        % [A]    - reverse saturation current
```

```
19 T_sim = 1e-6;      % [s]   - simulation time
20 Npts  = 1000;        % Number of points per period
21 %
22 % Initial settings
23 T_abs        = 273.15 + T_rel;
24 vt           = kb*T_abs/q;
25 nvt          = n*vt;
26 T            = 1/f;
27 omega        = 2*pi*f;
28 N_periods    = floor(T_sim/T);
29 t            = linspace(0,N_periods,N_periods)*T;
30 DT           = T/Npts;
31 Y_res     = 1/R + C/DT;
32 k1 = Is/nvt;
33 k2 = 1/R;
34 k3 = Cout/DT;
35 k4 = DT/L;
36 k5 = C/DT;
37 %
38 % Temporal variables
39 vd_old   = 0;
40 vout_old = 0;
41 % Initial conditions
42 il_o      = 0;
43 vc_o      = 0;
44 id_o      = 0;
45 vout      = zeros(1,N_periods);
46 %
47 tSimul = tic;
48 %
49 for ind2 = 2:N_periods
50     %
51     for ind1 = 1:Npts
52     %
53     vin      = v_i*sin(omega*(DT*ind1));
54     vin_end  = v_i*sin(omega*(DT*(ind1-1)));
55     Dvin     = vin - vin_end;
56     %
57     Yd        = Y_res + k1*exp(vd_old/nvt);
58     Dvout     = ((vc_o*k2 + Dvin*Y_res + il_o)*(1-Y_res/Yd
       )+(Y_res/Yd)*id_o )/(k3 +Y_res*(1-Y_res/Yd));
```

```
59      Dvd       = (vc_o*k2 - id_o  + Y_res*(Dvin-Dvout) +
            il_o)/Yd;
60      vd_new    = vd_old + Dvd;
61      vout_new  = vout_old + Dvout;
62      vc_o      = vin - vd_new - vout_new ;
63      %
64      vd_old    = vd_new;
65      vout_old  = vout_new;
66      il_o      = vc_o*k4 + il_o;
67      id_o      = Is*(exp(vd_old/nvt)-1);
68    end
69    %
70    vout(ind2)   = vout_new;
71    %
72  end
73  tSimulTot = toc(tSimul);
74  %
75  % Picture
76  figure, hold all;
77  plot(t,vout);
78  ylabel('v_{out}(t) [V]');
79  xlabel('t [s]');
80  grid on;
```

Appendix B

LTspice device models

B.1 Diode model

There are two types of diodes available: one is a conduction region-wise linear model, that yields representation of an idealized diode, and the other model available is the standard Berkeley SPICE semiconductor diode, with an exponential voltage-current relation.

B.1.1 Conduction region-wise linear model

The piece-wise linear diode model in LTspice is characterized by three conduction regions: ON, OFF and reverse breakdown. Forward conduction and reverse breakdown can non-linear by specifying some parameters. The main parameters for this type of diode are reported in table B.1:

Name	Parameter	Default value	Units
R_{on}	Resistance in forward conduction	1	Ω
R_{off}	Resistance in reverse conduction	$1/G_{min}$	Ω
V_{fwd}	Forward threshold voltage	0	V
V_{fwd}	Reverse threshold voltage	∞	V
R_{rev}	Breakdown impedance	R_{on}	Ω
I_{limit}	Forward current limit	∞	A
$RevI_{limit}$	Reverse current limit	∞	A
$Epsilon$	width of quadratic region	0	V
$Revepsilon$	width of quadratic region reverse	0	V

Table B.1: LTspice Diode model parameters

In this case just the idealized case is required, so just the parameters Ron, Roff,

Vfwd and Vrev must be defined, accordingly on the diode datasheet:

- $R_{on} = 6\ \Omega$
- $R_{off} = 1\ \mathrm{M}\Omega$
- $V_{fwd} = 0.25\ \mathrm{V}$
- $V_{rev} = 20\ \mathrm{V}$

The resulting characteristic is shown in figure B.1:

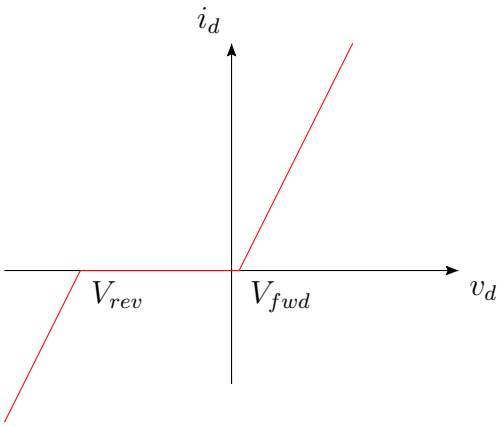

Figure B.1: Diode piece-wise model in LTspice

B.1.2 Berkeley diode model

The standard Berkeley SPICE semiconductor diode is diode model with an exponential characteristic. With appropriate precautions it is possible to refer to the shape of the Shockley equation. The equivalent circuit is shown in figure B.2:

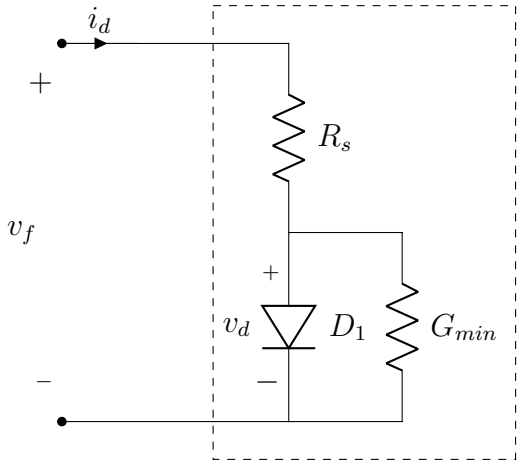

Figure B.2: DC Large-signal LTspice Diode model

This model contains an active diode D_1, a series resistance R_s and a shunt conductance G_{min}. The dc model variables are the voltage across the diode v_f, the voltage across the internal diode v_d and the terminal current i_d. In the table B.2 the most important parameters are reported:

Name	Parameter	Default value	Units
I_s	Saturation current	$10 \cdot 10^{-15}$	A
R_s	Series resistance	0	Ω
η	Emission coefficient	1	
G_{min}	Shunt conductance	$1 \cdot 10^{-12}$	S
EG	Activation energy	1.11	eV
XTI	I_s temperature exponent	3	
BV	Breakdown voltage	∞	V
I_{BV}	Saturation current	$1 \cdot 10^{-13}$	A

Table B.2: LTspice Diode model parameters

From these parameters it is possible to define the device characteristic from the following equations:

$$v_f = R_s \cdot i_d + v_d \tag{B.1}$$

$$i_d = f(v_d) \tag{B.2}$$

Four operative regions define the relation between the internal diode voltage and diode current:

1. For $vd \leq -5 \cdot \eta V_t$

$$i_d = I_s \cdot \left(e^{\frac{v_d}{\eta V_t}} - 1 \right) + G_{min} \cdot v_d \tag{B.3}$$

2. For $BV < vd < -5 \cdot \eta V_t$

$$i_d = -I_s + G_{min} \cdot v_d \tag{B.4}$$

3. For $vd = BV$

$$i_d = -I_{BV} \tag{B.5}$$

4. For $vd < BV$

$$i_d = -I_s \cdot \left(e^{-\frac{BV+v_d}{V_t}} - 1 + \frac{BV}{V_t} \right) \tag{B.6}$$

The model takes also into account the temperature effect on the parameters. T_{NOM} is the nominal temperature that have a default value of 27 °C. For the saturation current I_s the parameters η, EG and XTI are used to model its variation in function of the temperature:

$$I_s(T) = I_s(T_{NOM}) \cdot \left(\frac{T}{T_{NOM}} \right)^{\frac{XTI}{\eta}} \cdot e^{\left(\frac{qEG}{k_b \eta}\right) \cdot \left(\frac{1}{T_{NOM}} - \frac{1}{T}\right)} \tag{B.7}$$

The model is much more complicated than the one used to get the Euler solution. For this reason many parameters was set in order to get a model as similar as possible to the expression 3.2:

- $R_s = 0\ \Omega \ \rightarrow \ v_d = v_f$
- $XGI = 0$ and $EG = 0$ eV $\ \rightarrow \ I_s(T) = I_s(T_{NOM}) \ \forall \ T$

B.2 Inductor model

The inductor model model is represented in figure B.3:

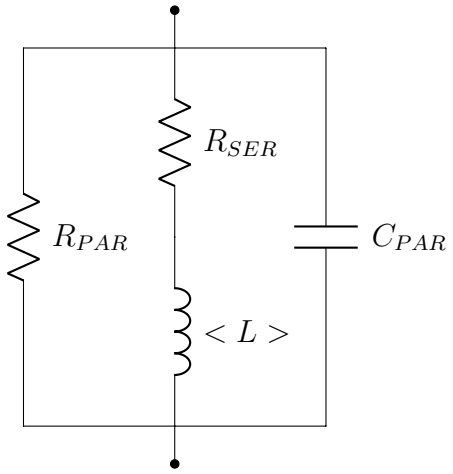

Figure B.3: LTspice inductor model

The parameter R_{SER}, that is a series resistance, has a default value of 1 mΩ that is not mentioned the inductance statement. This allows LTspice to integrate the inductance as a Norton equivalent circuit instead of Thevenin equivalent in order to reduce the size of the circuit's linearized matrix. This parameter makes errors in the simulation, especially when the value of L is quite low (that is the case of a patch with a high value of Q). In order to avoid this error this parameter has been set to a null value. The disadvantage is that LTspice requires to use the more cumbersome Thevenin equivalent of the inductor during transient analysis and consequently all the simulations are longer. In conclusions, for the inductor model:

- $R_{SER} = 0$
- $R_{PAR} = \infty$ (default)
- $C_{PAR} = 0$ (default)

Bibliography

[1] S. Ladan, N. Ghassemi, A. Ghiotto, and K. Wu. Highly efficient compact rectenna for wireless energy harvesting application. *IEEE Microwave Magazine*, 14(1):117–122, Jan 2013.

[2] Y. S. Chen and C. W. Chiu. Maximum achievable power conversion efficiency obtained through an optimized rectenna structure for rf energy harvesting. *IEEE Transactions on Antennas and Propagation*, 65(5):2305–2317, May 2017.

[3] Constantine A. Balanis. *Antenna Theory: Analysis and Design*. Wiley, 2016.

[4] Giuseppe Vecchi. Rectangular patch antenna: Design with slot radiation and transmission line model. University Lecture, 2015.

[5] B. Strassner and K. Chang. Microwave power transmission: Historical milestones and system components. *Proceedings of the IEEE*, 101(6):1379–1396, June 2013.

[6] Xiao Lu, D. Niyato, Ping Wang, Dong In Kim, and Zhu Han. Wireless charger networking for mobile devices: fundamentals, standards, and applications. *IEEE Wireless Communications*, 22(2):126–135, April 2015.

[7] M. Biey, M. Hasler, R. Lojacono, and A. Premoli. Pila: a computer program for fast and accurate analysis of piecewise linear circuits. In *1988., IEEE International Symposium on Circuits and Systems*, pages 1123–1126 vol.2, June 1988.

[8] R. Perfetti. *Circuiti elettrici*. Zanichelli, 2013.